

ISSN 0009-3084  
CPLIA 87 (1) 1-90

# CPL

Managing Editors

F. Paltauf (Graz, Austria)

I.H.O. Schmid (Austin, MN, USA)

## CHEMISTRY AND PHYSICS OF LIPIDS

ELSEVIER

VOL. 87 NO. 1 MAY 30th 1997

## CHEMISTRY AND PHYSICS OF LIPIDS

### SCOPE OF THE JOURNAL

Chemistry and Physics of Lipids publishes research papers and review articles in the field of molecular biology which emphasise chemical and physical aspects of lipids. Accordingly, the journal covers: advances in synthetic and analytical lipid methodology; chemical and physical characterisation of isolated structures; thermodynamics, phase behaviour, topology and dynamics of lipid assemblies; physicochemical studies into lipid-lipid and lipid-protein interactions in lipoproteins and in natural and model membranes; movement of lipids within, across and between membranes; intracellular lipid transfer; structure-function relationships and the nature of lipid-derived second messengers; chemical, physical and functional alterations of lipids induced by free radicals; and the role of lipids in the regulation of membrane-dependent biological processes. Reviews, full articles and short communications will be considered for publication in each issue. Special Issues will consist of invited contributions organized and edited to cover specific themes.

### MANAGING EDITORS

Prof. F. Paltauf, Institut für Biochemie und Lebensmittelchemie, Technische Universität Graz, Petersgasse 12, A-8010, Graz, Austria.

Prof. H.H.O. Schmid, The Hormel Institute, University of Minnesota, 801 16th Avenue N.E., Austin, MN 55912, U.S.A.

### EDITORIAL ADVISORY BOARD

Y. Barenholz, Jerusalem; R.L. Biltonen, Charlottesville, VA; R. Bittman, Flushing, NY; A. Blume, Kaiserslautern; J.M. Boggs, Toronto; R.E. Brown, Austin, MN; G. Ceve, Munich; W.W. Christie, Dundee; H. Egge, Bonn; R.M. Epand, Hamilton; H. Esterbauer, Graz; K. Gawrisch, Rockville, MD; R.H. Gigg, London; A. Gulik, Gif-sur-Yvette; F.D. Gunstone, Dundee; H. Hauser, Zürich; H.S. Hendrickson, Seattle, WA; H.J. Hinz, Münster; L. Huang, Pittsburgh, PA; M. Kates, Ottawa; P.K.J. Kinnunen, Helsinki; P. Laggner, Graz; D. Marsh, Göttingen; R.N. McElhaney, Edmonton; T.J. McIntosh, Durham, NC; J.D. Morrisett, Houston, TX; V. Natarajan, Indianapolis, IN; E. Niki, Tokyo; Y. Nozawa, Gifu; E. Oldfield, Urbana, IL; I. Pascher, Göteborg; M.C. Phillips, Philadelphia, PA; F. Schroeder, College Station, TX; J. Seelig, Basel; G. Shipley, Boston, MA; P. Yeagle, Buffalo, NY.

### FOUNDING EDITORS

L.D. Bergelson, Moscow; D. Chapman, London; J.B. Finean, Birmingham; G.H. de Haas, Utrecht; H.K. Mangold, Münster; D. Shapiro, Rehovot.

**Publication information:** *Chemistry and Physics of Lipids* 0009-3084. For 1997 volumes 86-90 are scheduled for publication. Subscription prices are available upon request from the publisher. Subscriptions are accepted on a prepaid basis only and are entered on a calendar year basis. Issues are sent by surface mail except to the following countries where Air delivery via SAL mail is ensured: Argentina, Australia, Brazil, Canada, Hong Kong, India, Israel, Japan, Malaysia, Mexico, New Zealand, Pakistan, PR China, Singapore, South Africa, South Korea, Taiwan, Thailand, USA. For all other countries airmail rates are available upon request. Claims for missing issues should be made within six months of our publication (mailing) date.

**Orders, claims and product enquiries:** please contact the Customer Support Department at the Regional Sales Office nearest you:

New York	Amsterdam	Tokyo	Singapore
Elsevier Science	Elsevier Science	Elsevier Science	Elsevier Science
P.O. Box 945	P.O. Box 211	9-15 Higashi-Azabu 1-chome	No. 1 Temasek Avenue
New York, NY 10159-0945	1000 AE Amsterdam	Minato-ku, Tokyo 106	# 17-01 Millenia Tower
USA	The Netherlands	Japan	Singapore 039192
Tel. (+1)212-633-3730	Tel. (+31)20-4853757	Tel. (+81)3-5561-5033	Tel. (+65)434-3727
[Toll free number for North American customers: 1-888-4ES-INFO (437-4636)]	Fax (+31)20-4853432	Fax (+81)3-5561-5047	Fax (+65)337-2230
Fax (+1)212-633-3680	e-mail nlinfo-f@elsevier.nl	e-mail kyf04035@niftyserve.or.jp	e-mail asiainfo@elsevier.com.sg
e-mail usinfo-f@elsevier.com			

Submission of a paper to Chemistry and Physics of Lipids is understood to imply that it is not being considered for publication elsewhere and that the author's permission to publish his/her article(s) in this journal implies the exclusive authorisation of the publisher to deal with all issues concerning copyright therein.

Submission of multi-authored manuscripts implies the consent of *each* of the authors. The publisher will assume that the senior or corresponding author has specifically obtained the approval of all other co-authors to submit the manuscript to this journal.

Periodicals postage paid at Rahway, New Jersey. Chemistry and Physics of Lipids (ISSN 0009-3084) is published monthly, except June and December, by Elsevier Science Ireland Ltd., Bay 15, Shannon Industrial Estate, Shannon, Co. Clare. The annual subscription in the USA is \$1422. Chemistry and Physics of Lipids is distributed by Virgin Mailing and Distribution, 10 Camptown Road, Irvington, New Jersey 07111-1105. POSTMASTER: Please send address corrections to Chemistry and Physics of Lipids, c/o Elsevier Science Regional Sales Office, Customer Support Department, 655 Avenue of the Americas, New York, NY 10010.



# **CHEMISTRY AND PHYSICS OF LIPIDS**



# CHEMISTRY AND PHYSICS OF LIPIDS

*Managing Editors*

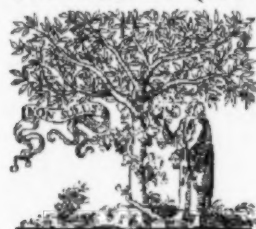
F. PALTAUF, Graz, Austria

H.H.O. SCHMID, Austin, MN, USA

*Editorial Advisory Board*

Y. Barenholz	L. Huang
R.L. Biltonen	M. Kates
R. Bittman	P.K.J. Kinnunen
A. Blume	P. Laggner
J.M. Boggs	D. Marsh
R.E. Brown	R.N. McElhaney
G. Ceve	T.J. McIntosh
W.W. Christie	J.D. Morrisett
H. Egge	V. Natarajan
R.M. Epand	E. Niki
H. Esterbauer	Y. Nozawa
K. Gawrisch	E. Oldfield
R.H. Gigg	I. Pascher
A. Gulik	M.C. Phillips
F.D. Gunstone	F. Schroeder
H. Hauser	J. Seelig
H.S. Hendrickson	G. Shipley
H.J. Hinz	P. Yeagle

VOLUME 87 (1997)



ELSEVIER

Amsterdam — Lausanne — London — New York — Shannon — Tokyo

Copyright © 1997, Elsevier Science Ireland Ltd. All rights reserved

This journal and the individual contributions contained in it are protected by the copyright of Elsevier Science Ireland Ltd., and the following terms and conditions apply to their use:

#### **Photocopying**

Single photocopies of single articles may be made for personal use as allowed by national copyright laws. Permission of the publisher and payment of a fee is required for all other photocopying, including multiple or systematic copying, copying for advertising or promotional purposes, resale, and all forms of document delivery. Special rates are available for educational institutions that wish to make photocopies for non-profit educational classroom use.

In the USA, users may clear permissions and make payment through the Copyright Clearance Center, Inc., 222 Rosewood Drive, Danvers MA 01923, USA. Tel.: (508) 750-8400; Fax: (508) 750-4744. In the UK, users may clear permissions and make payment through the Copyright Licensing Agency Rapid Clearance Service (CLARCS), 90 Tottenham Court Road, London W1P 0LP, UK. In other countries where a local copyright clearance centre exists, please contact it for information on required permission and payments.

#### **Derivative Works**

Subscribers may reproduce tables of contents or prepare lists of articles including abstracts for internal circulation within their institutions. Permission of the publisher is required for resale or distribution outside the institution.

Permission of the publisher is required for all other derivative works, including compilations and translations.

#### **Electronic Storage**

Permission of the publisher is required to store electronically any material contained in this journal, including any article or part of an article. Contact the publisher at the address indicated.

*Except as outlined above, no part of this publication may be reproduced, stored in a retrieval system or transmitted in any form or by any means, electronic, mechanical, photocopying, recording or otherwise, without prior written permission of the publisher.*

*No responsibility is assumed by the Publisher for any injury and/or damage to persons or property as a matter of products liability, negligence or otherwise, or from any use or operation of any methods, products, instructions or ideas contained in the material herein. Because of rapid advances in the medical sciences, independent verification of diagnoses and drug dosages should be made.*

*Although all advertising material is expected to conform to ethical (medical) standards, inclusion in this publication does not constitute a guarantee or endorsement of the quality or value of such product or of the claims made of it by its manufacturer.*



## Greater partitioning of small spin labels into interdigitated than into non-interdigitated gel phase bilayers

Joan M. Boggs<sup>a,b,\*</sup>, Godha Rangaraj<sup>b</sup>

<sup>a</sup> Department of Clinical Biochemistry, University of Toronto, Toronto, Canada

<sup>b</sup> Research Institute, Department of Biochemistry, Hospital for Sick Children, 555 University Ave., Toronto, Ont. M5G 1X8, Canada

Received 22 October 1996; received in revised form 9 January 1997; accepted 9 January 1997

### Abstract

Partitioning of the small amphipathic spin labels 2,2,6,6-tetramethylpiperidine-1-oxyl (TEMPO), 4-oxo-2,2,6,6-tetramethylpiperidiny-*N*-oxy (TEMPONE), and di-tertiary butyl nitroxide (DTBN) into interdigitated  $L_{\beta}$ I and non-interdigitated  $L'_{\beta}$ ,  $P'_{\beta}$ , and  $L_{\alpha}$  phases was compared. The double chain interdigitated phases examined were 1,2-dipalmitoylphosphatidylcholine (DPPC) in the presence of 2.17 M ethanol, dihexadecylphosphatidylcholine (DHPC), and the complexes of dipalmitoylphosphatidylglycerol (DPPG) with polymyxin B and myelin basic protein. The triple chain mixed interdigitated phase of the asymmetric chain 1-stearoyl-2-caproyl-phosphatidylcholine (18:10-PC) was also examined. The non-interdigitated lipids were DPPC, DPPC in the presence of 0.87 M ethanol, DPPG, and the complex of DPPG with polylysine. Quantitation of the percentage of the membrane-bound spectral contribution in the presence of  $\text{NiSO}_4$ , used to broaden the aqueous spectral contribution, showed that all three spin labels partitioned into the  $L_{\beta}$ I phase significantly more than into the  $L'_{\beta}$  phase. The hyperfine splitting values indicated that all three spin labels were located near the apolar/polar interface in the  $L_{\beta}$ I phase. The amount of TEMPO and DTBN bound to the  $L_{\beta}$ I phase was similar to that in the  $L_{\alpha}$  phase but more TEMPONE was bound to the  $L_{\beta}$ I phase than to the  $L_{\alpha}$  phase. This is attributed to the greater polarity of TEMPONE, its preference for a polar or amphipathic environment, and the larger volume between lipid head groups at the apolar/polar interface in the  $L_{\beta}$ I phase compared to the other phases. However, TEMPO binding to the mixed interdigitated gel phase of 18:10-PC was no greater than to the non-interdigitated  $L'_{\beta}$  phase of DPPC, reflecting the smaller volume at the apolar/polar interface of this triple chain interdigitated bilayer compared to the double chain interdigitated bilayers.

**Abbreviations:** DHPC, 1,2-dihexadecylphosphatidylcholine; DPPC, 1,2-dipalmitoylphosphatidylcholine; DPPG, 1,2-dipalmitoylphosphatidylglycerol; DTBN, di-tertiary butyl nitroxide; EtOH, ethanol;  $L_{\alpha}$ , liquid crystalline phase;  $L_{\beta}$ I, interdigitated gel phase;  $L'_{\beta}$ , non-interdigitated gel phase; MBP, myelin basic protein;  $P'_{\beta}$ , gel phase at temperatures above the premelt transition temperature; 18,10-PC, 1-stearoyl-2-caproyl-phosphatidylcholine; PMX, polymyxin B; TEMPO, 2,2,6,6-tetramethylpiperidine-1-oxyl; TEMPONE, 4-oxo-2,2,6,6-tetramethylpiperidiny-*N*-oxy.

\* Corresponding author at: Department of Biochemistry, Hospital for Sick Children, 555 University Ave., Toronto, Ont. M5G 1X8, Canada. Tel: +1 416 8135919; Fax: +1 416 8135022.

Thus interdigitation of the lipid bilayer, whether due to addition of a substance like ethanol, or spontaneous as in DHPC, can cause increased partitioning of other substances into the bilayer, provided that they are small enough to fit into the volume created at the apolar/polar interface. This increased partitioning could contribute to an increased permeability of small molecules across interdigitated bilayers. © 1997 Elsevier Science Ireland Ltd.

**Keywords:** Spin label; EPR spectroscopy; Ethanol; Polymyxin B; Phosphatidylcholine; Phosphatidylglycerol; Myelin basic protein

## 1. Introduction

Many amphipathic compounds such as alcohols (at low concentrations) decrease the phase transition temperature of lipids (Rowe, 1983; Sturtevant, 1984; Kaminoh et al., 1988). Thermodynamic analyses predict that these compounds have a greater solubility in the liquid crystalline phase than in the gel phase. Indeed, the increased solubility of the small amphipathic spin label TEMPO in the liquid crystalline phase has been frequently used to detect lipid phase transitions (Hubbell and McConnell, 1968; Shimshick and McConnell, 1973). However, other amphipathic compounds, such as glycerol, and alcohols themselves at higher concentrations, cause interdigitation of the lipid bilayer in the gel phase (McDaniel et al., 1983; Simon and McIntosh, 1984). The phase transition temperature of the interdigitated bilayer is usually similar to that of the non-interdigitated bilayer. This implies that these compounds are dissolved in the bilayer in the interdigitated gel phase to a similar extent as in the liquid crystalline phase. They cause lateral separation of the lipid head groups in the gel phase, probably accompanied by greater tilting of the lipid molecules (Nagel et al., 1992). When further tilting can no longer occur, interdigitation of the lipid fatty acid chains occurs and maximizes interaction between the chains while allowing separation of the lipid head groups by the solutes without tilting. The partition coefficient or solubility of these compounds in the interdigitated bilayer has only been measured in one study in which interdigitation was induced with butanol. Using titration calorimetry, Zhang and Rowe (1992) were able to show that the partition coefficient of butanol in the interdigitated  $L_{\beta}$ I gel phase of dipalmitoylphosphatidylcholine (DPPC) was considerably greater than that in the non-interdigitated  $L'_{\beta}$  gel phase and, indeed, was

similar to that in the  $P'_{\beta}$  phase. However, it proved impossible to directly detect membrane-bound [ $^{13}\text{C}$ ]butanol in the  $L'_{\beta}$  or  $L_{\beta}$ I phases using  $^{13}\text{C}$ -NMR (Herold et al., 1987).

The partition coefficient of other compounds may also be increased in interdigitated bilayers where the interdigitation is induced by amphipathic substances such as ethanol. It may be similarly increased in lipids which spontaneously form interdigitated bilayers in the absence of exogenous compounds such as dihexadecylphosphatidylcholine (DHPC) (Ruocco et al., 1985). Membrane binding of small spin labels such as TEMPO, DTBN, and TEMPONE can be detected from their EPR spectra. In the present study we compare the membrane concentrations of these probes in a number of interdigitated and non-interdigitated gel phase bilayers. The double chain interdigitated phases examined were DPPC in the presence of 2.17 M ethanol, DHPC, and the complexes of dipalmitoylphosphatidylglycerol (DPPG) with polymyxin B (PMX) and myelin basic protein (MBP). The triple chain mixed interdigitated phase of the asymmetric chain 1-stearoyl-2-caproyl-phosphatidylcholine (18:10-PC) was also examined. With the exception of the complex of MBP with DPPG, these phases have all been shown by others to be interdigitated using X-ray diffraction (Ranck and Tocanne, 1982; Hui et al., 1984; Simon and McIntosh, 1984; Ruocco et al., 1985). This has been confirmed by us using fatty acid and lipid spin labels with the nitroxide group near the end of the acyl chain (Boggs and Rangaraj, 1985; Boggs and Mason, 1986; Boggs et al., 1989). The latter technique also indicates that the complex of MBP with DPPG is interdigitated (Boggs et al., 1981; Boggs and Moscarello, 1982). The non-interdigitated lipids were DPPC, DPPC in the presence of 0.87



M ethanol (Simon and McIntosh, 1984), DPPG, and the complex of DPPG with polylysine (Carrier and Pezolet, 1986). The results show that the membrane concentrations of TEMPO, DTBN, and TEMPONE are considerably greater in the interdigitated gel phase bilayers formed by symmetric chain length lipids than in non-interdigitated gel phase bilayers. However, this was not the case for the mixed interdigitated gel phase of 18:10-PC. In addition, the hyperfine splitting of the spectra of these probes reveals the polarity of their environment (Griffith and Jost, 1976). Thus the location of these probes in the  $L_\beta$ I,  $L'_\beta$ ,  $P'_\beta$ , and  $L_\alpha$  phases could be compared.

## 2. Materials and methods

1,2-Di-*O*-hexadecyl-*sn*-glycero-3-phosphocholine (DHPC) was purchased from Calbiochem-Behring Corp. (La Jolla, CA), 1,2-Dipalmitoyl-*sn*-glycero-3-phosphocholine (DPPC) was from Sigma Chemical Co. (St. Louis, MO), 1,2-dipalmitoyl-*sn*-glycero-3-phosphoglycerol (DPPG) was from Avanti Chemical Co. and 1-stearoyl-2-caproyl-*sn*-glycero-3-phosphocholine (18:10-PC) was a generous gift from Dr. J.T. Mason. 2,2,6,6-Tetramethylpiperidine-1-oxyl (TEMPO), 4-oxo-2,2,6,6-tetramethylpiperidiny-*N*-oxy (TEMPONE), and di-tertiary butyl nitroxide (DTBN) were from Aldrich Chemical Co.; polymyxin B sulfate (PMX) was from Sigma, and 100% ethanol from Consolidated Alcohols. Polylysine ( $M_r > 20\,000$ ) was purchased from Miles-Yeda. Myelin basic protein (MBP) was prepared from bovine brain white matter as described (Cheifetz and Moscarello, 1985).

In the case of DHPC, DPPC with or without ethanol, and 18:10-PC, the lipids were dispersed in a 0.2 mM solution of the probe, prepared in distilled water with or without the desired amount of ethanol, by vigorous vortex mixing at a temperature above the lipid phase transition temperature. Samples with ethanol were prepared in capped tubes and were incubated at 45°C for 5 min to cause them to be in the  $L_\beta$ I phase when cooled to 9°C, the lowest temperature used for measurement of the EPR spectra (Boggs et al., 1989). Nambi et al. (1988) showed that at 2.17 M ethanol the transition temperature from the  $L'_\beta$  to the  $L_\beta$ I phase is about

12°C. The reverse transition from the  $L_\beta$ I to the  $L'_\beta$  phase on cooling is slow. Thus, our samples which were all cooled from 45°C within 1 h or less before measurement of the spectra, are in the  $L_\beta$ I phase at 9°C. DPPC in the absence of ethanol was treated similarly. Just before measurement of the spectra, an equal volume of 32% (w/w) sucrose, as used by Rowe (1982), with or without the desired amount of ethanol, was added and the sample was gently mixed. Preliminary measurements were made in the absence of sucrose and similar results were obtained. However, the sucrose prevented settling out of the lipid suspension during measurement of the EPR spectrum and allowed more quantitative comparisons. The final lipid concentration was either 4 mg/70  $\mu$ l or 6 mg/50  $\mu$ l. The probe solution measured for comparison was treated similarly. Thus, the final probe concentration was 0.1 mM. About 40-50  $\mu$ l of the sample were taken up in a 50  $\mu$ l capillary tube, sealed at one end with Critoseal, and positioned with the sample in the EPR cavity.

PMX-DPPG samples were prepared as described earlier by combining chloroform/methanol solutions of the lipid and PMX in a 5:1 mole ratio, evaporating the solvent and dispersing the PMX-DPPG complex in 0.1 mM TEMPO at a concentration of 4 mg DPPG/70  $\mu$ l (Boggs and Rangaraj, 1985). MBP or polylysine were dissolved in 0.1 mM TEMPO containing 10 mM acetate buffer, 10 mM NaCl, at pH 6, at a concentration of 4 mg/ml (Boggs et al., 1981; Boggs and Moscarello, 1982); 0.5 ml MBP or polylysine solution was added to 2 mg dry DPPG. All samples were dispersed by vigorous vortex mixing at a temperature above the lipid phase transition temperature. None of the samples with DPPG contained sucrose since they formed precipitates in the presence of PMX or proteins. They were centrifuged for 5 min in an Eppendorf bench centrifuge, all but about 25  $\mu$ l of the supernatant were removed, and the pellets were resuspended in the remaining supernatant. The suspension was taken up in a 50  $\mu$ l capillary tube which was sealed at one end with a torch and centrifuged at 2000 rev./min for 10 min. The pellet, which was about 1 cm long in all cases, was positioned in the cavity of the EPR spectrometer.

The presence of the interdigitated or mixed interdigitated  $L_\beta$ I phases, or the non-interdigitated

$L'_\beta$  or  $P'_\beta$  gel phases under the conditions used was confirmed on separate samples containing fatty acid or lipid spin labels as described earlier (Boggs and Rangaraj, 1985; Boggs and Mason, 1986; Boggs et al., 1989). Fatty acid or lipid spin labels with the nitroxide group near the end of the acyl chain are significantly more motionally restricted in the interdigitated phases than in the non-interdigitated phases allowing identification of the phase structure. Interdigitation still occurred in the presence of 16% sucrose and 0.125 M  $\text{NiSO}_4$ .

EPR spectra were measured on a Varian E-104B spectrometer equipped with a Varian temperature controller and a DEC LSI-11 based microcomputer system.

Most lipid samples were also prepared by hydration with 0.2 mM probe containing 0.125 M  $\text{NiSO}_4$ , with or without ethanol, in order to broaden the spectrum of the probe free in solution and thus reveal the spectrum in the lipid bilayer (Polnaszek et al., 1978). An equal volume of sucrose solution also containing  $\text{NiSO}_4$ , with or without ethanol as required, was then added to all samples except those with PMX as described above. The final lipid concentration was 6 mg/50  $\mu\text{l}$ . The broadening effect of  $\text{NiSO}_4$  increased with temperature. At 9°C the residual spectrum of the probe in the aqueous phase in 0.125 M  $\text{NiSO}_4$  was still significant (shown for TEMPO in Fig. 1C, dotted line; peak height was 5% of that in the absence of  $\text{NiSO}_4$ ), particularly when compared to the membrane-bound spectra (e.g. Fig. 1E, dotted line). However, the broadened spectrum was easier to subtract from the spectra of the lipid samples than the unbroadened spectrum of free probe in water. At higher temperatures, broadening of the spectrum due to the probe in the aqueous phase was more complete and the broadened spectrum due to free probe in solution had little effect on the visual appearance of the membrane-bound spectra, except in the case of TEMPONE where less of the probe was membrane-bound. However, subtraction of the spectrum of free probe in  $\text{NiSO}_4$  was still necessary in order to determine the fraction of probe in the membrane phase by integration of the spectra, since the integral of the broadened spectrum is

identical to that of the unbroadened spectrum.

Fractional amounts of the spectrum of the probe in solution in  $\text{NiSO}_4$ , measured at the same temperature as the lipid samples, were subtracted from the spectrum of the probe in the lipid sample in the presence of  $\text{NiSO}_4$  until a realistic appearing spectrum of the probe in the membranous phase was obtained, in which the baseline did not become negative either before or after double integration (Jost and Griffith, 1978; Wang et al., 1989). The resulting membrane spectra in the presence of  $\text{NiSO}_4$  resembled those in its absence in those cases where the membrane spectrum could be sufficiently revealed by subtraction of the spectrum of the free probe; these included TEMPO in DPPC in 2.17 M ethanol and DHPC in the gel phase. In the presence of  $\text{NiSO}_4$ , the original total spectrum and the spectrum of the probe in solution were integrated twice to give the values  $T$  and  $S$ , respectively and the amount of membrane-bound probe,  $M$ , was determined from  $M = T - fS$ , where  $f$  is the fractional amount of the solution spectrum  $S$  subtracted from the total spectrum  $T$  to give the result spectrum  $M$  of the membrane-bound probe. The percentage of probe in the membrane phase,  $m$ , was determined from  $m = M/T \times 100$ . Alternatively the result spectrum  $M$  was also integrated twice to give the value of the membrane-bound probe,  $M$ , directly, and  $m$  was determined as  $M/T \times 100$ . Both methods gave similar results. The endpoint of the subtraction was easier to determine for some samples than others. A range of values for the percentage of membrane-bound probe is given using all result spectra which appeared to be equally valid. This range is wider for those samples where it was difficult to determine the endpoint.

The isotropic hyperfine splitting constant,  $a_o$ , was determined from spectra characteristic of nearly isotropic motion as described earlier (Boggs and Moscarello, 1978).  $\text{NiSO}_4$  also caused significant broadening of the membrane-bound spectra, particularly at higher temperatures. This did not affect the value of the double integral. However, the motional parameter,  $\tau_o$ , or correlation time,  $\tau_c$ , could not be calculated from the width of the center peak and line height ratios.



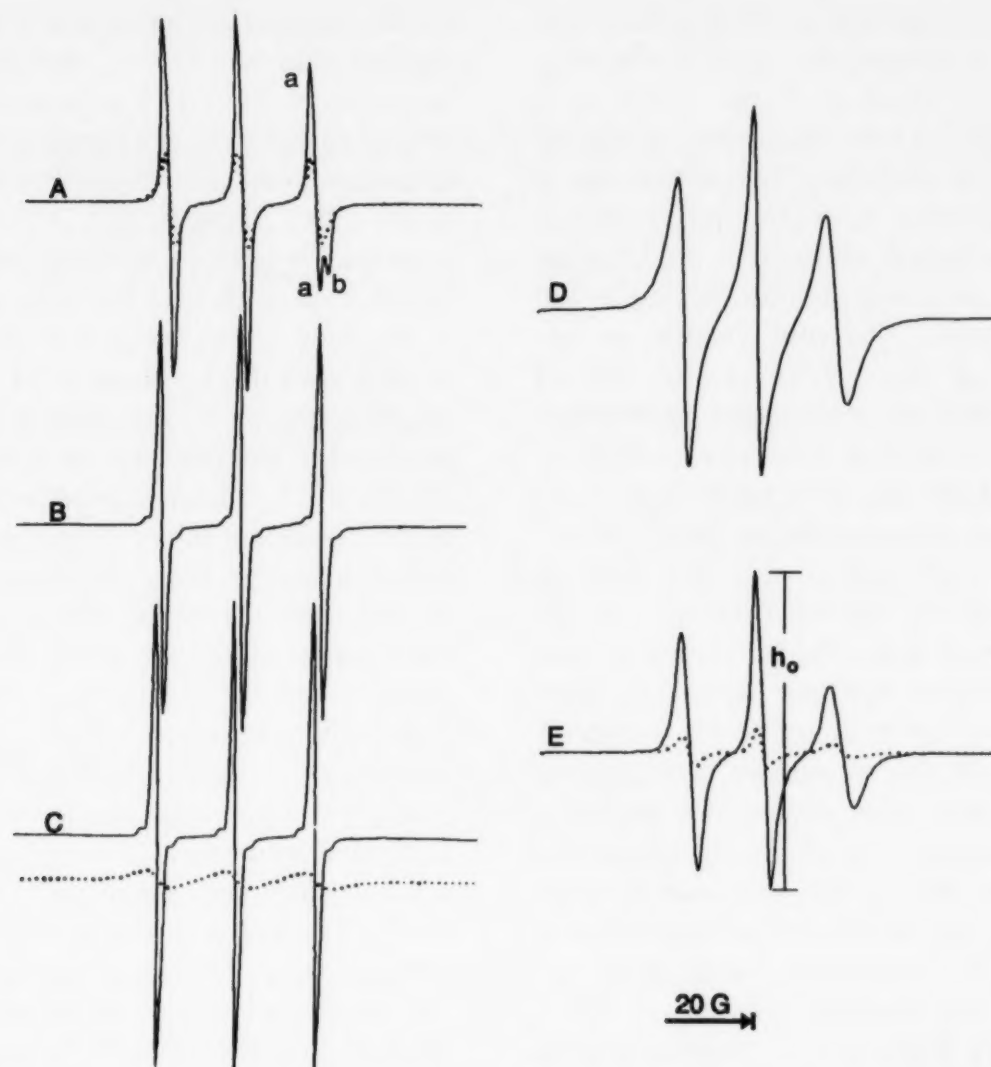


Fig. 1. EPR spectra of 0.1 mM TEMPO in (A) 120 mg/ml DPPC at 54°C in water (solid line) and in 0.125 M  $\text{NiSO}_4$  (dotted line), both plotted out at the same scale; (B) DPPC at 9°C in water, plotted out at the same scale as A; (C) TEMPO free in solution in water (solid line) and in 0.125 M  $\text{NiSO}_4$  (dotted line), both plotted out at the same scale as in A and B; (D) DPPC at 9°C in 0.125 M  $\text{NiSO}_4$ , plotted out amplified 7.8 times relative to other spectra; (E) membrane-bound spectral component of TEMPO in DPPC at 9°C in 0.125 M  $\text{NiSO}_4$  after subtraction of fractional amount of spectrum of TEMPO in solution in  $\text{NiSO}_4$ , plotted out amplified 7.8 times (solid line) and at the same scale as spectra in A, B, and C (dotted line). Peak (a) in (A) is due to membrane-bound TEMPO and peak (b) is due to TEMPO in the aqueous phase. Method of measurement of the height of the center peak,  $h_0$ , of the corrected membrane-bound spectrum is indicated in (E). Both the lipid suspension and the free TEMPO solution contain sucrose.

### 3. Results

#### 3.1. Non-interdigitated phases of DPPC

In the  $P'_\beta$  and  $L_\alpha$  phases of lipids, these probes are located in lower polarity environments which reduces the hyperfine splitting of the spectrum of the lipid-bound probe and allows resolution of the high field peak (a) of the spectrum of membrane-bound probe from that of the probe in aqueous solution as shown in Fig. 1A for TEMPO in the  $L_\alpha$  liquid crystalline phase of DPPC. In Fig. 1A,

the high field peak (b) due to free TEMPO in water can be resolved from that of membrane-bound TEMPO only below the baseline. The corresponding peak above the baseline has been offset by the larger membrane-bound peak (a) below the baseline. However, in the  $L'_\beta$  gel phase of DPPC, the membrane-bound spectrum of these probes is not resolved from that due to the probe in solution, as shown for TEMPO in Fig. 1B. The binding of these probes to the gel phase is revealed only by the fact that their spectra are a little more asymmetric and the height of the cen-

ter peak is reduced compared to the spectra of the probes in solution (shown for TEMPO in Fig. 1C). This is due to binding of the probe to a region of the bilayer where its motion is slowed compared to that in solution, but which has a relatively similar polarity as in the aqueous phase. This has been confirmed using  $\text{Ni}^{2+}$  to broaden the spectrum due to probe in solution and reveal the membrane-bound spectrum (Keith et al., 1977; Polnaszek et al., 1978) or by use of perdeuterated probes to resolve the membrane-bound peaks (Severcan and Cannistraro, 1988).

VHF W-band EPR has also been used to resolve the membrane-bound peaks in the  $P'_\beta$  and  $L_\alpha$  phases of DPPC although it was not able to detect probe in the  $L'_\beta$  phase (Smirnov et al., 1995). However, even when the membrane-bound peaks are distinguished by these techniques, their height is affected by the mobility of the spin label. In order to compare the amount of probe bound to the  $L'_\beta$  and  $L_\beta$  and other phases, it is necessary to resolve the spectrum of probe in the membrane environment from that in the aqueous environment by spectral subtraction and quantitate it by double integration. This has been done for TEMPO in non-interdigitated phases of DPPC (Wang et al., 1993). However, we found it difficult to subtract the sharp spectrum of the probe in solution from the composite spectrum. Therefore, in this study we use  $\text{NiSO}_4$  to broaden the spectrum of the probe in solution before subtracting the spectra.

The spectrum of TEMPO in DPPC at 9°C in  $\text{NiSO}_4$  is shown in Fig. 1D, amplified 7.8 times relative to that in Fig. 1B. At this temperature,  $\text{Ni}^{2+}$  does not completely eliminate the spectrum of TEMPO in the aqueous phase (see Fig. 1C, dotted line). The broadness of the spectrum in Fig. 1D indicates a significant contribution from the broadened spectrum of TEMPO in the aqueous phase. The spectrum of TEMPO in solution in  $\text{NiSO}_4$  in Fig. 1C (dotted line) was subtracted from that in DPPC in Fig. 1D to give the spectrum of TEMPO in the  $L'_\beta$  gel phase of DPPC itself, shown amplified in Fig. 1E (solid line). It is also shown in Fig. 1E (dotted line) plotted at the same scale as the total spectrum in the absence of  $\text{NiSO}_4$  in Fig. 1B. Integration of the membrane-

bound spectral component in Fig. 1E (dotted line) showed that 36–41% of the TEMPO giving the spectrum in Fig. 1B was located in the gel phase bilayer rather than the aqueous phase (Table 1). It is located in an environment only a little less polar than water as indicated by the value of the isotropic hyperfine splitting,  $a_o = 16.7$  G compared to a value of 17.2 G in water (Table 1).

The increase in amount bound to the  $P'_\beta$  phase at 34°C and the  $L_\alpha$  phase at 54°C was determined by integration of the membrane-bound spectra obtained in the presence of  $\text{NiSO}_4$  (shown in Fig. 1A for the  $L_\alpha$  phase, dotted line). The membrane-bound spectrum in the  $L_\alpha$  phase is broader and of lower intensity than the high field membrane-bound peak (a) in the absence of  $\text{NiSO}_4$  due to broadening of the spectrum of membrane-bound TEMPO by  $\text{Ni}^{2+}$ . This may be at least partially due to the accessibility of  $\text{Ni}^{2+}$  to TEMPO in the membrane. In addition, Pali et al. (1992) showed that  $\text{Ni}^{2+}$  could also cause dipolar relaxation of fatty acid spin labels in gel phase lipid bilayers by a solid state mechanism with a  $1/R^3$  dependence on the distance  $R$  of the nitroxide from the bilayer surface. However, this broadening does not affect the integrated value. Integration of the spectra showed that the amount bound increases to 42–64% in the  $P'_\beta$  phase and further to 81% in the  $L_\alpha$  phase (Table 1). TEMPO also is in a significantly more apolar environment in the  $P'_\beta$  phase than in the  $L'_\beta$  phase. Its environment in the  $P'_\beta$  phase is almost as apolar as in the  $L_\alpha$  phase (Table 1). Similar results were found for TEMPONE and DTBN (Table 1) except that their partition coefficients were less than that of TEMPO. The partition coefficient in all three phases decreased in the order TEMPO > DTBN > TEMPONE. The low amount of TEMPONE bound to the  $L'_\beta$  and  $P'_\beta$  phases of DPPC made quantitation in these phases more difficult and less accurate than for the other probes.

### 3.2. DPPC/ethanol

The amount of the probes in the gel phases of DPPC in the presence of 0.87 M and 2.17 M ethanol was then determined. DPPC has been shown by X-ray diffraction to form the non-inter-

Table 1  
Percentage of membrane-bound spin labels, hyperfine splitting,  $a_o$ , and center peak height,  $h_o$ , of spectrum of spin label in different phases of various lipids<sup>a</sup>

Sample	9°C				34°C				54°C			
	Phase	% bound	$a_o$ (G)	$h_o$	Phase	% bound	$a_o$ (G)	$h_o$	Phase	% bound	$a_o$ (G)	$h_o$
TEMPO												
DPPC	$L'_\beta$	<u>36-41</u>	16.69	1.72	$P'_\beta$	<u>42-64</u>	15.93	4.29	$L_\alpha$	<u>81-82</u>	15.79	5.13
DPPC/0.87 M EtOH	$L'_\beta$	<u>50-61</u>	16.79	1.88	$P'_\beta$	<u>62-66</u>	15.93	2.66	$L_\alpha$	83	15.79	3.71
DPPC/2.17 M EtOH	$L'_\beta$	<u>74-78</u>	16.79	3.12	$L'_\beta$	<u>62-77</u>	16.28	1.69	$L_\alpha$	76	15.79	2.69
DPPG/PMX	$L'_\beta$	<u>68-74</u>	<sup>c</sup>	2.85	$L'_\beta$	<u>58-85</u>	16.14	4.26	$L_\alpha$	75	15.73	4.02
DHPC	$L'_\beta$	<u>66-76</u>	<sup>c</sup>	3.59	$P'_\beta$	<u>69-73</u>	15.93	3.64	$L_\alpha$	79	15.93	3.73
DTNB												
DPPC	$L'_\beta$	<u>21-34</u>	16.43	0.53	$P'_\beta$	<u>17-34</u>	15.69	0.43	$L_\alpha$	<u>59-70</u>	15.54	3.42
DPPC/0.87 M EtOH	$L'_\beta$	38	16.69	0.78	$P'_\beta$	39	15.74	2.38	$L_\alpha$	<u>64-73</u>	15.58	3.52
DPPC/2.17 M EtOH	$L'_\beta$	<u>54-66</u>	16.48	1.97	$L'_\beta$	<u>58-64</u>	16.03	1.05	$L_\alpha$	<u>66-71</u>	15.64	2.66
TEMPONE												
DPPC	$L'_\beta$	<u>5-15</u>	15.24	0.21	$P'_\beta$	<u>5-15</u>	14.94	0.12	$L_\alpha$	<u>37-41</u>	14.74	1.71
DPPC/0.87 M EtOH	$L'_\beta$	<u>21-24</u>	15.89	0.49	$P'_\beta$	<u>26-30</u>	14.99	0.65	$L_\alpha$	<u>36-40</u>	14.89	1.26
DPPC/2.17 M EtOH	$L'_\beta$	<u>52-56</u>	15.79	1.49	$L'_\beta$	<u>53-57</u>	15.54	0.71	$L_\alpha$	<u>41-44</u>	14.93	0.83

<sup>a</sup>Determined from spectra in the presence of NiSO<sub>4</sub> after subtraction of spectrum of free spin label in NiSO<sub>4</sub>. Range of values given is for all result spectra which appeared valid. Hyperfine splitting  $a_o$  of free TEMPO in water is 17.20 G, of DTNB is 17.08 G, and of TEMPONE is 15.98 G. Center peak height,  $h_o$  (in arbitrary units), was determined for result spectrum giving % bound value which is underlined. If no value is underlined  $h_o$  was determined for spectrum giving a value in the middle of the range given.  $h_o$  increases with increased amount of bound TEMPO and with increase in mobility, but decreases with increased broadening by Ni<sup>2+</sup>. The spectrum of TEMPO in solution is broadened much more than that of membrane-bound TEMPO, but some broadening of the latter also occurs, especially at higher temperatures. The same lipid concentration is present in all cases except for DPPG/PMX.

<sup>b</sup>Measured at 29°C.

<sup>c</sup> $a_o$  was not calculated, as the motion appeared to be too slow ( $\tau_o > 10^{-9}$  s) (Schreier et al., 1978). EtOH, ethanol.



digitated  $L'_\beta$  gel phase at the lower ethanol concentration and an interdigitated  $L_\beta$ I gel phase at the higher concentration (Simon and McIntosh, 1984). In the  $L'_\beta$  gel phase in 0.87 M ethanol, the spectra (shown for TEMPO in Fig. 2A) appeared relatively similar to that in the absence of ethanol. The spectrum of TEMPO located in the membrane phase in the presence of  $\text{NiSO}_4$  at 9°C (after subtraction of the  $\text{Ni}^{2+}$ -broadened spectrum of TEMPO in the aqueous phase) is shown amplified in Fig. 2B (solid line), and also plotted at the same scale as that in Fig. 2A (dotted line in Fig. 2B). It is very similar to that in DPPC without ethanol (Fig. 1E), although  $a_o$  is larger (Table 1) indicating that TEMPO is in a slightly more polar environment. Integration of the spectrum indicated that the amount bound to DPPC in 0.87 M ethanol is greater than in the absence of ethanol (Table 1). As in the absence of ethanol, TEMPO is in a more apolar environment in the  $P'_\beta$  phase and the amount bound is a little greater than in the  $L'_\beta$  phase. In the  $L_\alpha$  phase the amount bound is similar to DPPC in the absence of ethanol.

In 2.17 M ethanol, the spectrum of TEMPO in the  $L_\beta$ I interdigitated gel phase of DPPC (Fig. 2C) is significantly different from the non-interdigitated  $L'_\beta$  gel phase bilayers at 0 and 0.87 M ethanol. Peaks or shoulders due to membrane-bound TEMPO could be distinguished from those due to TEMPO in the aqueous phase on both the low and high field sides. The membrane-bound spectrum in the presence of  $\text{NiSO}_4$  is shown in Fig. 2D. Interestingly, the polarity of the environment of TEMPO in the interdigitated bilayer at 9°C was similar to that in the non-interdigitated bilayer of DPPC, particularly that in the presence of 0.87 M ethanol (Table 1). However, integration of the spectrum showed that the amount of TEMPO bound to DPPC at 2.17 M was significantly greater than at 0.87 M (Table 1).

At 34°C it was in a more apolar environment than at 9°C but not as apolar as in the non-interdigitated bilayers. Greater broadening by  $\text{NiSO}_4$  occurred at this temperature for TEMPO in the interdigitated bilayer than in the non-interdigitated bilayers. This is evident from the decrease in peak height of the membrane-bound spectrum,  $h_o$ , on increasing the temperature from 9°C to 34°C

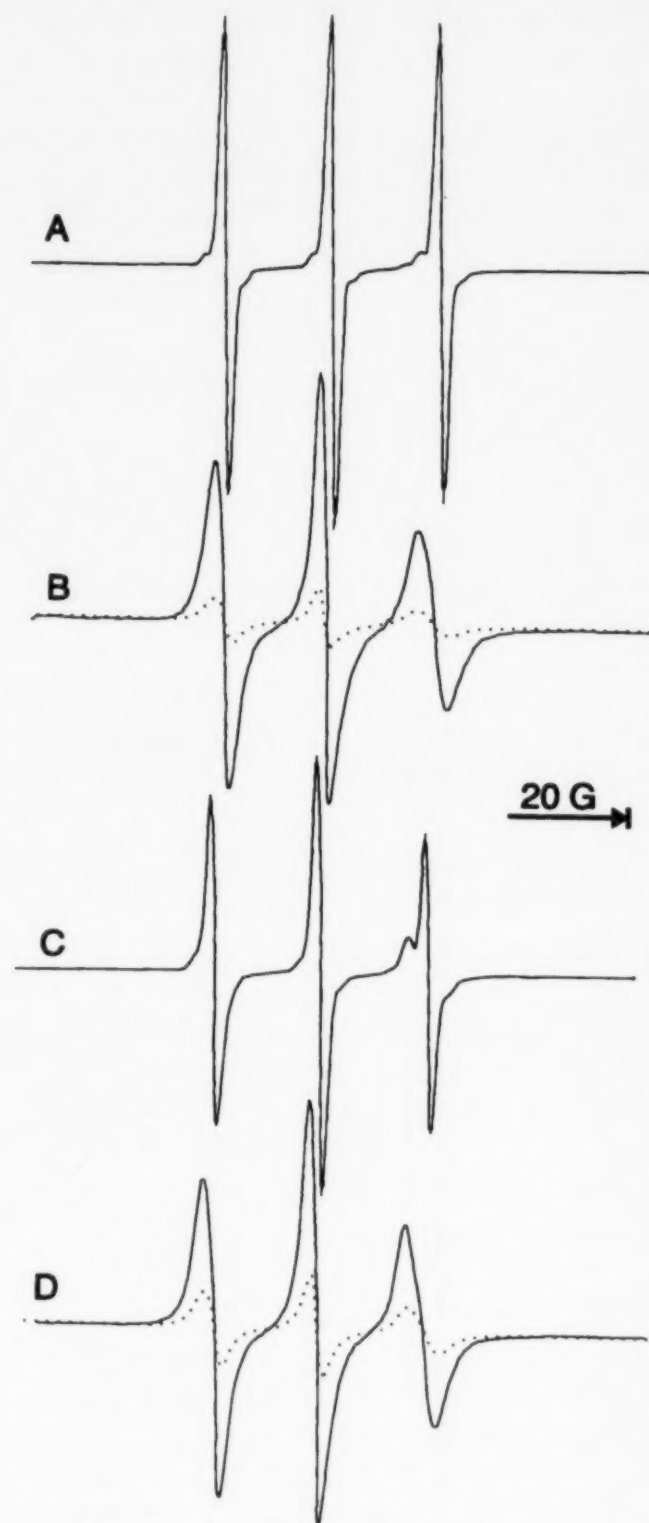


Fig. 2. EPR spectra of TEMPO at 9°C in 120 mg/ml DPPC suspended in water containing sucrose and (A) 0.87 M ethanol; (B) 0.87 M ethanol and 0.125 M  $\text{NiSO}_4$ , after subtraction of fractional amount of spectrum of TEMPO in  $\text{NiSO}_4$ . Membrane-bound spectrum is plotted amplified 9.5 times (solid line) and at the same scale as in A (dotted line); (C) 2.17 M ethanol, plotted at the same scale as in A; (D) 2.17 M ethanol and 0.125 M  $\text{NiSO}_4$ , after subtraction of fractional amount of spectrum of TEMPO in  $\text{NiSO}_4$ . Membrane-bound spectrum is plotted amplified 9.5 times (solid line) and at the same scale as in A and C (dotted line).



at 2.17 M in contrast to the increase in  $h_o$  which occurs at 0 and 0.87 M ethanol (Table 1). This decrease is not due to a decrease in the amount bound since integration shows that a similar amount is bound at both temperatures (Table 1). Thus membrane-bound TEMPO may be more accessible to  $\text{Ni}^{2+}$  at 34°C in the  $L_{\beta}$ I phase than in the  $P'_{\beta}$  phase. Broadening of the membrane-bound spectrum continued to increase with increase in  $\text{NiSO}_4$  concentration at concentrations where broadening of the spectrum of TEMPO in the aqueous phase was nearly complete (not shown). This indicates that broadening of the spectrum of membrane-bound TEMPO was not due to exchange with TEMPO in solution, since in that case it should have been affected in the same way by  $\text{Ni}^{2+}$  concentration as TEMPO in the aqueous phase (Kulikov and Likhtenstein, 1977). At lower temperatures, accessibility of  $\text{Ni}^{2+}$  to membrane-bound TEMPO may decrease since the height increased on cooling back to 9°C. This increase may also be due to the decreased ability of  $\text{Ni}^{2+}$  to cause dipolar relaxation at lower temperatures where the mobility is lower.

In the  $L_{\alpha}$  phase, the polarity of the environment and the amount bound were not significantly affected by ethanol up to 2.17 M. At 2.17 M ethanol, the amount of bound TEMPO did not increase further during the  $L_{\beta}$ I to  $L_{\alpha}$  phase transition. If TEMPO behaves like ethanol in the interdigitated gel phase, the lack of increase in amount bound to the  $L_{\alpha}$  phase compared to the  $L_{\beta}$ I phase is to be expected since 2.17 M ethanol has no effect on the phase transition temperature. However, at 0.87 M where ethanol causes a decrease in the phase transition temperature, the amount of membrane-bound TEMPO increased during the  $P'_{\beta}$  to  $L_{\alpha}$  phase transition. At a concentration of 10–50 mM, TEMPO behaves like ethanol and similar drugs in that it causes a decrease of 2–7°C in the phase transition temperature of DPPC (determined by differential scanning calorimetry, not shown), although no evidence has been found that it causes interdigitation. Thus, at low concentrations, in the presence of high concentrations of ethanol, its solubility in the bilayer could mimic that of ethanol.

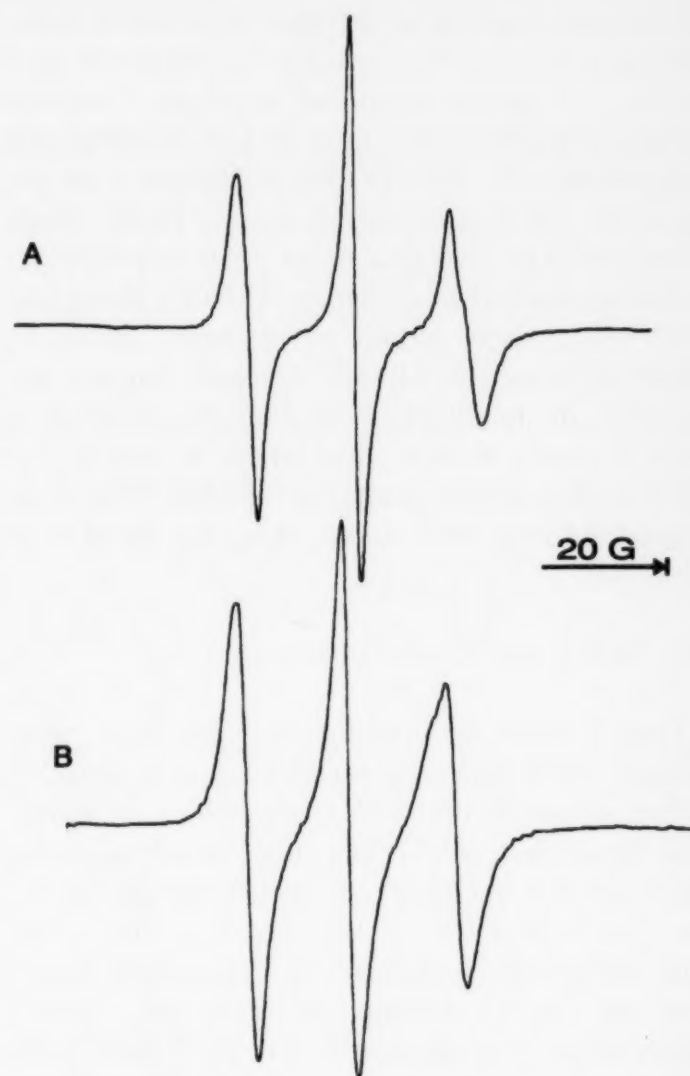


Fig. 3. Membrane-bound EPR spectra of (A) DTBN and (B) TEMPONE at 9°C in DPPC suspended in water containing sucrose, 0.125 M  $\text{NiSO}_4$  and 2.17 M ethanol after subtraction of fractional amounts of spectra of spin labels in  $\text{NiSO}_4$ .

Similar results were found for TEMPONE and DTBN. Their membrane-bound spectra in the  $L_{\beta}$ I phase of DPPC in 2.17 M ethanol, obtained in the presence of  $\text{Ni}^{2+}$  after subtraction of the  $\text{Ni}^{2+}$ -broadened spectra of the probes in solution, are shown in Fig. 3A and Fig. 3B, respectively. The amount of these probes bound to the  $L_{\beta}$ I phase, 52–66%, was significantly greater than to the  $L'_{\beta}$  or  $P'_{\beta}$  phases but it was less than for TEMPO (Table 1). Even though 52% of the TEMPONE was bound to the  $L_{\beta}$ I phase it had no detectable effect on the spectrum in the absence of  $\text{Ni}^{2+}$  except for a further increase in asymmetry and reduction of the height of the center line of the spectrum (not shown). A membrane-bound peak to the left of the high field

aqueous peak could be detected for DTBN, however (not shown). The amount of DTBN bound to the  $L_{\beta}$ I phase remained relatively constant through the phase transition as for TEMPO, but interestingly, for TEMPONE it decreased on going from the  $L_{\beta}$ I phase to the  $L_{\alpha}$  phase. Both probes were located in a more polar environment in the  $L'_{\beta}$  and  $L_{\beta}$ I phases than in the  $P'_{\beta}$  phase and went into a more apolar environment in the  $L_{\alpha}$  phase as found for TEMPO. Greater broadening by  $Ni^{2+}$  of membrane-bound probe occurred in the  $L_{\beta}$ I phase at 34°C than in the  $P'_{\beta}$  phase and the broadening was greater for TEMPONE in all phases at 34°C and above than for DTBN or TEMPO.

### 3.3. DHPC and 18:10-PC phases

DHPC forms an interdigitated gel phase up to around 35°C where it undergoes a  $L_{\beta}$ I to  $P'_{\beta}$  phase transition (Ruocco et al., 1985). A significant fraction of TEMPO is also dissolved in the interdigitated gel phase of DHPC as shown for the spectrum at 9°C in Fig. 4A. The low, center and high field peaks of the membrane-bound spectrum can be distinguished from the aqueous spectrum even more clearly than for DPPC in the presence of 2.17 M ethanol. The membrane-bound spectrum obtained in the presence of  $NiSO_4$  at this temperature (Fig. 4B) indicates that TEMPO has more anisotropic motion in the interdigitated gel phase of DHPC than in that of DPPC/ethanol.

Integration of the membrane-bound spectrum showed that the amount bound was greater than to non-interdigitated DPPC and similar to that in the interdigitated bilayer of DPPC induced by ethanol. At temperatures above 30°C, where DHPC forms a non-interdigitated  $P'_{\beta}$  phase (Ruocco et al., 1985), the spectrum in the presence of  $NiSO_4$  is more isotropic (Fig. 4C). There was little or no difference in binding of TEMPO to the  $L_{\beta}$ I,  $P'_{\beta}$ , or  $L_{\alpha}$  phases as found for DPPC in ethanol (Table 1). The  $a_o$  value was similar in all phases (Table 1). At 34°C, the height  $h_o$  was greater in the  $P'_{\beta}$  phase compared to the  $L_{\beta}$ I phase of DPPC in 2.17 M ethanol (Table 1), indicating less  $Ni^{2+}$  broadening in the  $P'_{\beta}$  phase than in the  $L_{\beta}$ I phase.

No membrane-bound component could be detected in spectra of TEMPO in the mixed interdigitated (triple chain) gel phase of 18:10-PC (Hui et



Fig. 4. EPR spectra of TEMPO in 57 mg/ml DHPC suspended (A) in water containing sucrose at 9°C; (B) in water containing sucrose and 0.125 M  $NiSO_4$  at 9°C, plotted amplified 5.8 times relative to A; (C) as in B at 34°C. Spectrum shown in (B) was not corrected by subtraction of spectrum of TEMPO in  $NiSO_4$ . This correction had only small effects on the lineshape of the spectrum, although it reduced the height by about 4% (center peak). However, the spectrum shown in (C) was corrected.

al., 1984) at 9°C in the absence of  $\text{NiSO}_4$  although the spectrum was a little more asymmetric than that in water as found for the non-interdigitated  $L'_\beta$  phase of DPPC, indicating interaction of some of the probe with the lipid. Since it appeared to be much less than in the double chain interdigitated gel phases, this lipid was not examined in the presence of  $\text{NiSO}_4$ .

### 3.4. DPPG/PMX, DPPG/MBP, and DPPG/polylysine bilayers

Polymyxin B (PMX) was shown to cause interdigitation of DPPG using X-ray diffraction by Ranck and Tocanne (1982). The phase transition temperature of the interdigitated bilayer is similar to or a little less than that of DPPG. The spectrum of TEMPO in the complex of DPPG-PMX (5:1 m/m) at 9°C is shown in Fig. 5A and shows that TEMPO is dissolved in the interdigitated gel phase of this lipid also. As for DHPC, the membrane-bound spectrum can be detected at the high, center, and low field positions, but it is broader than that found for DHPC. The membrane-bound spectrum obtained in the presence of  $\text{NiSO}_4$  (Fig. 5B) shows that TEMPO has slow motion in DPPG/PMX. The motion is more anisotropic than in DPPC but less than in DHPC. Integration of the membrane-bound spectra in DPPG/PMX in the presence of  $\text{NiSO}_4$  showed that the amount bound at 9°C was similar to the other  $L_\beta I$  phases and it did not increase with temperature (Table 1). The  $\text{Ni}^{2+}$  broadening of membrane-bound TEMPO at 29°C was less than in the other  $L_\beta I$  phases since  $h_o$  increased from its value at 9°C.

A similar spectrum to that in Fig. 5A is obtained for the complex of MBP with DPPG at pH 6 (Fig. 5C). This complex is also thought to be interdigitated since it causes motional restriction of lipid and fatty acid spin labels in which the nitroxide group is near the terminal methyl, similar to the behavior of other interdigitated bilayers (Boggs et al., 1981, 1989; Boggs and Moscarello, 1982). In contrast, no membrane-bound component could be detected in the spectrum of TEMPO added to the complex of polylysine-DPPG (not shown). The spectrum resembled that

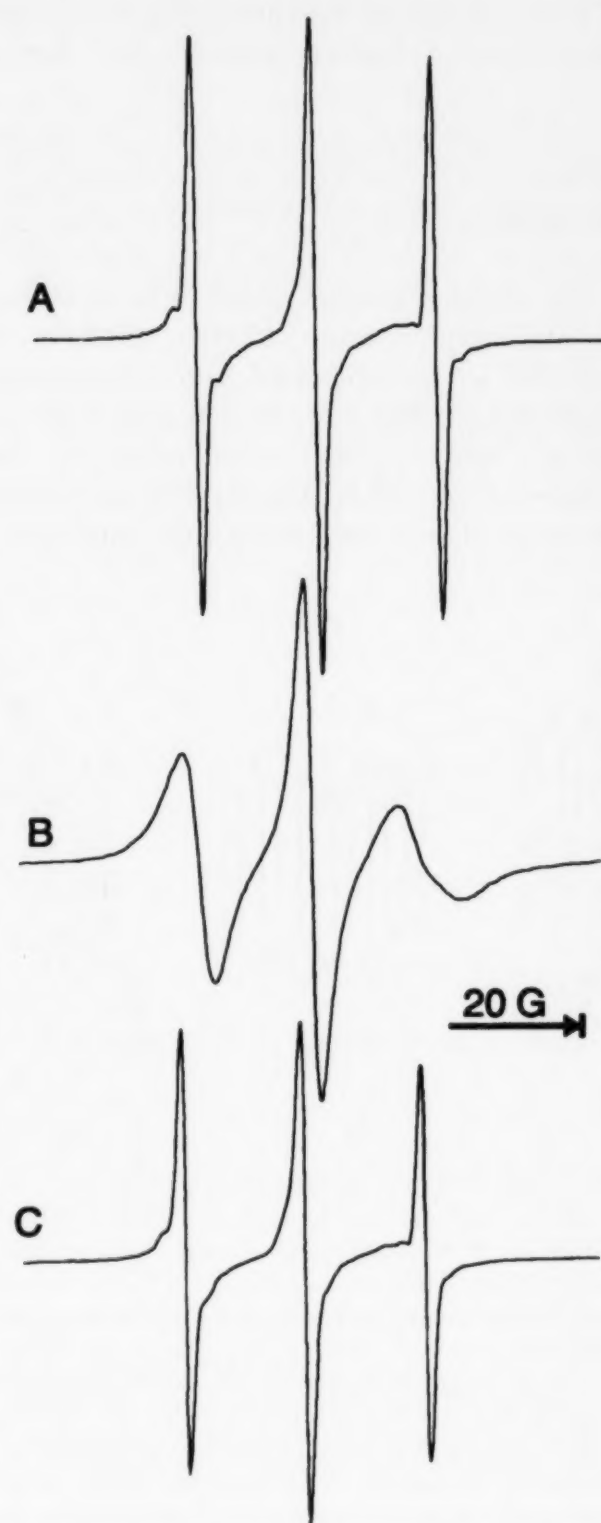


Fig. 5. EPR spectra of TEMPO at 9°C in (A) DPPG/PMX 5:1 (m/m) in buffer without  $\text{NiSO}_4$ ; (B) DPPG/PMX in buffer containing 0.125 M  $\text{NiSO}_4$  after subtraction of fractional amount of spectrum of TEMPO in  $\text{NiSO}_4$ , plotted amplified by an arbitrary amount relative to A; (C) DPPG/MBP in buffer without  $\text{NiSO}_4$ . Pelleted samples were used and the amount of material present is not known. However, the size of the pellets in the EPR capillary tube was similar in all cases.



of TEMPO in water. Polylysine does not cause interdigitation of DPPG (Carrier and Pezolet, 1986).

#### 4. Discussion

In this study we have been able to directly detect membrane-bound TEMPO, DTBN, and TEMPONE in interdigitated and non-interdigitated gel phases. We have shown that these amphipathic spin labels can partition into interdigitated gel phase bilayers formed of symmetric lipids significantly more than into non-in-

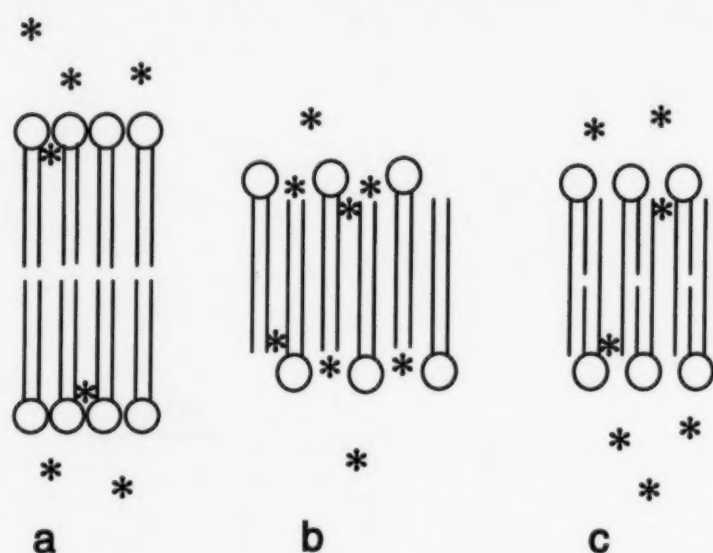


Fig. 6. Diagrammatic representation of different types of gel phase bilayers indicating the location of a small amphipathic spin label or other molecule (\*) in (a) non-interdigitated bilayer; (b) fully interdigitated double-chain bilayer formed by symmetric chain length lipids; (c) triple chain mixed interdigitated bilayer formed by asymmetric chain length lipids. A small amount of the spin label (\*) can partition into the gel phase of the non-interdigitated bilayer (a) or the mixed interdigitated bilayer (c) near the apolar/polar interface. Although not depicted in the model, the hydrocarbon chains below the interface region are probably too closely packed in all three gel phase bilayers to allow much spin label to partition into the hydrophobic region of the acyl chains. In the double chain interdigitated bilayer (c) additional spin label (\*) can partition into the larger space created at the interface region by separation of the lipid molecules by interdigitating lipid molecules from the other side of the bilayer. Insufficient space is available in the triple chain interdigitated bilayer to permit this additional binding of molecules of the size of the spin labels used. Amphipathic molecules which induce interdigitation of symmetric chain length lipids, such as ethanol, are probably located in the same regions as indicated by the \*.

terdigitated gel phase bilayers as depicted in Fig. 6. This is true for lipids where interdigitation is induced by amphipathic compounds or proteins and also for the symmetric lipid DHPC which spontaneously forms interdigitated bilayers. This increased solubility of other substances in the interdigitated bilayer is consistent with the increase in the  $L_{\beta}I$  to the  $P'_{\beta}$  phase transition temperature of DHPC caused by ethanol which indicates that it interacts preferentially with the interdigitated phase relative to the  $P'_{\beta}$  phase (Veiro et al., 1988). Thus, if interdigitated gel phase bilayers can form in natural membranes, they could allow a variety of other substances to partition into them. This might result in a greater permeability than for non-interdigitated bilayers as shown by Zeng et al. (1993) for the permeability of protons through interdigitated DPPC-ethanol bilayers. Komatsu and Okada (1995) recently showed that the permeability of the  $L_{\beta}I$  phase of DPPC to calcein was greater than that of the  $L'_{\beta}$  phase and similar to that of the  $L_{\alpha}$  phase of egg PC. The greater permeability may be partly due to the decreased bilayer thickness and, in the case of charged substances, to the decreased surface charge density of the interdigitated bilayer. The present results indicate that for amphipathic substances, increased binding to the interdigitated bilayer might also contribute to an increase in permeability.

The interdigitated bilayer might be expected to accommodate amphipathic substances better than non-interdigitated bilayers since there is a greater molecular area per lipid head group in the interdigitated bilayer, provided that they are small enough to fit in this region (Fig. 6b). TEMPO, TEMPONE, and DTBN all were small enough to do so. These substances are expected to locate near the apolar/polar interface, i.e. in the same site occupied by substances which cause interdigitation. This was supported by the high polarity of the environment of these probes in interdigitated bilayers at low temperatures. By measuring the thickness of the interdigitated bilayer in the presence of different chain length alcohols by X-ray diffraction, Adachi et al. (1995) showed that ethanol was oriented parallel to the acyl chains in the apolar/polar interface of the interdigitated

bilayer with two ethanol molecules packed end-to-end with the two fatty acid chains of each lipid molecule. On the other hand, large molecules such as prodan which are too big to fit in this space and not long enough to insert between the acyl chains and interact with them by van der Waals interactions are excluded from the interdigitated bilayer (Zeng and Chong, 1995). Compounds with long acyl chains, however, such as laurdan (Zeng and Chong, 1995) or fatty acid spin labels (Boggs and Moscarello, 1982; Boggs et al., 1989), which can insert between the acyl chains and interact with them by van der Waals interactions are not excluded.

The concentration of TEMPO and DTBN in the interdigitated phase did not change significantly with temperature and did not increase in the  $L_\alpha$  phase. This is to be expected for interdigitated bilayers such as DPPC/ethanol and DPPG/PMX whose phase transition temperatures are similar to that of non-interdigitated bilayers, if TEMPO behaves like the substance inducing the interdigitation. However, the interdigitated bilayer of DPPC induced by butanol has a lower phase transition temperature than DPPC alone. Consistent with this, butanol was found to have a lower partition coefficient in the interdigitated bilayer than in the  $L_\alpha$  phase (Zhang and Rowe, 1992). Although the partition coefficient of butanol in the non-interdigitated  $L'_\beta$  phase could not be measured, it must have been less than 50% of that in the  $L_\beta$ I phase, in agreement with the relative differences in TEMPO binding to the two phases found here.

In contrast to butanol, TEMPO, and DTBN, the concentration of TEMPONE was less in the  $L_\alpha$  phase than in the interdigitated phase. TEMPONE is more polar than TEMPO and would preferentially locate in the aqueous phase or in a more polar environment in the bilayer if sufficient space were available for it. The double chain interdigitated  $L_\beta$ I phase, with more space available between the lipid polar head groups at the apolar/polar interface than the other phases, can accommodate TEMPONE better than the  $L_\alpha$  phase despite the greater fluidity of the latter.

At low temperatures below the premelt transition of DPPC, the polarity of the environment of

these probes in interdigitated bilayers of DPPC/ethanol is similar to that of non-interdigitated gel phase bilayers suggesting that they are located in the same region of the bilayer when interdigitation is induced by ethanol as when it is not interdigitated. This is probably close to the apolar/polar interface region over the terminal methyl groups of interdigitated lipid molecules from the opposite side of the bilayer (Fig. 6).

At higher temperatures, the probes are located in a more apolar environment in both non-interdigitated and interdigitated gel phase bilayers. It is important to note, however, that they are in a more polar environment in the interdigitated bilayers in all cases at 34°C than in the non-interdigitated bilayer. Thus, the location of the probes in interdigitated bilayers remains more constant with temperature up to the gel to liquid crystalline phase transition temperature, than in non-interdigitated bilayers where a transition to the  $P'_\beta$  phase occurs. The presence of the interdigitated acyl chains from lipid on the other side of the bilayer may inhibit the movement of the probes to sites deeper within the bilayer. Furthermore, they prefer an amphipathic location if sufficient space is available for them. The greater broadening of the spectra of membrane-bound TEMPO and DTBN by  $\text{NiSO}_4$  at 34°C in the  $L_\beta$ I phases compared to the  $P'_\beta$  phases indicates greater accessibility of  $\text{Ni}^{2+}$  to these probes in the former than in the latter. This is also consistent with a location close to the interfacial region in the  $L_\beta$ I phase. The only exception was the  $L_\beta$ I phase of the DPPG/PMX complex. In this case, the presence of PMX may restrict accessibility of  $\text{Ni}^{2+}$  to TEMPO. However, TEMPONE was broadened more than the other probes even in the  $P'_\beta$  and  $L_\alpha$  phases indicating that it may be located closer to the apolar/polar interface in these phases than the other probes consistent with its greater water solubility.

In the triple chain mixed interdigitated gel phase bilayer of the asymmetric lipid 18:10-PC, however, TEMPO binding was no greater than to the non-interdigitated gel phase bilayers, suggesting that mixed interdigitated bilayers may not allow other substances to partition into them as readily as double chain interdigitated bilayers



formed of symmetric lipids. This is probably due to the smaller surface area per molecule for asymmetric lipids in the triple chain mixed interdigitated bilayer (Fig. 6c) compared to symmetric lipids in the double chain interdigitated bilayer (Fig. 6b). In the former, the lipid molecules are separated from each other by only one acyl chain of a lipid molecule on the other side of the bilayer, while in the latter bilayer, lipid molecules are separated by two acyl chains.

The increased partitioning of these small amphipathic spin labels into interdigitated bilayers formed by symmetric lipids represents another way to detect these bilayers in addition to X-ray diffraction (Ranck and Tocanne, 1982), fatty acid spin labels (Boggs et al., 1981, 1989), and fluorescent probes (Nambi et al., 1988; Zeng and Chong, 1995). We have shown that a nitroxide group on the 16th carbon of stearic acid can be used to diagnose the structure of most interdigitated bilayers of symmetric and asymmetric lipids since it is more motionally restricted at low temperatures in interdigitated bilayers than in non-interdigitated bilayers. However, some interdigitated bilayers such as DHPC and DPPC/ethanol are exceptions to this (Boggs et al., 1989). Use of other spin labels indicated that these latter bilayers were more disordered than the others. Higher temperatures and phospholipid spin labels rather than fatty acid spin labels had to be used in order to clearly distinguish them from non-interdigitated bilayers (Boggs et al., 1989). However, the present study shows that TEMPO binds as significantly to DPPC/ethanol and DHPC as to the other interdigitated bilayers indicating that it may be a more universal spin probe for diagnosis of interdigitation than fatty acid spin labels. The similar behavior of TEMPO in bilayers of DPPG/MBP as in the interdigitated bilayers of DPPC/ethanol, DHPC, and DPPG/PMX, in contrast to its behavior in DPPG with polylysine, supports our earlier studies using fatty acid spin labels, which indicated that MBP induced interdigitation of DPPG (Boggs et al., 1981; Boggs and Moscarello, 1982).

## Acknowledgements

This work was supported by a grant from the Medical Research Council of Canada to JMB. We thank Dr. J.T. Mason for a generous gift of 18:10-PC.

## References

- Adachi, T., Takahashi, H., Ohki, K. and Hatta, I. (1995) Interdigitated structure of phospholipid-alcohol systems studied by X-ray diffraction. *Biophys. J.* 68, 1850–1855.
- Boggs, J.M. and Mason, J.T. (1986) Calorimetric and fatty acid spin label study of subgel and interdigitated gel phases formed by asymmetric phosphatidylcholines. *Biochim. Biophys. Acta* 863, 231–242.
- Boggs, J.M. and Moscarello, M.A. (1978) Effects of basic protein from human CNS myelin on lipid bilayer structure. *J. Membr. Biol.* 39, 75–96.
- Boggs, J.M. and Moscarello, M.A. (1982) Interdigitation of fatty acid chains of dipalmitoylphosphatidylglycerol due to intercalation of myelin basic protein. *Biophys. J.* 37, 57–59.
- Boggs, J.M. and Rangaraj, G. (1985) Phase transitions and fatty acid spin label behavior in interdigitated lipid phases induced by glycerol and polymyxin B. *Biochim. Biophys. Acta* 816, 221–233.
- Boggs, J.M., Stamp, D. and Moscarello, M.A. (1981) Interaction of myelin basic protein with dipalmitoylphosphatidylglycerol: dependence on the lipid phase and investigation of a metastable state. *Biochemistry* 20, 6066–6072.
- Boggs, J.M., Rangaraj, G. and Watts, A. (1989) Behavior of a number of spin labels in a variety of interdigitated lipid bilayers. *Biochim. Biophys. Acta* 981, 243–253.
- Carrier, D. and Pezolet, M. (1986) Investigation of polylysine-dipalmitoylphosphatidylglycerol interactions in model membranes. *Biochemistry* 25, 4167–4174.
- Cheifetz, S. and Moscarello, M.A. (1985) Effect of bovine basic protein charge microheterogeneity on protein-induced aggregation of unilamellar vesicles containing a mixture of acidic and neutral phospholipids. *Biochemistry* 24, 1909–1914.
- Griffith, O.H. and Jost, P.C. (1976) Lipid spin labels in biological membranes, in L. Berliner (ed.), *Spin Labeling, Theory and Applications*. Academic Press, New York, pp. 453–523.
- Herold, L.L., Rowe, E.S. and Khalifah, R.G. (1987) <sup>13</sup>C-NMR and spectrophotometric studies of alcohol-lipid interactions. *Chem. Phys. Lipids* 43, 215–225.
- Hubbell, W.L. and McConnell, H.M. (1968) Spin label studies of the excitable membranes of nerve and muscle. *Proc. Natl. Acad. Sci. USA* 61, 12–16.
- Hui, S.W., Mason, J.T. and Huang, C.-H. (1984) Acyl chain interdigitation in saturated mixed-chain phosphatidylcholine bilayer dispersions. *Biochemistry* 23, 5570–5577.

- Jost, P.C. and Griffith, O.H. (1978) The spin-labeling technique. *Methods Enzymol.* 49, 369–418.
- Kaminoh, Y., Tashiro, C., Kamaya, H. and Ueda, I. (1988) Depression of phase-transition temperature by anesthetics: nonzero solid membrane binding. *Biochim. Biophys. Acta* 946, 215–220.
- Keith, A.D., Snipes, W. and Chapman, D. (1977) Spin label studies on the aqueous regions of phospholipid multilayers. *Biochemistry* 16, 634–641.
- Komatsu, H. and Okada, S. (1995) Increased permeability of phase-separated liposomal membranes with mixtures of ethanol-induced interdigitated and non-interdigitated structures. *Biochim. Biophys. Acta* 1237, 169–175.
- Kulikov, A.V. and Likhtenstein, G.I. (1977) The use of spin relaxation phenomena in the investigation of the structure of model and biological systems by the method of spin labels. *Adv. Mol. Relax. Interact. Processes* 10, 47–79.
- McDaniel, R.V., McIntosh, T.J. and Simon, S.A. (1983) Induction of an interdigitated gel phase in fully hydrated phosphatidylcholine bilayers. *Biochim. Biophys. Acta* 731, 97–108.
- Nagel, N.E., Cevc, G. and Kirchner, S. (1992) The mechanism of the solute-induced chain interdigitation in phosphatidylcholine vesicles and characterization of the isothermal phase transitions by means of dynamic light scattering. *Biochim. Biophys. Acta* 1111, 263–269.
- Nambi, P., Rowe, E.S. and McIntosh, T.J. (1988) Studies of the ethanol-induced interdigitated gel phase in phosphatidylcholines using the fluorophore 1,6-diphenyl-1,3,5-hexatriene. *Biochemistry* 27, 9175–9182.
- Pali, T., Bartucci, R., Horvath, L.I. and Marsh, D. (1992) Distance measurements using paramagnetic ion-induced relaxation in the saturation transfer electron spin resonance of spin-labeled molecules. *Biophys. J.* 61, 1595–1602.
- Polnaszek, C.F., Schreier, S., Butler, K.W. and Smith, I.C.P. (1978) Analysis of the factors determining the EPR spectra of spin probes that partition between aqueous and lipid phases. *J. Am. Chem. Soc.* 100, 8223–8232.
- Ranck, J.L. and Tocanne, J.F. (1982) Polymyxin B induces interdigitation in dipalmitoylphosphatidylglycerol lamellar phase with stiff hydrocarbon chains. *FEBS Lett.* 143, 175–178.
- Rowe, E.S. (1982) The effects of ethanol on the thermotropic properties of dipalmitoylphosphatidylcholine. *Mol. Pharmacol.* 22, 133–139.
- Rowe, E.S. (1983) Lipid chain length and temperature dependence of ethanol-phosphatidylcholine interactions. *Biochemistry* 22, 3299–3305.
- Ruocco, M.J., Siminovich, D.J. and Griffin, R.G. (1985) Comparative study of the gel phases of ether- and ester-linked phosphatidylcholines. *Biochemistry* 24, 2406–2411.
- Schreier, S., Polnaszek, C.F. and Smith, I.C.P. (1978) Spin labels in membranes: Problems in practice. *Biochem. Biophys. Acta* 515, 395–436.
- Severcan, F. and Cannistraro, S. (1988) Use of PDDTBN spin probe in partition studies of lipid membranes. *Chem. Phys. Lipids* 153, 263–267.
- Shimshick, E.J. and McConnell, H.M. (1973) Lateral phase separation in phospholipid membranes. *Biochemistry* 12, 2351–60.
- Simon, S.A. and McIntosh, T.J. (1984) Interdigitated hydrocarbon chain packing causes the biphasic transition behavior in lipid/alcohol suspensions. *Biochim. Biophys. Acta* 773, 169–172.
- Smirnov, A.I., Smirnova, T.I. and Morse II, P.D. (1995) Very high frequency electron paramagnetic resonance of 2,2,6,6-tetramethyl-1-piperidinyloxy in 1,2-dipalmitoyl-sn-glycero-3-phosphatidylcholine liposomes: Partitioning and molecular dynamics. *Biophys. J.* 68, 2350–2360.
- Sturtevant, J.M. (1984) The effects of water-soluble solutes on the phase transitions of phospholipids. *Proc. Natl. Acad. Sci. USA* 81, 1398–1400.
- Veiro, J.A., Nambi, P. and Rowe, E.S. (1988) Effect of alcohols on the phase transitions of dihexadecylphosphatidylcholine. *Biochim. Biophys. Acta* 943, 108–111.
- Wang, H.-Y., Tümmler, B. and Boggs, J.M. (1989) Use of spin labels to determine the percentage of interdigitated lipid in complexes with polymyxin B and polymyxin B nonapeptide. *Biochim. Biophys. Acta* 985, 182–198.
- Wang, D.-C., Taraschi, T.F., Rubin, E. and Janes, N. (1993) Configurational entropy is the driving force of ethanol action on membrane architecture. *Biochim. Biophys. Acta* 1145, 141–148.
- Zeng, J. and Chong, P.L.-G. (1995) Effect of ethanol-induced lipid interdigitation on the membrane solubility of prodan, acdan, and laurdan. *Biophys. J.* 68, 567–573.
- Zeng, J., Smith, K.E. and Chong, P.L.-G. (1993) Effects of alcohol-induced lipid interdigitation on proton permeability in L- $\alpha$ -dipalmitoylphosphatidylcholine vesicles. *Biophys. J.* 65, 1404–1414.
- Zhang, F. and Rowe, E.S. (1992) Titration calorimetric and differential scanning calorimetric studies of the interactions of n-butanol with several phases of dipalmitoylphosphatidylcholine. *Biochemistry* 31, 2005–2011.





## Oxidative stress effect on the integrity of lipid bilayers is modulated by cholesterol level of bilayers

Oren Tirosh <sup>a</sup>, Ron Kohen <sup>a</sup>, Jehoshua Katzhendler <sup>b</sup>, Anat Alon <sup>c</sup>,  
Yechezkel Barenholz <sup>c,\*</sup>

<sup>a</sup> Department of Pharmaceutics, School of Pharmacy, School of Medicine, The Hebrew University of Jerusalem, P.O. Box 12272, Jerusalem 91120, Israel

<sup>b</sup> Department of Pharmaceutical Chemistry, School of Pharmacy, The Hebrew University of Jerusalem, P.O. Box 12272 Jerusalem 91120, Israel

<sup>c</sup> Department of Biochemistry, School of Medicine, The Hebrew University of Jerusalem, P.O. Box 12272, Jerusalem 91120, Israel

Received 5 August 1996; received in revised form 14 February 1997; accepted 26 February 1997

### Abstract

Large unilamellar vesicles (120–160 nm) composed of egg phosphatidylcholine (egg PC) containing approximately 22 wt% of polyunsaturated fatty acids (PUFA) and various mol% (0, 10, 22, or 45) of cholesterol were exposed to oxidative stress. The hydrophilic azo compound 2,2'-azobis-(2-amidinopropane)2HCl (AAPH) which was thermally decomposed to produce a constant flux of peroxy radicals was the source of the oxidative stress ( $\leq 48$  h incubation at 37°C). Cholesterol loss following the oxidation was up to 33%, while PUFA were more extensively damaged; loss was up to 52, 88, and 100% for C-18:2, C-20:4, and C-22:6, respectively. (ii) Oxidizability of cholesterol when quantified in absolute amount was three-fold higher when its level was 45 mol%. The interrelationship between bilayer structure, especially its lateral organization and free volume, and lipid peroxidation are discussed. Differential scanning calorimetry of oxidized multilamellar vesicles lacking cholesterol revealed that a high level of oxidative damage to egg phosphatidylcholine PUFA resulted in the loss of the gel to liquid-crystalline phase transition of egg PC (broad peak at around  $-8^\circ\text{C}$ ). © 1997 Elsevier Science Ireland Ltd.

**Keywords:** Liposomes ; Lipid peroxidation; Acyl chains; Cholesterol

**Abbreviations:** LUV, large unilamellar vesicles; PUFA, polyunsaturated fatty acids; DSC, differential scanning calorimetry; PC, phosphatidylcholine; AAPH, 2,2'-azobis (2-amidinopropane)2HCl; MLV, multilamellar vesicles; SO, solid ordered; LD, liquid disordered; LO, liquid ordered; GC, gas chromatography.

\* Corresponding author. Tel.: + 97 2 6758507/9; fax: + 97 2 6411663/6784010; e-mail: yb@cc.huji.ac.il

### 1. Introduction

Auto and peroxidation of organic compounds are free radical chain processes which lead to deterioration of polyunsaturated acyl chains and

cholesterol. Three major stages in this process are recognized: initiation, propagation, and termination. Similar processes occur in plasma and organelle membranes surrounding cells and organelles, which contain polyunsaturated fatty acids (PUFA) and cholesterol [1,6].

Biological membranes are complex systems. They are composed of a large variety of lipids, proteins, glycocalyx (composed of glycolipids and glycoproteins), and cholesterol. Phospholipids, sphingolipids, and cholesterol are the main components of the membrane lipid bilayer. The ratio between them and the level of unsaturation determine membrane physical state regarding lateral organization and dynamics. Membrane phase transition temperature between the gel phase (solid ordered, SO) and the liquid-crystal phase (liquid disordered, LD) depends on the exact composition of the acyl chains in the phospholipid bilayer. Cholesterol molecules in the bilayer induce the formation of a third phase, referred to as liquid ordered (LO) [4,9,14]. A cholesterol molecule interacts with two phospholipid molecules and prevents them from going through the gel to liquid-crystal phase transition; at 33 mol% of cholesterol there is no apparent transition, as all the phospholipids of the membrane are in the liquid ordered phase (LO).

Physical state of the lipid bilayer has a major influence on many membrane functions, e.g. transport, signal transduction, membrane enzyme activities and receptor recognition [7,12].

Oxidative processes induce large alterations in membrane composition and physical state [12]. Loss of PUFA, cross-linking between oxidized lipids in the acyl chain regions and in the phospholipid headgroup, as well as interdigitation of oxidized phospholipids of the opposing monolayers in the lipid bilayer, lead to higher membrane rigidity, thereby decreasing the lateral diffusion and free volume within the bilayer [7,12]. However, the exact details of the relationship between membrane oxidative damage and changes in chemical and physical properties of membranes containing cholesterol are not fully understood. In this paper we are trying to clarify some aspects of this gap.

## 2. Materials and methods

### 2.1. Liposome preparation

Multilamellar vesicles (MLV) and large unilamellar vesicles (LUV) were prepared from mixtures of egg phosphatidylcholine (egg PC) and various mol% of cholesterol in 50 mM HEPES buffer pH 7.4. The lipids were dissolved in *t*-butanol and lyophilized. The powder was then hydrated with the buffer to form MLV and vortexed vigorously for 5 min. The MLV were downsized to LUV by extrusion through a 100 nm pore size polycarbonate filter according to an already published procedure [2]. All of the liposome preparations were in the size range of 120–160 nm as evaluated by dynamic light-scattering measurements [2].

### 2.2. Phospholipid phosphorus determination

Phospholipid phosphorus was determined as described elsewhere [3].

### 2.3. Acyl chain composition

100  $\mu$ l LUV (19 mM phospholipids) before and after exposure to oxidative stress was diluted with 900  $\mu$ l water. The lipids were extracted from the aqueous phase by adding 1 ml ethanol and 1 ml chloroform (containing 1 mg/ml BHT) and vortexing for 1 min. Two phases were formed, and the organic phase was collected and dried by a stream of nitrogen, followed by 2 h of lyophilization to remove all traces of water. The dry lipids were dissolved in 50  $\mu$ l toluene, 10  $\mu$ l methanol and 20  $\mu$ l Meth-Prep II methanol esterification reagent (Alltech). The mixture of lipids was analyzed by gas chromatography using a Perkin Elmer 1020 plus GC, with a Silar 10C chromatographic column (Alltech) using a temperature gradient of 5°C/min from 140 to 240°C [2].

### 2.4. Cholesterol determination

100  $\mu$ l LUV containing cholesterol before and after oxidative stress were extracted by chloroform containing (1 mg/ml BHT):methanol:HCl 0.1N (1:1:1 by vol). Two phases were formed. The chloroformic lower phase was separated, and 20

Table 1  
Residual PUFA (in wt%) after exposure to AAPH

Time (h)	Cholesterol concentration (mol%)											
	0			10			22			45		
PUFA:	18:2	20:4	22:6	18:2	20:4	22:6	18:2	20:4	22:6	18:2	20:4	22:6
0	100	100	100	100	100	100	100	100	100	100	100	100
24	87	80	58	82	36	35	82	56	47	82	58	51
48	66	26	25	48	12	0	64	28	36	67	32	27

PUFA remaining in wt% after incubation of LUV with 20 mM AAPH as measured by GC. Liposomes contained 19 mM phospholipid and 0, 10, 22, and 45 mol% of cholesterol.

Results represent the average of two separate oxidation experiments (differing between at most by 3%).

$\mu$ l of the samples was injected directly into the HPLC. Detection was performed at 212 nm, mobile phase-heptane:isopropanol 500:6 (v/v), flow-2 ml/min, column-normal phase Econosphere silica column (Alltech)  $100 \times 4.6$  mm, 3  $\mu$ m. [2]. Cholesterol was eluted after 6 min.

#### 2.5. Oxidative stress by 2,2'-azobis (2-amidinopropane) 2 HCL (AAPH)

SUV (19 mM phospholipids) containing different cholesterol concentrations were incubated with 20 mM AAPH (a hydrophilic thermal-dependent peroxy radical generator) at 37°C for up to 48 h ([6]).

#### 2.6. DSC measurements of MLV

MLV were prepared as previously described, with a phospholipid concentration of 100 mM. Liposomes were exposed to oxidative stress induced by 20 mM AAPH for a 1 week period at 37°C. As a control, an aliquot of the same liposome preparation was kept under nitrogen and at 4°C. Following the oxidation, the liposome preparations were concentrated by centrifugation and weighed. To the concentrated liposomes, ethyleneglycol was added to a final concentration of 40 wt% in order to prevent freezing. The mixtures were allowed to reach equilibrium (1 h incubation). The thermotropic behavior of the oxidized and the control liposomes was studied by Heat Flow DSC using a Mettler Thermal Analyzer model 4000. Scanning was conducted from  $-20$  to  $60^\circ\text{C}$  at the rate of  $2^\circ\text{C}$  per min.

#### 2.7. Statistical analysis

The oxidation rates of the different liposome preparations were analyzed according to the Kruskal-Wallis one way analysis of variances on ranks, and pairwise multiple comparison procedures (Dunns method), using the Sigmastat statistics program. The control was liposomes without cholesterol.

### 3. Results

#### 3.1. Effect of oxidation on phospholipid acyl chain composition of liposomes

Oxidative degradation of PUFA in liposomes containing various concentrations of cholesterol was determined by GC after 0, 24, and 48 h incubation with AAPH. Three PUFA were followed: linoleic, arachidonic, and docosahexaenoic (18:2, 20:4, and 22:6, respectively), and their loss was normalized to the internal standard of the saturated palmitic 16:0 acyl chain, which was not affected by the oxidation process. Extensive loss was recorded in all liposome preparations. The results are summarized in Table 1 and Table 2. Maximum oxidative damage was recorded at 10 mol% of cholesterol (which was statistically significantly different from the other compositions). We found no statistical difference in the loss of acyl chains between all of the other preparations, irrespective of their cholesterol content.



Table 2  
Damaged phospholipids (in mol%) after exposure to AAPH

Time (h)	Cholesterol concentration(mol%)			
	0	10	22	45
0	0	0	0	0
24	9.6	15.2	9.6	9.2
48	17.2	24.4	16.8	16.0

Since most phospholipids contain only one PUFA, the maximum amount of oxidizable phospholipids was estimated as 40 mol% (44 wt%).

### 3.2. Effect of AAPH on cholesterol oxidation in liposomes

Oxidative degradation of cholesterol in LUV of various cholesterol mol% was measured by HPLC following 0, 24, and 48 h incubation with 20 mM AAPH. Results are summarized in Table 3. Maximum oxidative damage to cholesterol as a percent of the control occurred in LUV with 10 mol% cholesterol. However in absolute values the most extensive damage to cholesterol was in the order: 45 mol% cholesterol > 10 mol% = 22 mol% (Table 4).

### 3.3. Differential scanning calorimetry of oxidized liposomes

MLV composed of egg PC (without cholesterol) were exposed, or not exposed, to oxidative damage by AAPH and analyzed by heat flow DSC. The results demonstrated that the gel-to-liquid-crystalline phase transition of egg PC, for which  $T_m$  at  $-8^\circ\text{C}$  (a broad transition) (Fig. 1, lower thermogram) was abolished following extensive and almost complete oxidation of PUFA (20 mM

Table 3  
Residual cholesterol (in mol% after exposure to AAPH)

Time(h)	Cholesterol concentration (mol%)		
	10	22	45
0	100	100	100
24	65	86	83
48	63	82	79

Results represent the average of two experiments (differing at most by 5%).

Table 4  
Amount ( $\mu\text{mol}$ ) of oxidized cholesterol

Time(h)	Cholesterol conc (mol%)		
	10	22	45
0	0	0	0
24	0.73 $\mu\text{mol}$	0.66 $\mu\text{mol}$	2.64 $\mu\text{mol}$
48	0.77 $\mu\text{mol}$	0.85 $\mu\text{mol}$	3.2 $\mu\text{mol}$

AAPH for 1 week at  $37^\circ\text{C}$ ) (Fig. 1, upper thermogram).

## 4. Discussion

Cholesterol is one of the main modulators of physical properties of membranes. Phase structure of membranes containing cholesterol can be classified into three states: liquid disordered (LD), which occurs at low cholesterol levels and at temperatures well above matrix main lipid gel-to-liquid-crystal phase transition temperature ( $T_m$ ); liquid ordered (LO), which occurs at high cholesterol mol% (above 20 mol%); and solid ordered (SO), which occurs at temperatures below matrix lipid  $T_m$  and at low cholesterol levels (below 20 mol%). Phase separation and coexistence between the three phases depend on the exact membrane composition and temperature. Most membrane physical properties are affected by its phase structure ([4,9,14]).

The oxidation rates of the PUFA in the lipid bilayers were hardly affected by the elevation of cholesterol concentration. Only at 10 mol% of cholesterol, a faster oxidation was observed (Table 1). The faster oxidation at 10 mol% could be attributed to the coexistence of LD and LO phases. This phase separation may be selective due to the preferential interaction of cholesterol with saturated and monosaturated egg PC acyl chains (Biterswijk et al., 1987; Mitchell and Litman, 1996). This selectivity may result in the LO phase rich in the 1-palmitoyl 2-oleyl PC and cholesterol and LD domains poor in cholesterol and enriched with PCs having polyunsaturated acyl chains at position 2. It is possible that this organization leaves the polyunsaturated PC unprotected. However, recent

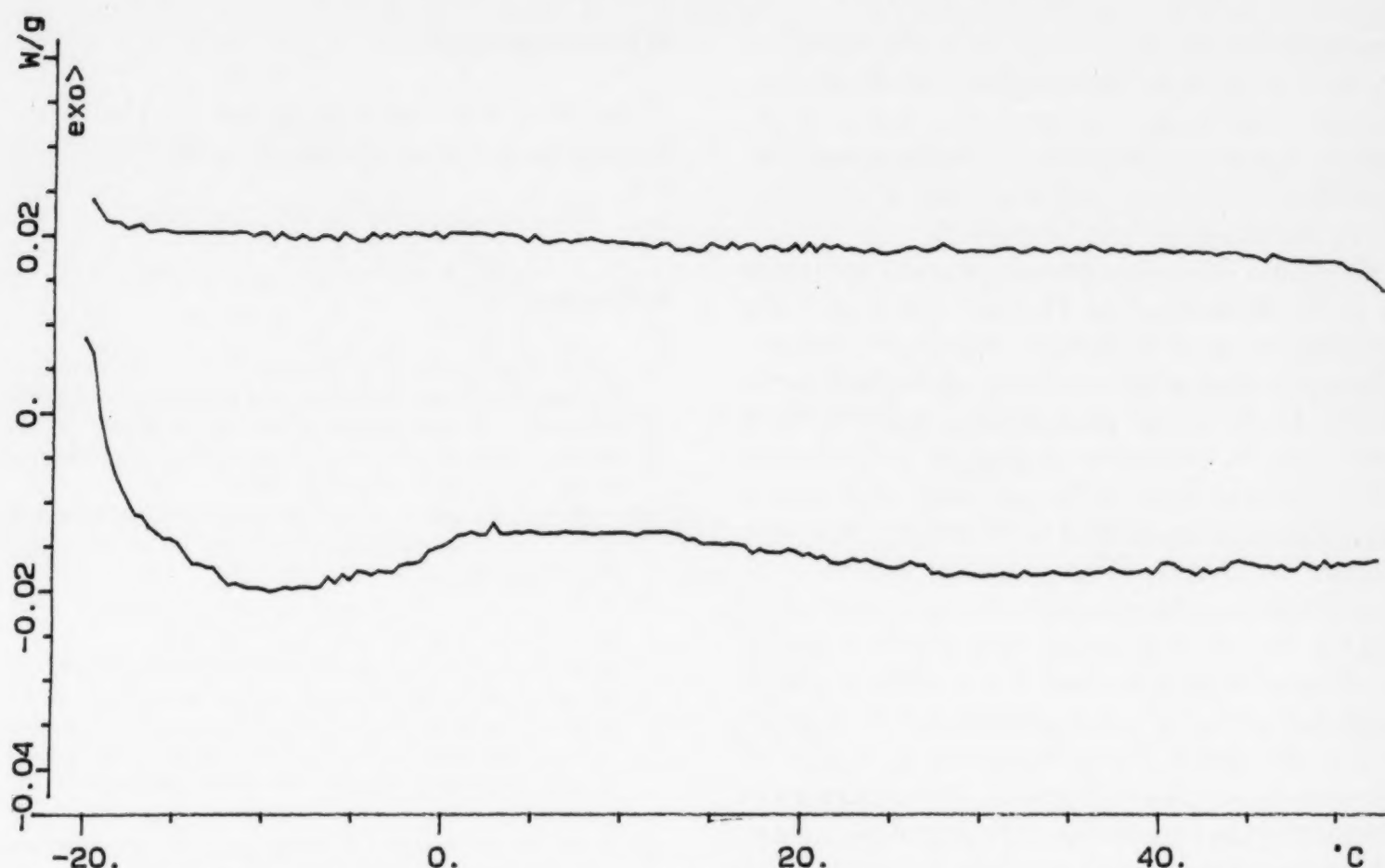


Fig. 1. Differential scanning calorimetry of multi-lamellar vesicles egg PC (MLV) (lower thermogram) and of oxidized egg PC (MLV) (upper thermogram). The heat flow profile showed a broad phase transition at  $-8^{\circ}\text{C}$ , which was completely lost following the oxidative modification.

observations suggest that cholesterol interaction with the polyunsaturated acyl chains of PC is much weaker than with saturated or mono unsaturated acyl chains (Mitchell and Litman, 1996). This supports the phase-separation-induced facilitation of AAPH, peroxy and other radicals penetration and movement as the main cause of enhanced oxidative damage. Such increased penetration and motion in cholesterol-induced LO/LD phase separation is discussed in detail by Damman et al. (1996). This explanation is also supported by the finding of Sankaram and Thompson (1992) showing that in a membrane poor in cholesterol the cholesterol molecules are located in large 'pores' which interdigitate both monolayers of the bilayer, partially phase separated from 40 mole % of the egg PC which contain PUFA (at position 2). Although only 40% of PC molecules have polyunsaturated acyl chains, their complete oxidation seems to alter the bilayer thermotropic behavior and completely abolishes the phase transition. A greater degree of

interdigitation and/or some degree of covalent cross-linking between oxidized acyl chains in the bilayer caused changes in the lateral organization of the bilayer, leading to the loss of the phase transition.

The new observations described here should lead to further studies aiming to clarify the contribution of lipid peroxidation induced interdigitation and/or cross-linkage, and of cholesterol oxidised products to the organization and dynamics of the membrane, while in membranes rich in cholesterol the cholesterol molecules are distributed in both monolayers between the phospholipids in a tight pack almost without any free volume. Straume and Litman [13] using time resolved fluorescence anisotropy of DPH investigated the influence of cholesterol on membranes that contain unsaturated phospholipids. Their findings showed that increasing cholesterol mol% modulates the effect of temperature and degree of saturation on the bilayer order and free volume. In addition they found that as cholesterol

concentration increases above 15 mol% there is a decrease in the water penetration into the bilayer, probably due to the formation of a tighter pack. Faster oxidation induced by cholesterol was also described by McLean and Hagaman in metal-induced oxidation of lipid bilayers [8].

Oxidation of cholesterol was identical at 10 and 22 mol% cholesterol. At 45 mol% cholesterol, the absolute extent of cholesterol oxidation was three-fold higher than at the two lower mol% cholesterol (Table 4). A similar phenomenon was described previously for enzymatic cholesterol oxidation by cholesterol oxidase [10]. It was explained by lateral organization of cholesterol in the bilayer plane. The oxidant we used (AAPH) is a water soluble compound which oxidized initially the outer layer of the bilayer. This layer maintains a maximum mol ratio of cholesterol:phospholipid of 1:2, while the inner layer has a higher ratio of cholesterol up to 42 mol% [12]. Above this mol% lateral separation of cholesterol occurs and domains of cholesterol not shielded by the phospholipids head groups, appear. These domains are more accessible to oxidation by AAPH.

The DSC results of oxidized MLV (complete oxidation of the polyunsaturated acyl chains) indicated that the cooperative phase transition of the phospholipids in the lipid bilayer was lost due to oxidation. The low phase transition temperature,  $-8^{\circ}\text{C}$ , of egg PC in MLV probably results from the large mol% ( $\sim 60\%$ ) of 1-palmitoyl-2-oleyl PC which is at least partially phase separated from 40 mol% of the egg PC which contain PUFA (at position 2). Although only 40% of PC molecules have polyunsaturated acyl chains, their complete oxidation seems to alter the bilayer thermotropic behavior and completely abolishes the phase transition. A greater degree of interdigitation and/or some degree of covalent cross-linking between oxidized acyl chains in the bilayer causes large changes in the lateral organization of the bilayer, leading to the loss of the phase transition.

The new observations described here should lead to further studies aiming to clarify the contribution of lipid peroxidation induced interdigitation and/or cross-linkage, and of cholesterol oxidized products to the organization and dynamics of the membrane.

## Acknowledgements

This work was supported in part by The Israel-United States Science Foundation, BSF 95/318 to Y.B.

## References

- [1] L.R.C. Barclay and K.U. Ingold (1981) Autoxidation of biological molecules; The autoxidation of model membrane. A comparison of the autoxidation of egg lecithin phosphatidylcholine in water and in chlorobenzene. *J. Am. Chem. Soc.* 103, 6478–6485.
- [2] Y. Barenholz and S. Amselem (1993) in: G. Gregoriadis (Ed.), *Liposome Technology*, Volume I, 2nd ed., CRC Press, Boca Raton, FL, pp. 501–525.
- [3] G.R. Bartlett (1959) Phosphorus assay in column chromatography. *J. Biol. Chem.* 234, 466–468.
- [4] B. Dammann, H.C. Fogedby, J.H. Ipsen, C. Jeppesen, K. Jorgensen, O.G. Mouritsen, J. Risbo, M.C. Sabra, M.M. Sperotto and M.J. Zuckermann (1996) in: D.D. Lasic and Y. Barenholz (Eds.), *Handbook of Nonmedical Applications of Liposomes*, Vol. 1, CRC Press, Boca Raton, FL, pp. 85–128.
- [5] M.M. Dooley, N. Sano, H. Kaeashima and T. Nakamura, (1990) Effects of 2,2'-azobis (2-amidinopropane) hydrochloride in vivo and protection by vitamin E. *Free Rad. Biol. Med.* 9, 199–204.
- [6] B. Halliwell and J.M.C. Gutteridge (Eds.) (1989) in: *Free Radicals in Biology and Medicine*, 2nd ed., Clarendon Press, Oxford, pp. 22–81.
- [7] D. Hegner (1980) Mechanism of Aging and Development. 14, 101–118.9
- [8] L.R. McLean and K.A. Hagaman (1992) Effect of lipid physical state on the rate of peroxidation of liposomes. *Free Rad. Biol. Med.* 12, 113–119.
- [9] D. Needham, T.J. McIntosh and A. Evans (1988) Thermomechanical and transition properties of dimyristoylphosphatidylcholine/cholesterol bilayers. *Biochemistry* 27, 4668–4673.
- [10] R. Pal, Y. Barenholz and R. Wagner (1980) Effect of cholesterol concentration on organization of viral and vesicle membranes. Probed by accessibility to cholesterol oxidase. *J. Biol. Chem.* 225 (12), 5820–5826.
- [11] M.B. Sankaram and T.E. Thompson (1991) Cholesterol-induced fluid-phase immiscibility in membranes. *Proc. Natl. Acad. Sci. USA*, 88, 8686–8690.
- [12] H.R. Shmeeda, E.B. Golden and Y. Barenholz, (1994) in: M. Shinitzky (Ed.), *Biomembranes*, Vol. 2, Structural and Functional Aspects, VCH, Weinheim, pp. 1–82.
- [13] M. Straume and B.J. Litman, (1987) Unsaturated acyl chain phosphatidylcholine vesicles as determined from higher order analysis of fluorescence anisotropy decay. *Biochemistry* 26 (16), 5121–5126.
- [14] P.L. Yeagle (1985) Cholesterol and the cell membrane. *Biochim. Biophys. Acta* 822, 267–287.



## Novel cationic liposomes for DNA-transfection with high efficiency and low toxicity

Tommi Paukku<sup>a,\*</sup>, Satu Lauraeus<sup>b</sup>, Ilpo Huhtaniemi<sup>a</sup>, Paavo K.J. Kinnunen<sup>b</sup>

<sup>a</sup> Department of Physiology, Institute of Biomedicine, University of Turku, Kiinamyllynkatu 10, 20520 Turku, Finland

<sup>b</sup> Department of Medical Chemistry, Institute of Biomedicine, University of Helsinki, Siltavuorenpenger 10, 00014 Helsinki, Finland

Received 2 December 1996; received in revised form 3 March 1997; accepted 5 March 1997

### Abstract

Liposomes containing the natural cationic amphiphile, sphingosine and some of its derivatives were used for transfection of DNA in vitro. Multilamellar liposomes comprised of dioleoylphosphatidylethanolamine (DOPE), different sphingosine derivatives, and diacylglycerols with varying fatty acid chains, preincubated with DNA, transfected efficiently the KK-1 murine granulosa cells. Most efficient transfection on this cell line was achieved with liposomes composed of phytosphingosine, DOPE, and dioctanoylglycerol (DC<sub>8</sub>G) (64:31:4.8, molar stoichiometry), which gave expression of the transfected gene 2–10-fold higher than the commercial reagent Lipofectin<sup>®</sup>. At higher doses the new liposomes also caused markedly less cell death of KK-1 cells. On COS-7 cells these liposomes showed slightly, but significantly lower transfection, of approximately 70%, of that gained with Lipofectin<sup>®</sup>. The murine Sertoli cells, MSC-1, selectively resisted transfection by the sphingosine derivative based liposomes tested, giving only 11–14% of the expression detected in Lipofectin<sup>®</sup> transfected cells of the same line. In conclusion, the novel liposomes formulated offer an effective, technically easy and economical method of transfection for a variety of cultured cell lines. © 1997 Elsevier Science Ireland Ltd.

**Keywords:** Transfection; Cationic liposomes; Sphingosine; Diacylglycerol

### 1. Introduction

Cationic liposomes are widely used for delivering foreign DNA into mammalian cells in vitro

[1,6,10,17,23,25]. Also liposome-based in vivo transfection systems have been developed recently [27–29,37,42]. The transfection efficiency of the currently available liposomes is rather low in vivo [43] and in some cell lines in vitro [18]. The toxicity of some of the commercially available cationic lipids has been assigned to their non-natural, non-biodegradable nature [9,35], e.g. N-[1-

\* Corresponding author. Fax: +358 2 2502610; e-mail: tommy.paukku@utu.fi

(2,3-dioleoyloxy)propyl]-*N,N,N*-trimethylammonium chloride (DOTMA) in Lipofectin®. In addition, their high cost is somewhat restrictive to their use.

Sphingosine and some of its derivatives are cationic lipids (Fig. 1) which occur naturally in mammalian and non-mammalian cells [11,15,26,44]. Accordingly, cells should be able to control their levels using the normal metabolic routes for these lipids. Sphingosine-containing liposomes complex strongly with DNA [21,22]. Sphingosine also inhibits protein kinase C (PKC) [2] [16]. To this end, inhibition of PKC has been proposed to be a critical factor determining the transfection efficiency and toxicity of cationic liposomes [35].

In addition to the synthetic cationic lipids required for the attachment of the liposomes to DNA, DOPE has been included in the liposomal formulations as it has been found to enhance transfection efficiency (for a review, see [45]). In contrast to most of the other lipids abundant in biomembranes and forming lamellar bilayers, DOPE as such adopts the so-called inverted hexagonal  $H_{II}$  arrangement and in general promotes the formation of this phase [4,34,39,40]. Diacylglycerol (DAG) is another well known promoter of  $H_{II}$  formation [3,5,7,8]. Lipids forming or promoting the formation of  $H_{II}$  as well as other inverted non-lamellar phases also enhance membrane fusion [20]. The tendency for the  $H_{II}$  arrangement derives from an imbalance in the relative cross-sectional effective areas of the lipid headgroups and its hydrophobic part, which further results in negative spontaneous curvatures for membranes containing this type of lipids [38]. In this study we wanted to examine, in addition to using sphingosine and its derivatives as natural cationic lipids for potentially reduced toxicity, whether the combined presence of DOPE and DAG results in increased transfection efficiency.

## 2. Materials and methods

### 2.1. Cell lines and media

The cell line KK-1 is derived from transgenic

murine ovarian tumour cells immortalized by expression of the simian virus 40 large and small tumor (*T*) antigens under the control of the murine inhibin- $\alpha$  subunit promoter [19]. HeLa cells are derived from human uterine cervix carcinoma. COS-7 and MSC-1 cell lines are derivatives of the simian kidney cell line CV-1 transformed with a mutant of simian virus 40 [12] and transgenic mice carrying a fusion gene composed of the human anti-Müllerian hormone (AMH) transcriptional regulatory sequences linked to the simian virus 40 *T*-antigen [31], respectively. The cells were grown on plastic tissue culture plates in Dulbecco's modified Eagle's medium with 10% fetal bovine serum (DMEM-10) in an incubator in an atmosphere of 5%  $CO_2$  in air at 37°C.

### 2.2. Liposomes

Phorbol myristoyl acetate (PMA), dioctanoylglycerol, dioleoylglycerol, phytosphingosine, sphingosine and sphingosyl phosphoryl choline were purchased from Sigma (St. Louis, MO). DOPE was obtained from Avanti Polar Lipids, (Alabaster, Ala). Multilamellar liposomes were prepared as described earlier ([21]). Briefly, DOPE and the different sphingosine derivatives (Fig. 1) were mixed in a 33:67 molar stoichiometry in

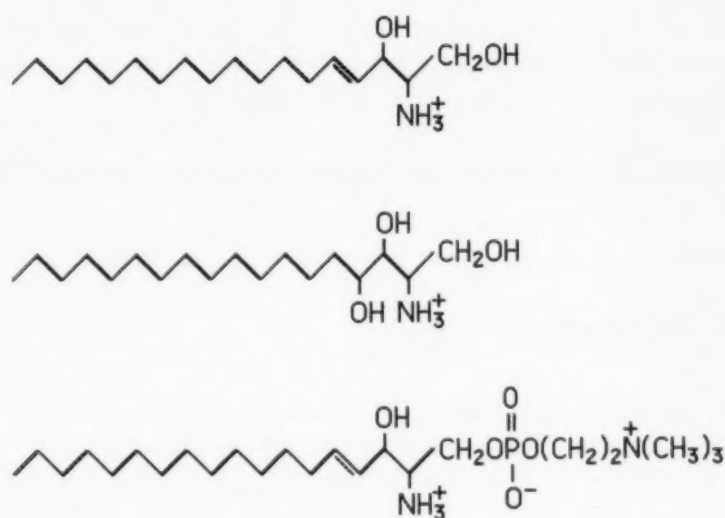


Fig. 1. Chemical structures of the different sphingosine derivatives used, sphingosine (top), phytosphingosine (middle), and sphingosyl phosphoryl choline (bottom).

chloroform, and the indicated amounts of dioleoylglycerol (DOG) or dioctanoylglycerol (DC<sub>8</sub>G) in chloroform were added to obtain the desired compositions. The mixtures were evaporated to dryness under a stream of nitrogen and the residual solvent was removed under vacuum overnight. The dry lipid mixture was hydrated for 30 min with 20 mmol/l Hepes buffer, containing 150 mmol/l NaCl and 0.1 mmol/l EDTA (pH 7.4) at 40°C in a water bath, and vortexed briefly every 5 min. At the end of hydration the liposomes were irradiated at 40°C in a bath-type sonicator (Branson, Danbury, CT) for 5 min. The total lipid concentration of the liposomes was 100 mg/l buffer. Lipofectin® (Gibco BRL, Gaithersburg, MD) was used as the reference liposome according to instructions of the manufacturer.

### 2.3. DNA

The pCMV-luciferase construct used in the experiments was designed to carry the promoter area of the cytomegalo virus (CMV) in front of the firefly luciferase coding sequence in an expression vector pUHC13-1 [13]. The DNA preparation was purified twice with CsCl gradient centrifugation and dissolved in sterile water for the transfections. The identity of the CMV-luciferase construct was verified using specific restriction endonuclease digestions.

### 2.4. Preparation of DNA–lipid complexes

One  $\mu$ g of DNA and 10  $\mu$ g of total lipid were each diluted into 100  $\mu$ l of serum-free DMEM (DMEM-SF) and then mixed, followed by an incubation for 15 min at 23°C. Thereafter, the total volume of the mixture was adjusted to 1 ml with DMEM-SF.

### 2.5. Lipofection

At least 80% confluent six-well cell culture plates were washed with DMEM-SF and the DNA–lipid complexes were laid over the cells. After a 10-h incubation period, the DNA–lipid

mixture was replaced by 2 ml of DMEM-10. Three days after the beginning of transfection, the cells were harvested by scraping off the culture plates. The cell extracts were prepared and a luminometric assay for luciferase activity was performed as described in details elsewhere [14,30]. In brief, 50  $\mu$ l of the total 100  $\mu$ l of the cell extracts were mixed with 360  $\mu$ l of assay buffer by short vortexing in a disposable cuvette. The cuvettes were thereafter placed in a Bio-Orbit Luminometer 1251 (Bio-Orbit, Turku, Finland) and the luminescence was measured after adding 200  $\mu$ l of luciferin solution (200  $\mu$ mol/l luciferin in 25 mmol/l glycylglycine, pH 7.8). If the luciferase activity of a sample exceeded the measuring range, a lower amount (10 or 20  $\mu$ l) of the cell extract was used.

### 2.6. PKC stimulation

PMA at a level of 1 mol% of total lipid was added to the liposome solutions. The transfection and expression analyses were performed as described above.

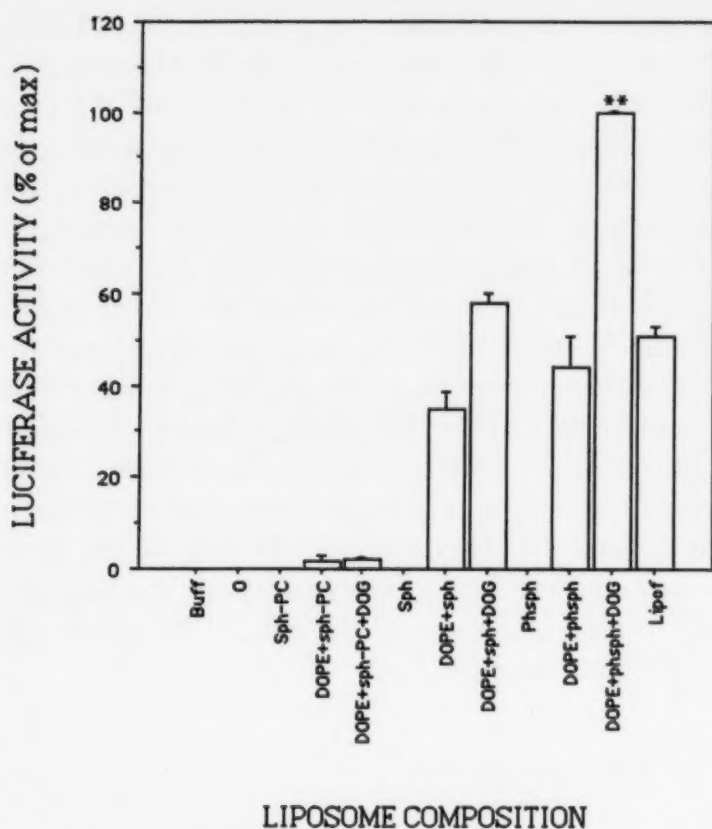
### 2.7. Statistical analysis

One-way analysis of variance, followed by Duncan's new multiple range test, was performed. When non-Gaussian by distribution, the data were subjected to logarithmic transformation before statistical evaluation. A *P*-value less than 0.05 was chosen as the limit of statistical significance.

## 3. Results

One  $\mu$ g of DNA mixed with 10  $\mu$ g of the lipid was tested to be the optimal amount of Lipofectin® for KK-1 cells, 2  $\mu$ g of DNA with 10  $\mu$ g of the lipid for HeLa cells and 1  $\mu$ g of DNA with 20  $\mu$ g of the lipid and 0.5  $\mu$ g of DNA with 10  $\mu$ g of the lipid for COS-7 and MSC-1 cells, respectively (data not shown). To compare the transfection efficiency, we chose the same concentrations





LIPOSOME COMPOSITION

Fig. 2. Effect of the different liposomal lipid combinations on transfection efficiency of pCMV-luc in KK-1 cells. KK-1 cells were transfected with 10  $\mu$ g lipid and 1  $\mu$ g CMV-luc plasmid. After harvest the luciferase activities of the cell lysates were measured. Buff = cells not transfected; 0 = cells transfected with 1  $\mu$ g DNA only, with no liposomes; sph-PC = sphingoylphosphorylcholine; sph = sphingosine; phsph = phytosphingosine. DOPE and sphingosine derivatives were mixed 1:1 (wt:wt) and 10 mol% DOG were added when indicated. The data presented as mean  $\pm$  S.E.M. of three replicate cultures. One of three similar experiments is presented. \*\*  $P < 0.01$  vs. Lipofectin<sup>®</sup> (Lipof).

for the sphingosine derivative-based liposomes. The DNA-lipid complexes formed rapidly after mixing and displayed stable transfectability at least for 1 h at the concentration used (data not shown).

The phytosphingosine and sphingosine containing liposomes gave good transfection efficiency in KK-1 cells, comparable to or exceeding that of Lipofectin<sup>®</sup>. Without DOPE the sphingosine derivatives showed very little transfection activity (Fig. 2). In COS-7 cells the sphingosine liposomes had slightly lower transfection efficiency than Lipofectin<sup>®</sup> (Fig. 3). MSC-1 cells showed selective resistance to DNA transfer with sphingosine derivatives. They gave only 11–14% of the activ-

ity with Lipofectin<sup>®</sup> transfection when transfected with the novel formulae (Fig. 3).

After the incubation of KK-1 cells with liposomes for 16 h or longer, the cells transfected with Lipofectin<sup>®</sup> had almost all died, whereas the sphingosine liposomes caused no marked cell death by that time. The other cell lines tolerated the novel compounds well and also Lipofectin<sup>®</sup> better than KK-1 cells. They showed only minor damage after incubation periods longer than 10 h.

Combining of the diacylglycerols with the sphingosine liposomes affected the transient luciferase expression in a biphasic dose-dependent manner in KK-1 cells. Dioleoylglycerol doubled the transfection at the optimum of 5 mol%, dioctanoylglycerol being most effective with an optimum at approx. 5–10 mol% (Fig. 4). Concentrations higher than optimum caused lower expression.

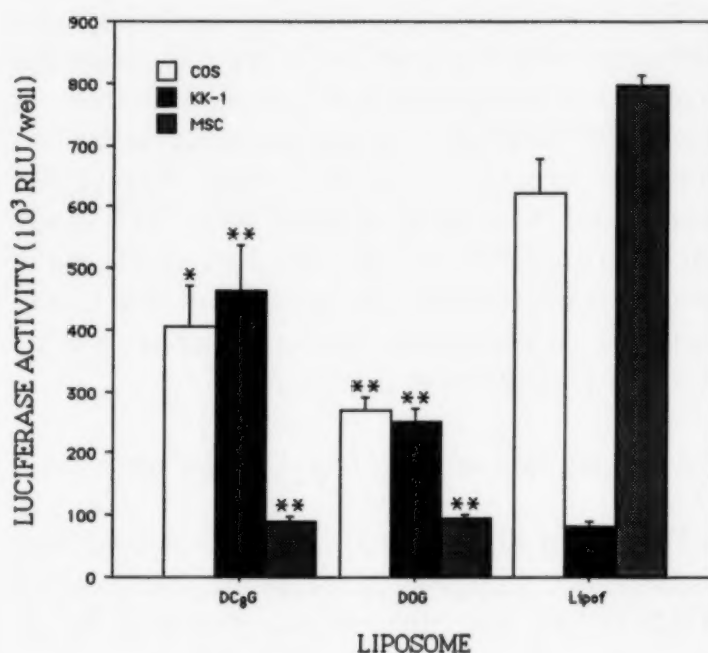


Fig. 3. Transfection efficiency of DOPE-phytosphingosine liposomes supplemented with 5 mol% of dioctanoylglycerol (DC<sub>8</sub>G) or dioleoylglycerol (DOG) and tested on KK-1, COS-7 and MSC-1 cells. 10  $\mu$ g of lipid with 1  $\mu$ g (KK-1 cells) or 0.5  $\mu$ g (MSC-1 cells) of DNA or 20  $\mu$ g of lipid with 1  $\mu$ g of DNA (COS-7 cells) was used in transfection. The data are presented as mean  $\pm$  S.E.M. of three replicate cultures. One of two similar experiments is presented. The expression was compared with that in the cells transfected with Lipofectin<sup>®</sup> (Lipof). \*  $P < 0.05$ , and \*\*  $P < 0.01$  vs. Lipofectin<sup>®</sup> in the same cell line. RLU = relative luciferase unit.

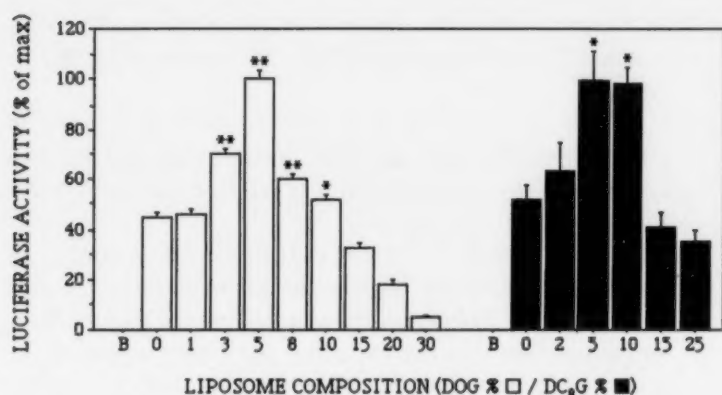


Fig. 4. The effect of varying contents of DOG or DC<sub>8</sub>G (in mol%) in DOPE-phytosphingosine liposomes on transfection efficiency. 10  $\mu$ g of total lipid and 1  $\mu$ g of DNA were used to transfect KK-1 cells. The data are presented as mean  $\pm$  S.E.M. of three replicate cultures. One of two similar experiments is presented. \*  $P < 0.05$ , and \*\*  $P < 0.01$  vs. DOPE-phytosphingosine liposomes with no DOG or DC<sub>8</sub>G. B = cells not transfected.

In wells stimulated by PMA (1 mol% of liposomal lipids) the expression of luciferase in KK-1 cells was only 22.4% of that in those not stimulated ( $P < 0.01$ ), when lipofected with phytosphingosine/DOPE/DC<sub>8</sub>G (64:31:4.8 mol%) containing liposomes. Despite PMA, the conditions were as described above in Section 2 for the other lipofections.

#### 4. Discussion

Our aim was to study the feasibility of sphingosine derivative containing liposomes for DNA transfer into mammalian cells. We also wanted to examine effects of DOPE and DAG, when combined in these liposomes. For this purpose we constructed liposomes comprised of DOG, phytosphingosine and DOPE. Notably, these liposomes clearly exceed the transfection efficiency of Lipofectin<sup>®</sup> in an immortalized murine granulosa cell line (KK-1). In addition, the toxicity of the novel liposomes was lower than that of Lipofectin<sup>®</sup> for these cells. In the COS-7 cell line these novel liposomes gave an essentially similar level of expression as Lipofectin<sup>®</sup> at a dose optimized for the latter. Only MSC-1 cells showed resistance to lipofection specific for sphingosine liposomes when compared to the commercial reference lipo-

somes. Taken together, the fact that the lipid components are commercially available at a reasonable cost, makes the use of the liposomes practical in many transfection applications, where large amounts of the reagents are needed, e.g. in vivo.

Positively charged cationic liposomes complex effectively with negatively charged DNA [9,35]. These complexes have a net positive charge and can interact with the negatively charged cell membrane and be endocytosed by cells [9,24]. The hydrophilic, cationic headgroup of sphingosine binds tightly to DNA [21]. Interestingly, the affinity of phytosphingosine for DNA is slightly higher than that of sphingosine, whereas a reduced affinity of sphingosylphosphorylcholine containing liposomes to DNA was evident [22]. Compared to sphingosine, the extra hydroxyl group makes the polar head of phytosphingosine more hydrophilic, which may result in the location of the amino group in a less apolar environment, thus suppressing deprotonation and sterically facilitating the interaction with DNA [22]. The observed DNA affinities of the liposomes containing different sphingosine derivatives seem to correlate with their transfection efficiency.

DOPE is a commonly used 'helper' lipid in liposomal transfection compounds. It fuses spontaneously with other lipid bilayers at low pH and may facilitate the efficient liberation of DNA from endocytic vesicles to cytoplasm [36,41,45]. Some cationic lipids, e.g. dioleyltrimethylammonium (DOTMA), can mediate DNA transfer themselves, without a helper lipid [9]. On the contrary, the tested cationic sphingolipids needed DOPE to transfect efficiently (Fig. 2).

Diacylglycerols affected the transfection efficiency in a dose-dependent manner, the optimum content being approximately 5 mol%. The phase transition temperature adjusted by diacylglycerols probably partly determines the structure and stability of the liposomes and their interaction with other lipid membranes. Liposomal transfection uses mainly the endosomal pathway [24]. The multiple steps should all be optimized to achieve maximal transfection efficiency. Addition of more than one or two components to a liposome, to maximize its DNA transfer, seems necessary.



The PKC activators can affect the transfection efficiency by the calcium phosphate method depending on the cell line transfected [32,33]. In our hands, adding PMA to the liposome solution lowered the expression of the luciferase gene in KK-1 cells, indicating a role for PKC activity in modulating liposomal gene transfer pathway.

The toxicity of the sphingosine derivative containing liposomes on KK-1 cells was apparently lower than that of Lipofectin®. The non-biodegradable DOTMA in Lipofectin® may account for the difference [35]. Especially sensitive cell lines could more easily be handled with less toxic liposomes. Some special cellular functions may also be disturbed in dying cells, e.g. promoter function experiments might be aberrated due to toxic effects.

For practical applications the availability, at low cost, of the liposomal components is highly desirable. Liposomes are easily and quickly prepared. Hence, the sphingosine derivative based liposomes characterized in the present study provide an efficient, low toxicity and moderate cost alternative for transient DNA transfection of cells in vitro. They may also be of use in transfection of other materials, stable transfections as well as in in vivo applications.

### Acknowledgements

We thank Ms Riikka Kytömaa for excellent technical assistance. These studies were supported by research contracts and grants from the Academy of Finland (P.K., I.H.), The Sigrid Juselius Foundation (P.K. and I.H.), and by the Biocentrum of University of Helsinki (P.K.), and T.P. by the Turku University Graduate School for Medical Sciences. S.L. is supported by the University of Helsinki PhD program for biotechnology.

### References

- [1] L.S. Belkowski, X. Fan and B.R. Bloom (1989) Transfection of murine and human macrophage-like cell lines by cationic liposomes. *Focus* 11, 35–36.
- [2] R. Bottega and R.M. Epand (1992) Inhibition of protein kinase C by cationic amphiphiles. *Biochemistry* 31, 9025–9030.
- [3] K.H. Cheng and S.W. Hui (1986) Correlation between bilayer destabilization and activity enhancement by diacylglycerols in reconstituted Ca-ATPase vesicles. *Arch. Biochim. Biophys.* 244, 382–386.
- [4] P.R. Cullis and B.D. Kruijff (1976) <sup>31</sup>P NMR studies of unsonicated aqueous dispersions of neutral and acidic phospholipids. Effects of phase transitions, p2H and divalent cations on the motion in the phosphate region of the polar headgroup. *Biochim. Biophys. Acta* 436, 523–540.
- [5] S. Das and R.P. Rand (1986) Modification by diacylglycerol of the structure and interaction of various phospholipid bilayer membranes. *Biochemistry* 25, 2882–2889.
- [6] L. Dorman and H. Yong (1989) Cationic liposomes-mediated transfection of suspension cultures. *Focus* 11, 37.
- [7] R.M. Epand (1985) Diacylglycerols, lysolecithin, or hydrocarbons markedly alter the bilayer to hexagonal phase transition temperature of phosphatidylethanolamines. *Biochemistry* 24, 7092–7095.
- [8] R.M. Epand, R.F. Epand and C.R.D. Lancaster (1985) Modulation of the bilayer to hexagonal phase transition of phosphatidylethanolamines by acylglycerols. *Biochim. Biophys. Acta* 945, 161–166.
- [9] P.L. Felgner, T.R. Gadek, M. Holm, R. Roman, H.W. Chan, M. Wenz, J.P. Northrop, G.M. Ringold and M. Danielsen (1987) Lipofection: A highly efficient, lipid-mediated DNA-transfection procedure. *Proc. Natl. Acad. Sci.* 84, 7413–7417.
- [10] P.L. Felgner and G.M. Ringold (1989) Cationic liposome-mediated transfection. *Nature* 337, 387–388.
- [11] N. Flamand, P. Justine, F. Bernaud, A. Rougier and Q. Gaetani (1994) In vivo distribution of free long-chain sphingoid bases in the human stratum corneum by high performance liquid chromatographic analysis of stripings. *J. Chromatogr. B. Biomed. Appl.* 656, 65–71.
- [12] Y. Gluzman (1981) SV40-transformed simian cells support the replication of early SV40 mutants. *Cell* 23, 175–182.
- [13] M. Gossen and H. Bujard (1992) Tight control of gene expression in mammalian cells by tetracyclin-responsive promoters. *Proc. Natl. Acad. Sci.* 89, 5547–5551.
- [14] S.J. Gould and S. Subramani (1988) Firefly luciferase as a tool in molecular and cell biology. *Anal. Biochem.* 7, 5–13.
- [15] S.K. Gross, T.A. Lyster, J.E. Evans and R.H. McCluer (1994) Expression of glycosphingolipids in serum-free primary cultures of mouse kidney cells: male-female differences and androgen sensitivity. *Mol. Cell Biochem.* 137, 25–31.
- [16] Y.A. Hannun, C.R. Loomis A.H.M. Jr and R.M. Bell (1986) Sphingosine inhibition of protein kinase C activity and phorbol diburate binding in vitro and in human platelets. *J. Biol. Chem.* 261, 12 604–12 609.
- [17] P. Hug and R.G. Sleight (1991) Liposomes for the transformation of eukaryotic cells. *Biochim. Biophys. Acta* 1097 1–17.



- [18] S. Jiao, G. Acsadi, A. Jani, P.L. Felgner and J.A. Wolff (1992) Persistence of plasmid DNA and expression in rat brain cells in vivo. *Exp. Neurol.* 115, 400–413.
- [19] K. Kananen, M. Markkula, E. Rainio, J.-G.J. Su, A.J.W. Hsueh and I.T. Huhtaniemi (1995) Gonadal tumorigenesis in transgenic mice bearing the mouse inhibin  $\alpha$ -subunit promoter/simian virus T-antigen fusion gene: characterization of ovarian tumors and establishment of gonadotropin-responsive granulosa cell lines. *Mol. Endocrinol.* 9, 616–627.
- [20] P.K.J. Kinnunen (1992) Fusion of lipid bilayers: a model involving mechanistic connection to  $H_{II}$  phase forming lipids. *Chem. Phys. Lipids* 63, 251–258.
- [21] P.K.J. Kinnunen, M. Rytömaa, A. Kõiv, J. Lehtonen, P. Mustonen and A. Aro (1993) Sphingosine-mediated membrane association of DNA and its reversal by phosphatidic acid. *Chem. Phys. Lipids* 66, 75–85.
- [22] A. Kõiv and P.K.J. Kinnunen (1994) Binding of DNA to liposomes containing different derivatives of sphingosine. *Chem. Phys. Lipids* 72, 77–86.
- [23] J.-Y. Legendre and F.C. Szoka (1992) Delivery of plasmid DNA into mammalian cell lines using pH-sensitive liposomes: Comparison with cationic liposomes. *Pharm. Res.* 9, 1235–1242.
- [24] D. Litzinger and L. Huang (1992) Phosphatidylethanolamine liposomes: drug delivery, gene transfer and immunodiagnostic applications. *Biochim. Biophys. Acta* 1113, 201–227.
- [25] R.A. Maurer (1989) Cation liposome-mediated transfection of primary cultures of rat pituitary cells. *Focus* 11, 25–27.
- [26] J. Muthing, U. Maurer, K. Sostaric, U. Neumann, H. Brandt, S. Duvar, J. Peter-Katalinic and S. Weber-Schurholz (1994) Different distributions of glycosphingolipids in mouse and rabbit skeletal muscle demonstrated by biochemical and immunohistological analyses. *J. Biochem. Tokyo* 115, 248–256.
- [27] E.G. Nabel, D. Gordon, Z.-Y. Yang, L. Xu, H. San, G.E. Plautz, B.-Y. Wu, X. Gao, L. Huang and G.J. Nabel (1992) Gene transfer in vivo with DNA–liposome complexes: Lack of autoimmunity and gonadal localization. *Human Gene Therapy* 3, 649–656.
- [28] E.G. Nabel, G. Plautz and G.J. Nabel (1990) Site-specific gene transfer in vivo by direct gene transfer into arterial wall. *Science* 249, 1285–1288.
- [29] G.J. Nabel, A. Chang, E.G. Nabel, G. Plautz, B.A. Fox, L. Huang and S. Shu (1992) Clinical Protocol: Immunotherapy of malignancy by in vivo gene transfer into tumors. *Human Gene Therapy* 3, 399–410.
- [30] V.T. Nguyen, M. Morange and O. Bensuade (1988) Firefly luciferase luminescence assays using scintillation counters for quantitation in transfected mammalian cells. *Anal. Biochem.* 71, 404–408.
- [31] J.J. Pechon, R.R. Behringer, R.L. Cate, K.A. Harwood, R.L. Idzerda and R.D. Palmiter (1992) Directed expression of an oncogene to Sertoli cells in transgenic mice using Müllerian inhibiting substance regulatory sequences. *Mol. Endocrinol.* 6, 1403–1411.
- [32] J.T. Reston, S. Gould-Fogerite and R.J. Mannino (1991) Potentiation of DNA mediated gene transfer in NIH3T3 cells by activators of protein kinase C. *Biochim. Biophys. Acta* 1088, 270–276.
- [33] J.T. Reston, S. Gould-Fogerite, R.J. Mannino (1993) Differential effects of the phorbol ester TPA on DNA-mediated transfection in a variety of cell lines. *Biochim. Biophys. Acta* 1177, 49–53.
- [34] E. Shyamsunder, S.M. Gruner, M.W. Tate, D.C. Turner, P.T.C. So (1988) Observation of inverted cubic phase in hydrated dioleoylphosphatidylethanolamine membranes. *Biochemistry* 27, 2332–2336.
- [35] A. Singhal, L. Huang (1994) Gene transfer in mammalian cells using liposomes as carriers, in: J.A. Wolff (Ed.), *Gene Therapeutics*, Birkhäuser, Boston, pp. 118–142.
- [36] L. Stamatatos, R. Leventis, M.J. Zuckerman and J.R. Silvius (1988) Interactions of cationic lipid vesicles with negatively charged phospholipid vesicles and biological membranes. *Biochemistry* 27, 3917–3925.
- [37] M.J. Stewart, G.E. Plautz, L.D. Buono, Z.Y. Yang, L. Xu, X. Gao, L. Huang, E.G. Nabel and G.J. Nabel (1992) Gene transfer in vivo with DNA–Liposome complexes: safety and acute toxicity in mice. *Human Gene Therapy* 3, 267–275.
- [38] M.W. Tate, E.F. Eikenberry, D.C. Turner, E. Shyamsunder and S.M. Gruner (1991) Nonbilayer phases of membrane lipids. *Chem. Phys. Lipids* 57, 147–164.
- [39] C.P.S. Tilcock, M.B. Bally, S.B. Farren and P.R. Cullis (1982) Influence of cholesterol on the structural preferences of dioleoylphosphatidylethanolamine-dioleoylphosphatidylcholine systems: a phosphorus-31 and deuterium nuclear magnetic resonance study. *Biochemistry* 21, 4596–4601.
- [40] C.P.S. Tilcock and P.R. Cullis (1982) The polymorphic phase behaviour and miscibility properties of synthetic phosphatidylethanolamines. *Biochim. Biophys. Acta* 684, 212–218.
- [41] E. Wagner, C. Plank, K. Zatloukal, M. Cotten and M.L. Birnstiel (1992) Influenza virus hemagglutinin HA-2 N-terminal fusogenic peptides augment gene transfer by transferin-polylysine-DNA complexes: toward a synthetic virus-like gene-transfer vehicle. *Proc. Natl. Acad. Sci.* 89, 7934–7938.
- [42] N. Welsh, C. Oberg, C. Hellerstrom and M. Welsh (1990) Liposome mediated in vivo transfection of pancreatic islet cells. *Biomed. Biochim. Acta* 49, 1157–1164.
- [43] J.A. Wolff, R.W. Malone, P. Williams, W. Chong, G. Acsadi, A. Jani and P.L. Felgner (1990) Direct gene transfer into mouse muscle in vivo. *Science* 247, 1465–1468.
- [44] C. Zhao, T. Beeler and T. Dunn (1994) Suppressors of the  $Ca^{2+}$ -sensitive yeast mutant (*csg2*) identify genes involved in sphingolipid biosynthesis; Cloning and characterization of SCS 1, a gene required for serine palmitoyltransferase activity. *J. Biol. Chem.* 269, 21480–21488.
- [45] X. Zhou (1992) Liposome mediated gene transfer in mammalian cells, Thesis, University of Tennessee.



## New nucleoside-5'-alkylphosphonophosphates and related compounds containing 2'-deoxycytidine, thymidine and adenosine as nucleoside component. Syntheses and their effects on tumor cell growth in vitro

H. Brachwitz <sup>a,\*</sup>, Y. Thomas <sup>b</sup>, J. Bergmann <sup>a</sup>, P. Langen <sup>a</sup>, W.E. Berdel <sup>b</sup>

<sup>a</sup> Max-Delbrück-Centrum für Molekulare Medizin, Robert-Rössle-Str. 10, 13122 Berlin, Germany

<sup>b</sup> Freie Universität Berlin, Universitätsklinikum Benjamin Franklin, Abt. Hämatologie and Onkologie, Berlin, Germany

Received 4 November 1996; received in revised form 18 March 1997; accepted 19 March 1997

### Abstract

Recent studies have shown that phosphono analogs of cytidine-5'-diphosphate diacylglycerol (CDP-DAG) possessing a structurally modified lipid moiety exhibit antiproliferative activity in vitro. As an extension of our previous work we tried to elucidate whether the presence of the cytidine component is necessary for cytostatic activity. In this context we have synthesized similarly structured nucleoside-phospholipid conjugates containing nucleoside components other than cytidine, which also do not exhibit cytostatic properties as such. The compounds include 5'-alkyldiphosphates and 5'-alkylphosphonophosphates of 2'-deoxycytidine, thymidine and adenosine with different alkyl chain length as well as selected 3-hexadecyl-2-chloro-2-deoxyglycero-(1)-diphosphates and -phosphonophosphates of these nucleosides. The chemical structures of the newly synthesized nucleoside-phospholipid conjugates were confirmed by fast atom bombardment (FAB) and electrospray ionization (ESI) mass spectrometry. It was found that these compounds also inhibit the cell growth of different human cell lines, i.e. the presence of the cytidine component is not a necessary prerequisite for the antiproliferative activity of these nucleoside-phospholipid conjugates. © 1997 Elsevier Science Ireland Ltd.

**Keywords:** Nucleoside-5'-alkylphosphonophosphate; Nucleoside-5'-alkyldiphosphate; Nucleoside-phospholipid conjugates; Antiproliferative activity; Fast atom bombardment mass spectrometry (FAB-MS); Electrospray ionizations mass spectrometry (ESI-MS)

\* Corresponding author. Tel.: +49 30 94063347; fax: +49 30 94063347; e-mail: hbrachw@orion.rz.mdc-berlin.de



## 1. Introduction

Analogues of the naturally occurring cytidine diphosphate diacylglycerol (CDP-DAG) possessing a cytostatically active nucleoside as molecular component, e.g. ara-5'-cytidinediphosphate-alkyl(acyl)glycerols and -thioglycerols (Hong et al., 1986; Berdel et al., 1988; Hong et al., 1995), function as prodrugs of the nucleoside. The presence of the lipid moiety protect the parent nucleoside from rapid inactivation by enzymes. In addition, the nucleoside-phospholipid conjugates are more efficiently incorporated into cells and can be metabolized as CDP-DAG itself, resulting in the intracellular release of the nucleoside monophosphate (the precursor of the effective nucleoside triphosphate), bypassing possible deficiencies in nucleoside kinase activities of the target cells. This concept of intracellular conversion of nucleoside-phospholipid conjugates into the nucleoside monophosphates and triphosphates has also been used in the case of virostatically active 3'-deoxythymidine and 2',3'-dideoxycytidine derivatives (Brachwitz and von Janta-Lipinski, 1990; van Wijk et al., 1991a,b).

Previous work led to the first report from our laboratory that some types of alkyldeoxyglycero analogs of CDP-DAG exhibit potent antitumor activity in vitro though lacking a cytostatically active nucleoside component (Brachwitz et al., 1990b,c; Langen et al., 1992).

Further structure-activity studies have shown that CDP-DAG analogs such as 5'-cytidine-alkyldiphosphates possessing only a long chain alkyl group instead of the alkyldeoxyglycero residue as molecular component also show antiproliferative activity against various tumor cells in vitro, indicating that the presence of the glycerodeoxy moiety is not a necessary prerequisite for cytotoxicity (Brachwitz et al., 1990c; Langen et al., 1992). Furthermore, the structurally related 5'-cytidine-alkylphosphonophosphates bearing a nonhydrolysable C-P-bond, resistant to hydrolytic cleavage by phospholipase C exhibited an improved antitumoral efficacy in vitro (Brachwitz et al., 1996). The mechanism of action of these CDP-DAG analogs is not clearly understood, but it appears to be completely different from that of conventional antitumor drugs based on nucleosides

interfering with DNA synthesis. Apparently, the antiproliferative effects of these compounds are mainly attributed to the lipid component or their metabolites rather than to the nucleoside.

As an extension of our previous work we tried to elucidate whether the presence of the cytidine component is necessary for cytostatic activity.

In this context we synthesized similarly structured nucleoside-phospholipid conjugates containing nucleoside components other than cytidine, which also do not exhibit cytostatic properties as such, and studied their antiproliferative properties against various cell lines in vitro. The new compounds studied include 5'-alkyl-diphosphates and 5'-alkylphosphonophosphates of 2'-deoxycytidine, thymidine and adenosine with different alkyl chain length as well as selected 3-hexadecyl-2-chloro-2-deoxyglycero-(1) diphosphates and phosphonophosphates of these nucleosides. In Fig. 1

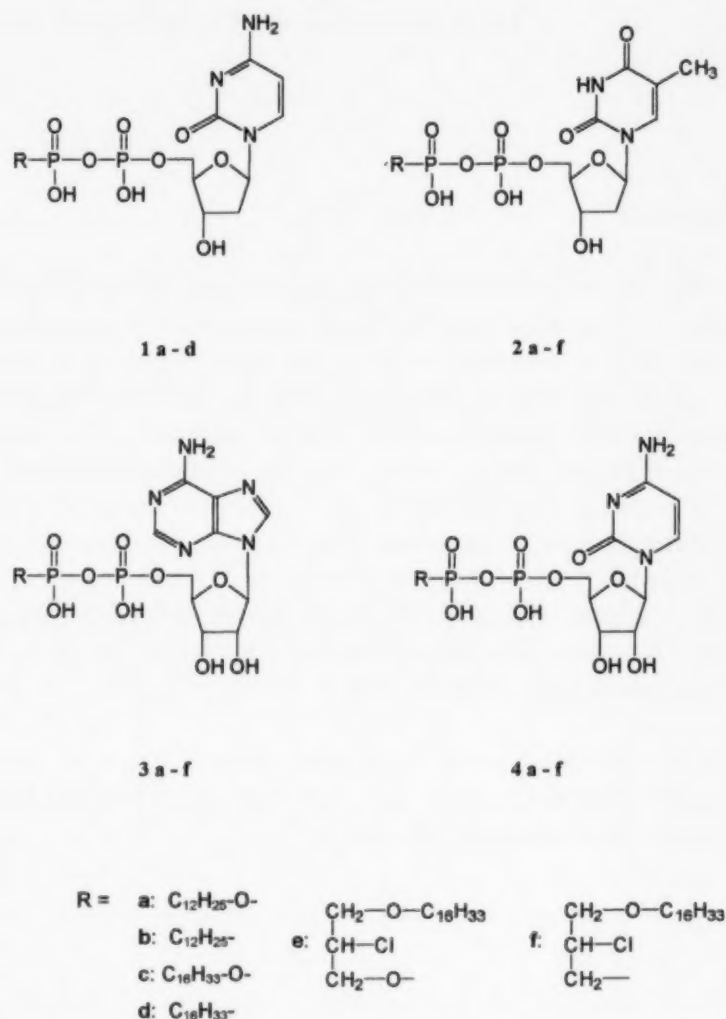


Fig. 1. Chemical structure of the newly synthesized deoxycytidine-(1), thymidine-(2) and adenosine-(3) phospholipid derivatives and the cytidine-phospholipid derivatives (4).

the chemical structures of the newly synthesized nucleoside–phospholipid conjugates together with corresponding cytidine derivatives **4** are listed. It was found that nucleoside-phospholipid conjugates of the type **1–3** also inhibit the cell growth of different human cell lines, i.e. the presence of the cytidine component is no necessary prerequisite for antiproliferative activity. The compounds **2d** and **3d** were found to show the highest cytostatic activity against a variety of tumor cell lines.

## 2. Experimental

### 2.1. Material and methods

#### 2.1.1. Materials

The long chain alkylphosphates and the *O*-alkyldeoxyglycerophosphates were obtained by reaction of the respective alcohols with phosphorus oxychloride in hexane in the presence of triethylamine similar to the method previously described (Brachwitz et al., 1982). The alkylphosphonates and the *O*-alkyldeoxyglycerophosphonates were prepared by the Michaelis-Arbuzov reaction of alkylbromides with triethylphosphite via the diethyl alkylphosphonates and bis(trimethylsilyl) alkylphosphonates (Brachwitz et al., 1996). The 5'-monophosphomorpholides of deoxycytidine, thymidine and adenosine (4-morpholine-*N,N'*-dicyclohexylcarboxamidinium salts) were obtained from Sigma.

#### 2.1.2. Cell cultures

We used a human mammary tumor cell line (MATU) and a benzpyrene induced, immortalized, but nontumorigenic human breast epithelial cell line (H 184A<sub>1</sub>N<sub>4</sub>) which was obtained from Dr M. Stampfer (Livermore Lab., University of California, Berkeley). Cells were grown as described in (Bergmann et al., 1994). The H184<sub>v-erb</sub> cells were obtained by transfection of the H184A<sub>1</sub>N<sub>4</sub> cells with *v-erb* B-DNA and cotransfection with neomycin-DNA. H184<sub>neo</sub> cells were transfected with neomycin-DNA only and serve as control (Jungahn et al., 1995). HL-60 promyelocytic leukemia cells (ATCC No 240) were routinely cultivated as described in (Langen et al., 1992).

#### 2.1.3. Measurement of the antiproliferative activity

Cell proliferation was determined using the XTT assay (Scudiero et al., 1988) (Cell Proliferation Kit II, Boehringer, Mannheim).

H184 and MATU cells were seeded in 96 microwell plates ( $5 \times 10^2$  cells/well) and were incubated for 48 h. The compounds were added, and the culture was continued further for 48 h. HL60 cells ( $1 \times 10^4$  cells/well) were seeded in the microwell plates and the compounds were added immediately. 48 h later the XTT assay was started. After incubation with the labeling mixture for 4 h at 37°C and 5% CO<sub>2</sub> the plates were measured in an ELISA reader with 450 nm and a reference wavelength with 600 nm. Decreasing of absorbance correlates with the inhibition of cell growth. The mean concentration of a compound required to cause 50% decrease in the absorbance in treated cells as compared with nontreated cells was calculated (ID<sub>50</sub>).

### 2.2. Analytical methods

Analytical thin-layer chromatography (TLC) was carried out on Merck silica gel 60 F<sub>254</sub> plates using solvent system A: chloroform-methanol-water-acetic acid (50:30:4:8, v/v/v/v); solvent system B: *n*-propanol-NH<sub>3</sub> (25%)-water (66:10:20, v/v/v).

Preparative thin-layer chromatography was carried out on Merck silica gel 60 F<sub>254</sub> preparative plates using solvent system A.

Phosphorus containing compounds were visualized with Zinzade's reagent modified according to Beiss (Kates, 1972).

The column chromatography was performed with carboxymethylcellulose (Servacel CM 52, sodium form) using chloroform/methanol mixtures with increasing polarity as eluent.

The purification by HPLC was carried out on a semipreparative RP-18-silica gel column using methanol-water gradient with increasing polarity.

The fast atom bombardment (FAB) mass spectrometry and electrospray ionization (ESI) mass spectrometry was performed on a Finnigan MAT 95 fitted with an ESI-II/APCI source. The instrument was operated in the negative mode. FAB: ionization source temperature 50°C, matrix glyc-



erol or 'magic bullet'. Resolution: 1000 at 10% valley. Cs-gun parameter: 25 kV (working voltage), 4  $\mu$ A (emission current). ESI: compressed air was used as the nebulization gas. Ionization source temperature 40°C, capillary temperature 270°C, vaporizer temperature 470°C. Resolution (low): 1000 at 10% valley, resolution (high): 6500 at 10% valley. Water–methanol (5:95) was used as mobile phase.

### 2.3. Chemical synthesis

#### 2.3.1. 2'-Deoxycytidine-5'-dodecyldiphosphate **1a**

A mixture of *n*-dodecylphosphate (288 mg, 1.1 mmol) and 2'-deoxycytidine-5'-monophosphomorpholidate (833 mg, 1.24 mmol) was codistilled twice with dry toluene and dried in vacuo over P<sub>2</sub>O<sub>5</sub> over night. Both compounds were dissolved in 40 ml of dry pyridine and stirred at room temperature under an anhydrous atmosphere for 74 h. Then pyridine was evaporated to dryness. The residue was partitioned between 80 ml of CHCl<sub>3</sub>–MeOH–H<sub>2</sub>O (1.5:3:2.5, v/v/v) and the pH was adjusted to 3–4 with formic acid. The aqueous layer was extracted twice with CHCl<sub>3</sub>. The organic layers were combined and dried over Na<sub>2</sub>SO<sub>4</sub>. Then the pH was adjusted to 9 with methanolic NH<sub>3</sub> and the solution was evaporated to dryness.

The crude product containing unreacted alkylphosphate was purified by column chromatography on CM-cellulose (sodium form, 25 g). The elution was performed with CHCl<sub>3</sub>–MeOH mixtures with increasing polarity (95:5 up to 2:3, v/v) (Comfurius and Zwaal, 1977). Fractions containing the pure diphosphate were collected and evaporated to dryness. The residue was treated with acetone. The suspension was filtered to give 207 mg of the pure compound **1a** as colorless crystals.

#### 2.3.2. Compound **1b–d**, **2a–f**, **3a–f**

The compounds were prepared as described for the synthesis of **1a** starting from the corresponding nucleosidemonophosphomorpholidate and the alkylphosphate or -phosphonate.

The compounds **2a–d** were purified by preparative TLC (see Section 2.2).

Purification of the compounds **3a–c** was carried out by HPLC on a semipreparative RP-18 column.

The analytical data of the new compounds are shown in Table 1.

### 3. Results and discussion

Previous experiments have shown that cytidine–phospholipid conjugates of type **4** exhibit antiproliferative properties in vitro though lacking a cytostatically active nucleoside component (Brachwitz et al., 1990b,c; Langen et al., 1992; Brachwitz et al., 1996). In order to elucidate the influence of the nucleoside component on the antitumoral efficacy in more detail we have synthesized the nucleoside-phospholipid conjugates **1–3**, possessing deoxycytidine, thymidine and adenosine as nucleoside components. Since the cytidine derivatives of type **4** with an alkyl chain of less than 12 C-atoms have been found to be practically ineffective, while the hexadecyl derivatives have proved to be the most effective ones, we have prepared the dodecyl- and hexadecylesters of the 5'-nucleosidediphosphates (**1a,c–3a,c**) and of the phosphonophosphates (**1b,d–3b,d**) to compare them with the corresponding 5'-cytidine derivatives (**4a–d**). Moreover, we have synthesized some selected 5'-thymidine- and 5'-adenosine-alkyldeoxyglycerodiphosphates (**2e, 3e**) and -phosphonophosphates (**2f, 3f**), the phospholipid moiety of which has been used as the decisive structural element in other cytostatically active phospholipids (Brachwitz et al., 1982; 1990a,b,c; Langen et al., 1992).

#### 3.1. Chemistry

The new nucleoside-phospholipid conjugates were synthesized by condensation reaction of 5'-nucleoside monophosphomorpholidate with the alkylphosphates, alkylphosphonates and the corresponding *O*-alkyldeoxyglycero derivatives, respectively, following the procedure described for the synthesis of cytidinediphosphate-diacylglycerol analogs (Moffatt and Khorana, 1961; Brachwitz et al., 1996). The reaction was performed by



Table 1  
Analytical data of the compounds 1–3

Compound	UV <sup>a</sup>	TLC		MS <sup>d</sup>	Formula	Elemental analysis calculated (found)		
		R <sub>f</sub> (A) <sup>b</sup>	R <sub>f</sub> (B) <sup>c</sup>			C	H	N
1a	272	0.33	0.53	554 [M-H] <sup>-</sup>	C <sub>21</sub> H <sub>37</sub> N <sub>3</sub> Na <sub>2</sub> O <sub>10</sub> P <sub>2</sub> ·2H <sub>2</sub> O	40.23 (40.12)	6.41 (6.36)	6.69 (6.44)
1b	272	0.35	0.53	538 [M-H] <sup>-</sup>	C <sub>21</sub> H <sub>37</sub> N <sub>3</sub> Na <sub>2</sub> O <sub>9</sub> P <sub>2</sub> ·2H <sub>2</sub> O	40.78 (40.15)	6.52 (6.71)	6.79 (7.58)
1c	272	0.39	0.54	610 [M-H] <sup>-</sup>	C <sub>25</sub> H <sub>45</sub> N <sub>3</sub> Na <sub>2</sub> O <sub>10</sub> P <sub>2</sub> ·2H <sub>2</sub> O	43.42 (43.01)	7.14 (6.85)	6.08 (5.64)
1d	272	0.40	0.54	594 [M-H] <sup>-</sup>	C <sub>25</sub> H <sub>53</sub> N <sub>5</sub> O <sub>9</sub> P <sub>2</sub> ·3H <sub>2</sub> O	43.88 (44.48)	8.63 (8.59)	10.24 (9.49)
2a	268	0.43	0.55	569 [M-H] <sup>-</sup>	C <sub>22</sub> H <sub>38</sub> N <sub>2</sub> Na <sub>2</sub> O <sub>11</sub> P <sub>2</sub> ·2H <sub>2</sub> O	40.06 (40.15)	6.57 (6.00)	4.24 (3.69)
2b	268	0.41	0.55	575 [M-2H + Na] <sup>-</sup>	C <sub>22</sub> H <sub>38</sub> N <sub>2</sub> Na <sub>2</sub> O <sub>10</sub> P <sub>2</sub>	41.77 (41.87)	6.96 (7.20)	8.86 (8.57)
2c	268	0.49	0.54	647 [M-2H + Na] <sup>-</sup>	C <sub>26</sub> H <sub>46</sub> N <sub>2</sub> Na <sub>2</sub> O <sub>11</sub> P <sub>2</sub> ·3H <sub>2</sub> O	43.10 (43.14)	7.23 (6.48)	3.87 (3.42)
2d	267	0.45	0.54	609 [M-H] <sup>-</sup>	C <sub>26</sub> H <sub>46</sub> N <sub>2</sub> Na <sub>2</sub> O <sub>10</sub> P <sub>2</sub> ·3H <sub>2</sub> O	44.06 (42.90)	7.68 (6.80)	3.95 (3.43)
2e	268	0.45	0.56	717 [M-H] <sup>-</sup>	C <sub>29</sub> H <sub>51</sub> ClN <sub>2</sub> Na <sub>2</sub> O <sub>12</sub> P	42.99 (42.72)	6.97 (6.70)	3.46 (3.41)
2f	267	0.48	0.56	723 [M-2H + Na] <sup>-</sup>	C <sub>29</sub> H <sub>51</sub> ClN <sub>2</sub> Na <sub>2</sub> O <sub>11</sub> P·2H <sub>2</sub> O	44.47 (44.41)	7.08 (7.03)	3.66 (3.66)
3a	260	0.37	0.52	594 [M-H] <sup>-</sup>	C <sub>22</sub> H <sub>43</sub> N <sub>6</sub> O <sub>10</sub> P <sub>2</sub> ·2H <sub>2</sub> O	40.74 (40.85)	7.15 (7.31)	12.96 (13.37)
3b	260	0.33	0.52	578 (i) [M-H] <sup>-</sup>	C <sub>22</sub> H <sub>39</sub> N <sub>5</sub> O <sub>9</sub> P <sub>2</sub> ·2H <sub>2</sub> O	42.31 (41.88)	7.10 (7.11)	11.22 (11.66)
3c	260	0.39	0.51	650 [M-H] <sup>-</sup>	C <sub>26</sub> H <sub>53</sub> N <sub>7</sub> O <sub>10</sub> P <sub>2</sub> ·2H <sub>2</sub> O	43.26 (43.00)	7.96 (7.66)	13.58 (13.12)
3d	260	0.37	0.51	634 (i) [M-H] <sup>-</sup>	C <sub>26</sub> H <sub>45</sub> N <sub>5</sub> Na <sub>2</sub> O <sub>9</sub> P <sub>2</sub> ·2H <sub>2</sub> O	44.19 (43.45)	6.85 (6.58)	9.91 (10.08)
3e	260	0.38	0.56	742 (i) [M-H] <sup>-</sup>	C <sub>29</sub> H <sub>50</sub> ClN <sub>5</sub> Na <sub>2</sub> O <sub>11</sub> P·2.3H <sub>2</sub> O	41.35 (41.11)	6.70 (6.48)	8.31 (8.10)
3f	260	0.38	0.56	726 [M-H] <sup>-</sup>	C <sub>29</sub> H <sub>50</sub> ClN <sub>5</sub> Na <sub>2</sub> O <sub>10</sub> P·2H <sub>2</sub> O	43.10 (43.00)	6.73 (6.42)	8.67 (8.45)

<sup>a</sup>  $\lambda_{\max}$  (nm), MeOH; <sup>b</sup> Solvent system A: CHCl<sub>3</sub>-MeOH-H<sub>2</sub>O-AcOH 50:30:8:4; <sup>c</sup> Solvent system B: PrOH-H<sub>2</sub>O-NH<sub>3</sub> (25%) 66:20:10;

<sup>d</sup> Mass spectrometry: negative ion ESI-MS, (i) negative ion FAB-MS.

stirring a mixture of the dry reaction components in pyridine for about 70–100 h under an anhydrous atmosphere at 35–42°C. Although in all experiments an excess of the phosphates and phosphonates, respectively, has been used under various reaction temperatures, a complete conversion of the nucleoside component could not be achieved. Yields of the conjugates range between 10 and 30% only. The alternative strategy for the synthesis of the conjugates involving the reaction of the lipidphosph(on)ate morpholides with the

nucleoside monophosphates, which has also been successfully used for the preparation of nucleoside-phospholipid conjugates (Brachwitz and von Janta-Lipinski, 1990; van Wijk et al., 1992) did not give improved yields (results not given).

The desired products were isolated from the reaction mixture by carboxymethylcellulose column chromatography, using a discontinuous chloroform-methanol gradient with increasing solvent polarity as described previously (Comfurius and Zwaal, 1977; Brachwitz et al., 1996).

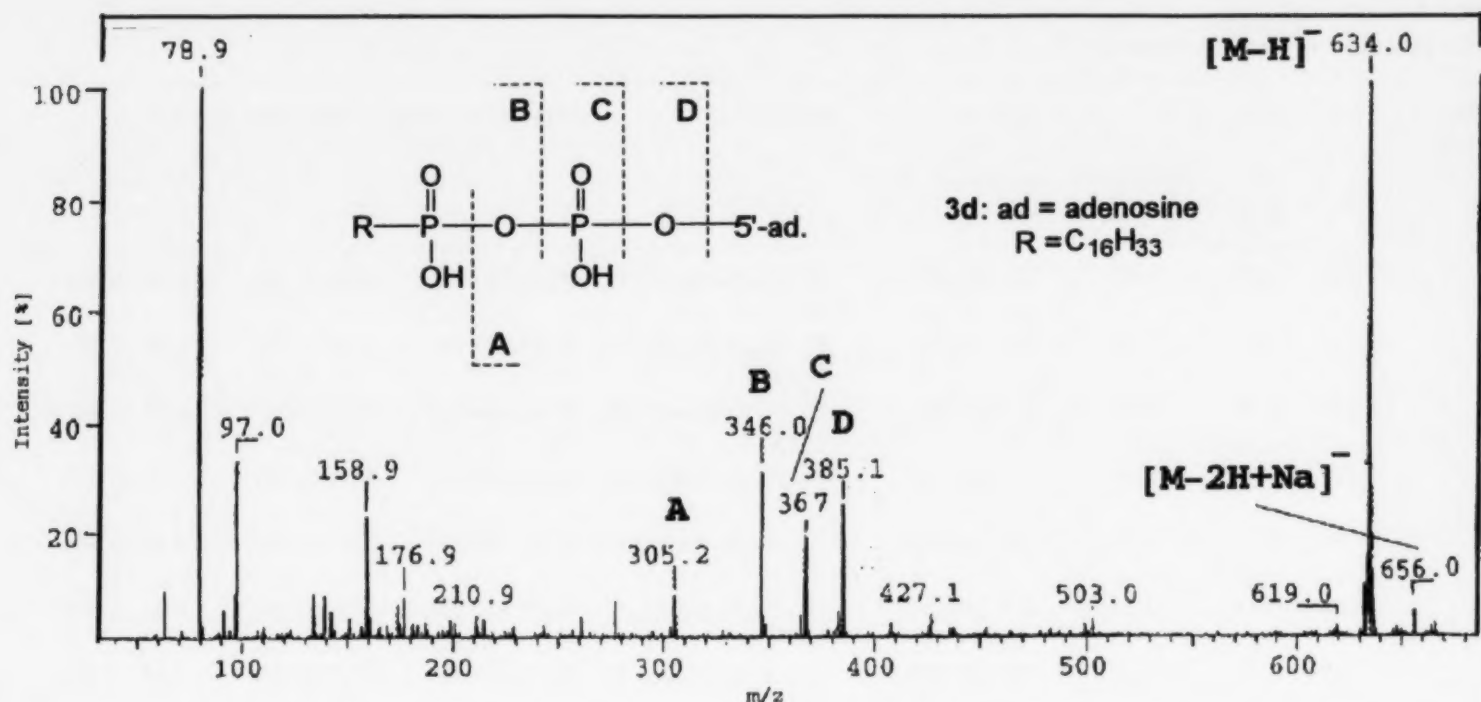


Fig. 2. Negative-ion fast atom bombardment mass spectra and fragmentation of compound 3d.

However, in the case of compounds **2a–d** and **3a–c**, the unreacted phosph(on)ates could not be completely removed from the reaction mixtures by this method. The pure thymidine derivatives **2a–d** were obtained in small amounts by preparative thin layer chromatography on silica gel. The adenosine derivatives **3a–c** were successfully purified by semipreparative reversed-phase HPLC on RP-18-silicagel using chloroform-methanol gradient as eluent.

### 3.2. Analytical

The purity of all new compounds was checked by thin layer chromatography (TLC). The chemical structure was confirmed by elemental analysis, negative-ion electrospray ionization (ESI) mass spectrometry and negative-ion fast atom bombardment (FAB) mass spectrometry, as well as UV-spectrometry.

The negative-ion ESI spectra of the compounds are characterized by the presence of the  $[M-H]^-$  ions and the intensive  $[M-2H+Na]^-$  ions, the latter being the base peaks in the spectra of the compounds **1a**, **1c**, **2c**, **2e–f**, **3d–f**. The  $[M-H]^-$  ions are the base peaks in the spectra of **1b** and

**3c**. Additional ions of lower intensity (4.3–15.1% of the corresponding base peak), attributable to the sodium adducts  $[M-3H+2Na]^-$ , are found in the spectra of the compounds **1a**, **1c**, **2c**, **2e–f**, **3c** and **3f**. In the case of compound **2c** this peak shows an intensity of 34% of the base peak.

Similar ions are also observed in the negative-ion FAB spectra. In these the compounds **1a**, **1b**, **1d**, **2a**, **2f**, **3a–e** contain the  $[M-H]^-$  ions as base peak, in the spectra of the compounds **1c**, **2c**, **2e**, **2f**, **3e** and **3f** the base peaks are represented by the  $[M-2H+Na]^-$  ions. In addition to the ions described, in most cases a series of fragment ions are present. As an example the negative-ion FAB mass spectrum of the compound **3d** is given in Fig. 2. The fragmentation led to the formation of the  $m/z$  305 ion (fragment A), which was generated by expulsion of the adenosine monophosphate moiety from the molecular ion, and the  $m/z$  346 ion representing the fragment B. A further characteristic peak is found at  $m/z$  385, which corresponds to the alkyl diphosphate ion (fragment C). The fragment D produced by the loss of the adenosine residue from the molecular ion is found at  $m/z$  367.

Table 2

Cytostatic activity (halfmaximal inhibitory concentration, ID<sub>50</sub>) of nucleoside-phospholipid derivatives 1–4

Compound	ID <sub>50</sub> -values [ $\mu$ M] $\pm$ S.E.				
	H184A <sub>1</sub> N <sub>4</sub>	H184 v-erb B	H184 B4 neo	MATU	HL 60
1a	> 100	> 100	> 100	> 100	> 100
1b	> 100	> 100	> 100	> 100	> 100
1c	34.3 $\pm$ 1.9	47.5 $\pm$ 5.5	58.0 $\pm$ 2.0	42.5 $\pm$ 0.5	> 100
1d	16.0 $\pm$ 3.0	1.0 $\pm$ 1.0	15.0 $\pm$ 1.0	21.5 $\pm$ 1.5	50.00 $\pm$ 1.0
2a	> 100	> 100	> 100	> 100	> 100
2b	> 100	> 100	> 100	> 100	> 100
2c	54.7 $\pm$ 0.7	69.0 $\pm$ 1.5	98.5 $\pm$ 11.5	58.3 $\pm$ 8.1	> 100
2d	12.0 $\pm$ 4.0	8.5 $\pm$ 1.5	11.5 $\pm$ 3.5	11.5 $\pm$ 5.5	57.0 $\pm$ 7.4
2e	42.5 $\pm$ 0.5	30.0 $\pm$ 1.0	42.5 $\pm$ 2.5	51.0 $\pm$ 2.0	> 100
2f	41.7 $\pm$ 2.9	41.5 $\pm$ 3.5	35.0 $\pm$ 1.0	37.2 $\pm$ 4.5	> 100
3a	> 100	> 100	> 100	> 100	> 100
3b	> 100	> 100	> 100	> 100	> 100
3c	35.0 $\pm$ 3.0	43.5 $\pm$ 2.5	42.5 $\pm$ 0.5	36.0 $\pm$ 2.0	92.8 $\pm$ 8.1
3d	10.5 $\pm$ 1.4	10.5 $\pm$ 3.5	11.5 $\pm$ 0.5	7.0 $\pm$ 0.7	32.7 $\pm$ 2.2
3e	35.0 $\pm$ 7.1	25.0 $\pm$ 1.0	29.0 $\pm$ 2.0	42.5 $\pm$ 2.5	> 100
3f	34.3 $\pm$ 5.4	32.0 $\pm$ 1.0	34.5 $\pm$ 1.5	41.5 $\pm$ 1.5	81.7 $\pm$ 3.0
4a	> 100	> 100	> 100	> 100	> 100
4b	> 100	> 100	> 100	> 100	> 100
4c	79.5 $\pm$ 8.2	66.0 $\pm$ 3.0	67.0 $\pm$ 2.5	> 100	> 100
4d	16.0 $\pm$ 1.0	17.0 $\pm$ 2.8	14.8 $\pm$ 1.3	15.7 $\pm$ 1.4	65.7 $\pm$ 5.2
4e	52.5 $\pm$ 11.5	—	—	56.5 $\pm$ 0.5	—
4f	40.5 $\pm$ 5.5	40.0 $\pm$ 1.0	42.0 $\pm$ 1.0	29.5 $\pm$ 4.5	> 100

### 3.3. Antiproliferative activity

The newly synthesized nucleoside-phospholipid conjugates 1–3 were tested for antiproliferative activity against the mammary epithelial cell line H184A<sub>1</sub>N<sub>4</sub> before and after transfection with the v-erbB oncogene, whose gene products are involved in the dysregulation of signal transduction. In this context it was of interest whether the change of the mammary epithelial cell line H184A<sub>1</sub>N<sub>4</sub> by the v-erbB oncogene is reflected by an altered sensitivity against the new nucleoside-phospholipid conjugates. In addition, the effects of these compounds against the promyelocytic leukemia cells HL 60 and the human mammary tumor cell line MATU were studied. The results are summarized in Table 2 in the form of the ID<sub>50</sub>-values, i.e. the concentration of the compounds resulting in 50% inhibition of the cell growth. Previously we have found that cytidine-phospholipid conjugates containing special lipid components exhibited cytostatic activity against

human normal and tumor cells (Brachwitz et al., 1996). The data concerning these derivatives are given for comparison.

The present studies clearly indicate that structurally related compounds in which cytidine is exchanged by deoxycytidine, thymidine and adenosine show antiproliferative effects, too. In Fig. 3 the dependence of the ID<sub>50</sub>-value on the type of the nucleoside and the lipid residue is given for the cell lines H184. The dodecylphosphates (1a–3a) and the dodecylphosphonophosphates (1b–3b) were ineffective, the ID<sub>50</sub> values were higher than 100  $\mu$ M, as was found for the cytidine derivatives (4a,b). The exchange of cytidine by deoxycytidine, thymidine and adenosine in the hexadecylphosphates (1c–3c) causes an increase in the antiproliferative activity against H184 and MATU. Especially the antiproliferative activity of the deoxycytidine and the adenosine derivatives (1c, 3c) were remarkably superior to the corresponding cytidine derivative 4c (Fig. 3a). Surprisingly the HL 60 cells were not found to be



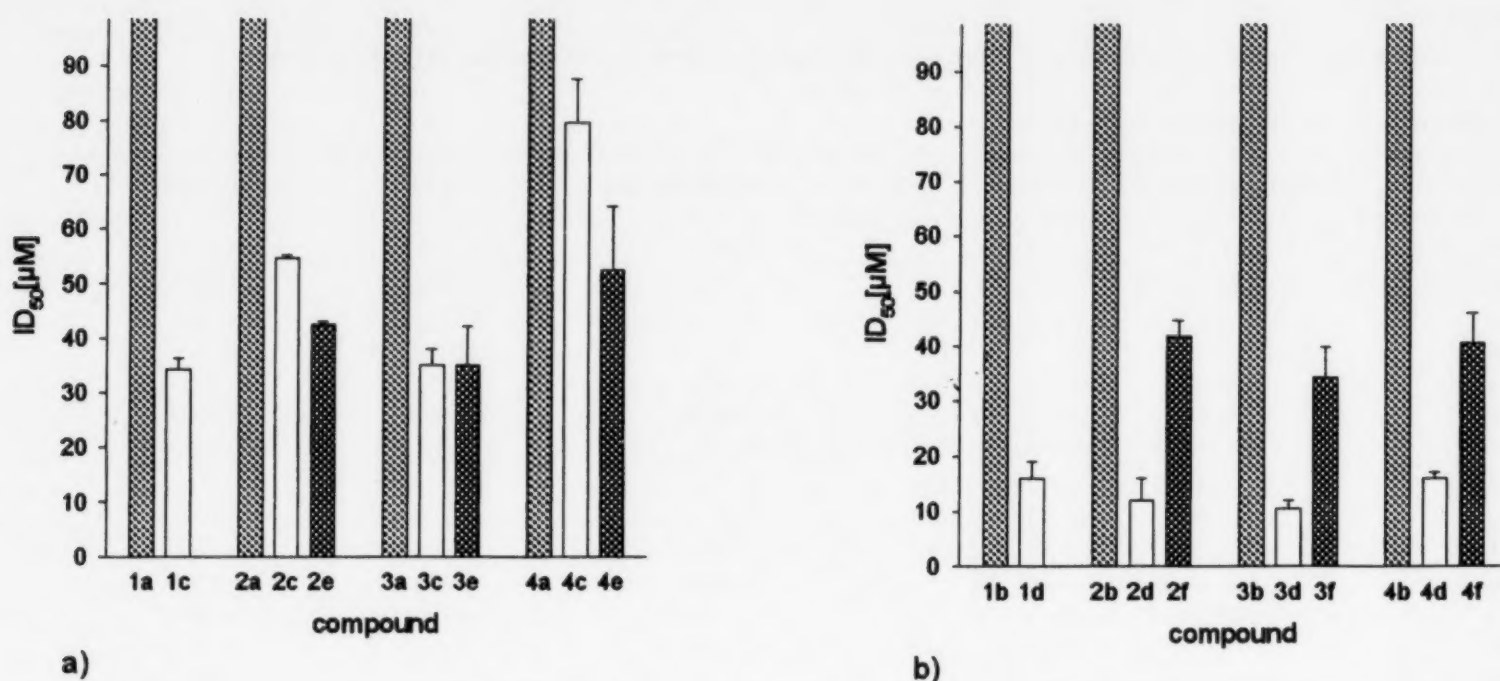


Fig. 3.  $ID_{50}$ -values of nucleoside-5'-diphosphates (a) and nucleoside-5'-phosphonophosphates (b) for the cell line H184.

sensitive to the hexadecyldiphosphates (**1c–3c**) as already shown for the cytidine derivative (**4c**). In the case of the halogene-containing glycerodeoxydiphosphates (**2e**, **3e**) the change of the nucleoside residue did not strongly influence the cytostatic activity. Thus, the  $ID_{50}$ -values of the substances **2e–3e** are similar to that of the cytidine derivative **4e** (Fig. 3a). Contrary to the corresponding cytidine diphosphate, the introduction of the halogen-containing alkyldeoxyglycerol group instead of the hexadecyl group in the thymidine and adenosine derivatives did not improve the antiproliferative efficacy in all cell lines used (except HL 60).

The hexadecylphosphonophosphates of the four nucleosides (**1d–4d**) show a greater activity than the corresponding hexadecyldiphosphates (**1c–4c**) as shown in Fig. 3b presumably due to the increased biostability of the P-C bond against cleavage by phospholipase C. Their  $ID_{50}$ -values are in the range of 7–20  $\mu$ M. The adenosine derivative **3d** was found to be the most effective compound ( $ID_{50}$ -value 7–10  $\mu$ M) in MATU and H184 cell lines.

We did not find obvious differences between the antiproliferative activity of the H184 cells before and after transfection with the *erb B* oncogen and between that of the nontumorigenic cell line H184 and the tumor cell line MATU.

The mode of action of the new nucleoside-phospholipid conjugates is still unknown, but the results obtained demonstrate the potential interest of these compounds in cancer treatment.

#### Acknowledgements

The authors thank Ms I. Thun for the tests of cytostatic activity. This work was supported in part by a grant from the BMBF, grant no. 01GB9402.

#### References

- Berdel, W.E., Danhauser, S., Hong, C.I., Schick, H.D., Reichert, A., Busch, R., Rastetter, J., Vogler, W.R., 1988. Influence of 1-beta-D-arabinofuranosylcytosine conjugates of lipids on the growth and metastasis of Lewis lung carcinoma. *Cancer Res.* 48, 826–829.
- Bergmann, J., Junghahn, I., Brachwitz, H., Langen, P., 1994. Multiple effects of antitumor alkyl-lysophospholipid analogs on the cytosolic free  $Ca^{2+}$  concentration in a normal and a breast cancer cell line. *Anticancer Res.* 14, 1549–1556.
- Brachwitz, H., Hintsche, R., Langen, P., Schildt, J., 1982. Halo Lipids. 5. Synthesis, Nuclear Magnetic-Resonance Spectra and Cytostatic Properties of Halo Analogs of Alkyllysophospholipids. *Chem. Phys. Lipids* 31, 33–52.

- Brachwitz, H., Lachmann, U., Thomas, Y., Bergmann, J., Berdel, W.E., Langen, P., 1996. Synthesis and antiproliferative activity of cytidine-5'-alkylphosphonophosphates and structurally related compounds. *Chem. Phys. Lipids* 83, 77–85.
- Brachwitz, H., Langen, P., Dube, G., Schildt, J., Paltauf, F., Hermetter, A., 1990a. Halo lipids. 10. Synthesis and cytostatic activity of *O*-alkylglycerophospho-L-serine analogs. *Chem. Phys. Lipids* 54, 89–98.
- Brachwitz, H., Langen, P., Paltauf, F., 1990b. Cytidine-5'-diphosphate-alkylglycerol analogs (CDP-AG) — a new class of cytostatically active phospholipids. *Cancer. Res. Clin. Oncol. (Supplement)* 116, 993.
- Brachwitz, H., Schönfeld, R., Langen, P., Paltauf, F., Hermetter, A., 1990c. New cytidine-5'-diphosphate alkanols and glycerols, a process for preparing them and their use. Patent PCT WO 90/02134.
- Brachwitz, H., von Janta-Lipinski, M., 1990. Verfahren zur Herstellung von 2',3'-Dideoxythymidin-5'-diphosphat-1,2-di-*O*-alkylglycerolen und von deren Salzen. Deutsches Patent DD 279, 249.
- Comfurius, P., Zwaal, R.F.A., 1977. The enzymatic synthesis of phosphatidylserine and purification by CM-cellulose column chromatography. *Biochim. Biophys. Acta* 488, 36–42.
- Hong, C.I., An, S.H., Buchheit, D.J., Nechaev, A., Kirisits, A.J., West, C.R., Berdel, W.E., 1986. Nucleoside Conjugates. 7. Synthesis and Antitumor of 1-beta-D-Arabinofuranosylcytosin Conjugates of Ether Lipids. *J. Med. Chem.* 29, 2038–2044.
- Hong, C.I., Nechaev, A., Kirisits, A.J., Vig, R., Hui, S.W., West, C.R., 1995. Nucleoside conjugates. 14. synthesis and antitumor activity of 1-beta-d-arabinofuranosylcytosine conjugates of ether lipids with improved water solubility. *J. Med. Chem.* 38, 1629–1634.
- Junghahn, I., Bergmann, J., Langen, P., Thun, I., Vollgraf, C., Brachwitz, H., 1995. Effect of alp analogs on inositol trisphosphate formation in h183 mammary epithelial cells before and after transfection with *v-erb b* oncogene. *Anti-cancer Res.* 15, 449–454.
- Kates, M., 1972. Techniques of lipidology: isolation, analysis and identification of lipids, In: Work, T.S. and Work, E. (Eds.), *Laboratory techniques in biochemistry and molecular biology*. American Elsevier Publishing, New York, pp. 421.
- Langen, P., Maurer, H.R., Brachwitz, H., Eckert, K., Veit, A., Vollgraf, C., 1992. Cytostatic effects of various alkyl phospholipid analogues on different cells in vitro. *Anticancer Res.* 12, 2109–2112.
- Moffatt, J.G., Khorana, H.G., 1961. Nucleoside Polyphosphates. X. The Synthesis and Some Reactions of Nucleoside-5'Phosphoromorpholides and Related Compounds. Improved Methods for the Preparation of Nucleoside-5'Polyphosphates. *J. Am. Chem. Soc.* 83, 649–658.
- Scudiero, D.A., Shoemaker, R.H., Paull, K.D., Monks, A., Tierney, S., Nofziger, T.H., Currens, M.J., Seniff, D., Boyd, M.R., 1988. Evaluation of a Soluble Tetrazolium/Formazan Assay for Cell Growth and Drug Sensitivity in Culture Using Human and Other Tumor Cell Lines. *Cancer Res.* 48, 4827–4833.
- van Wijk, G.M.T., Hostetler, K.Y., Schlame, M., van den Bosch, H., 1991a. Cytidine diphosphate diglyceride analogs of antiretroviral dideoxynucleosides: evidence for release of dideoxynucleoside-monophosphates by phospholipid biosynthetic enzymes in rat liver subcellular fractions. *Biochim. Biophys. Acta* 1086, 99–105.
- van Wijk, G.M.T., Hostetler, K.Y., van den Bosch, H., 1991b. Lipid conjugates of antiretroviral agents: release of antiretroviral nucleoside monophosphates by a nucleoside diphosphate diglyceride hydrolase activity from rat liver mitochondria. *Biochim. Biophys. Acta* 1084, 307–310.
- van Wijk, G.M.T., Hostetler, K.Y., van den Bosch, H., 1992. Antiviral nucleoside diphosphate diglycerides: improved synthesis and facilitated purification. *J. Lipid Res.* 33, 1211–1219.





## Monolayer properties of monosialoganglioside in the mixed diacetylene lipid films on the air/water interface

Quan Cheng, Raymond C. Stevens \*

*Department of Chemistry, University of California, Berkeley, CA 94720, USA  
Materials Sciences Division, Lawrence Berkeley Laboratory, Berkeley, CA 94720, USA*

Received 4 December 1996; received in revised form 19 March 1997; accepted 19 March 1997

### Abstract

By combining the cellular membrane receptor GM1 with diacetylenic lipids, blue monolayer films can be created that undergo a colorimetric transition to red upon exposure to cholera toxin. The monolayer behaviour of GM1 in diacetylenic films was studied using the Langmuir-Blodgett technique with the goal of building colorimetric biosensors. Macroscopic characteristics of the films were obtained through analysis of surface pressure-area isotherms of GM1 and derivatized diacetylenic lipids at the air/water interface. Film optical properties and colorimetric response were optimized through modification of the ratio of receptor GM1 to diacetylene lipids and detection of the target analyte cholera toxin. Isothermic compression studies show that the mixed monolayers exhibit favourable film compressibility and high transferability as compared to the monolayers consisting of pure GM1. The impact of ionic strength and sub-phase pH on molecular interactions of lipids and miscibility of the mixed films is discussed. Contrary to usual temperature dependence observed for saturated fatty lipids, GM1/diacetylenic monolayers display an inverse relationship between temperature and surface pressure. © 1997 Elsevier Science Ireland Ltd.

**Keywords:** Gangliosides; Polydiacetylene; Monolayers; Biosensors

### 1. Introduction

The incorporation of biological receptor–ligand molecules into organized lipid matrix as biosensors has enormous potential. Construction of such biosensory materials typically involves the appropriate mixing of more than two components

at the two dimensional aqueous surface. Deviation from ideal mixing is often found in mixed films when two structurally different molecules are involved (Gaines, 1966). As the orientation and interactions of biological ligands residing in the film ultimately determine the sensors' recognition ability and effectiveness, the film properties such as molecular packing, compressibility, stability and miscibility must be characterized for

\* Corresponding author. Tel.: +1 510 6438285.

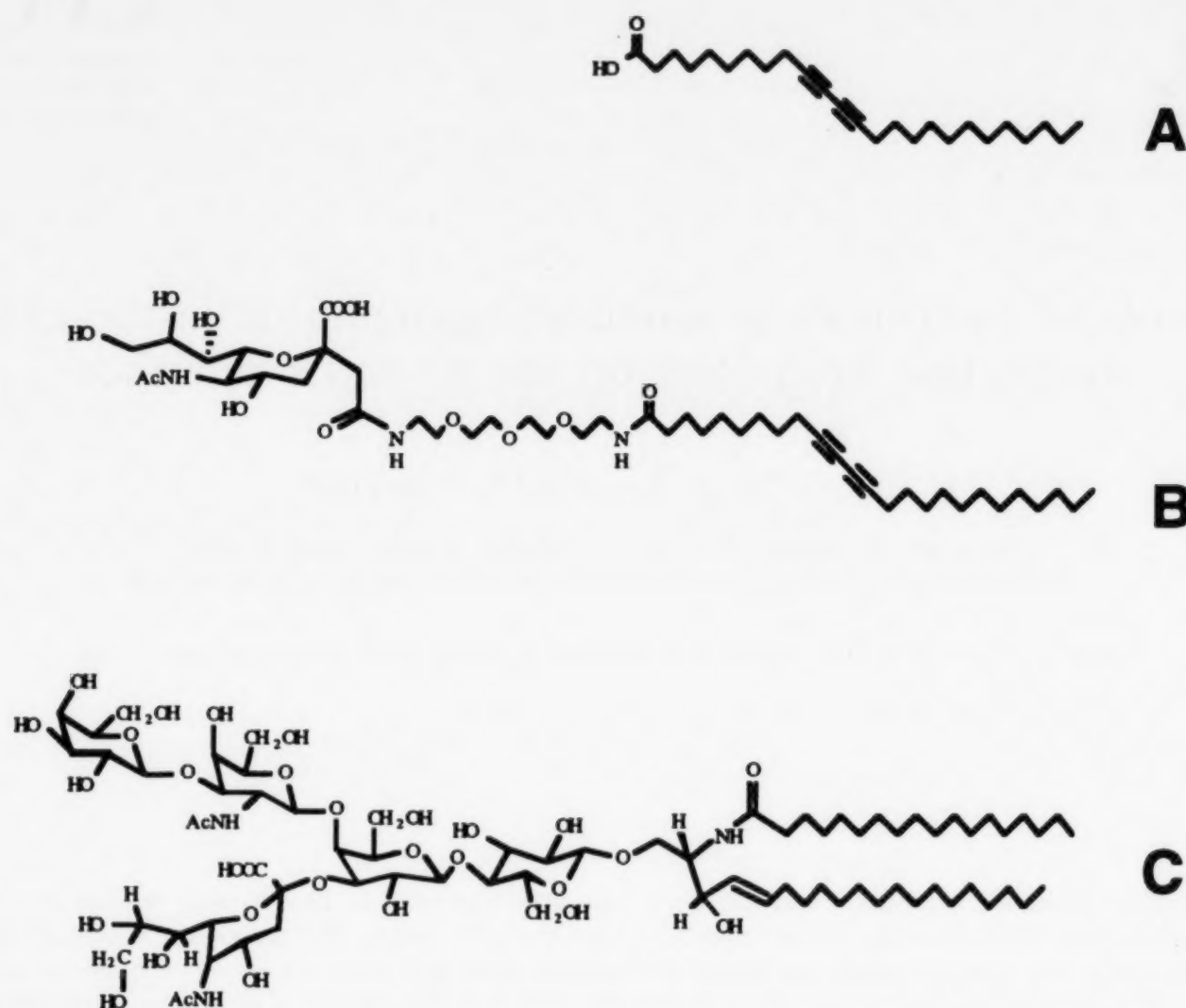


Fig. 1. Structure of lipid molecules used in the investigation. (A) 10,12-pentacosadiynoic acid (PDA); (B) Sialic acid derivatized 10,12-pentacosadiynoic acid (SA-PDA); (C) Monosialoganglioside GM1.

achieving maximal sensing capability of the biomaterials.

The Langmuir-Blodgett (LB) monolayer technique provides a useful means to study molecular interactions in a two-dimensional array of molecules (Roberts, 1990; Ulman, 1991). By monitoring the spread and compression of molecules at the water/air interface, phase transitions, molecular packing, and head-group interaction can be analyzed on the basis of the pressure-area ( $\pi$ -A) isotherm. In addition, the LB monolayer allows for precise control in monolayer formation and transfer. Well-defined lipid assemblies with various surface functionality can thus be built on both aqueous surface and solid substrates for biosensor study or biological membrane modelling (Lukes et al., 1992; Terrettaz et al., 1993;

Tronin et al., 1994; Fujita et al., 1994).

We are particularly interested in constructing monolayer biosensors for biological pathogens. By taking advantage of the unique stress-induced chromatic properties of polydiacetylene film made from 10,12-pentacosadiynoic acid (PDA), we developed a colorimetric film sensor for cholera toxin (CT) in which membrane receptor ganglioside GM1 was embedded (Charych et al., 1996). Gangliosides are glycolipids located in the plasma membrane of vertebrate cells. These molecules play a variety of roles in neuronal differentiation, neuronal growth, synapse formation, and maintenance of neuronal plasticity (Svennerholm, 1994). Fig. 1 illustrates the molecular structure of PDA, sialic acid derivatized PDA (SA-PDA), and monosialoganglioside (GM1)

used in the biosensor design. The interaction between the ganglioside and the toxin provides the molecular basis of the recognition event, which is consequently amplified into a measurable colour change in the PDA films. The presence of SA–PDA in the films promotes the colour transition by lowering the activation barrier of the chromatic transition, making the films metastable and thus ready to respond to molecular recognition events (Charych et al., 1996).

This paper reports the isothermic investigation of ternary GM1/SA–PDA/PDA Langmuir monolayers on aqueous sub-phase as a function of composition, temperature, sub-phase ionic content, and sub-phase pH. As part of a systematic approach of optimizing the biosensing response of the films, this study addressed the macroscopic features of the film that strongly influence the monolayer formation and transfer, and consequently the sensing patterns. Much of the effort was placed on characterizing the 5%GM1/5%SA–PDA/90%PDA film, as the ternary features of this film have been found to create the most effective biosensors for the detection of cholera toxin. Comparison of 5% GM1/5%SA–PDA/90%PDA films to the pure and binary PDA films were made to reveal the nature of interactions of GM1 with diacetylenic lipids and the effect of such interactions on monolayer formation and films' sensing capability.

## 2. Experimental procedures

### 2.1. Materials

Monosialoganglioside (GM1) was purchased from Matreya (Pleasant Gap, PA), and was > 98% purity according to the manufacturer. 10,12-Pentacosadiynoic acid (PDA) was obtained from Farchan (Gainesville, FL), and was purified through filtration before use. Sialic acid derivatized PDA (SA–PDA) was a gift of Dr Jon Nagy of Lawrence Berkeley Laboratory and was synthesized according to literature (Spevak, 1984). Chloroform and methanol were obtained

from Aldrich (Milwaukee, WI) with the best available grade. Cadmium chloride and sodium phosphate were obtained from Mallinckrodt (St. Louis, MO). All chemicals were used without further purification. The water used in all experiments was doubly distilled deionized water purified with a Nanopure water system.

### 2.2. Apparatus

A Langmuir-Blodgett trough (KSV mini-trough, KSV Instruments, Finland) was used for the preparation of the samples. The dimensions of the trough are 300 × 75 mm. The movement of the barrier for compressing the spread of molecules at the water/air interface was controlled through a micromotor, and the surface pressure was measured and monitored by a Wilhemy balance. The temperature was controlled by a water bath circulator (Fisher Scientific). The humidity was maintained at 45 ± 5%.

### 2.3. Methods

PDA and SA–PDA were dissolved in chloroform, while the ganglioside GM1 was dissolved in a 2:1 CHCl<sub>3</sub>:CH<sub>3</sub>OH (v:v) mixed solvent. The above solutions were then mixed to the designated molar ratios while the total concentration was brought to ca. 2 mM. The PDA solutions were spread on the aqueous sub-phase by using a microsyringe, and rested for 30 min to allow organic solvent to evaporate before compression. The isotherms of 100% PDA and 100% GM1 were monitored as a function of evaporation time to determine if there was any material loss during the resting period. We found, between 5 min and 1 h evaporation period, the difference in molecular area and surface pressure for both compounds was insignificant (< 2%). The compression speed was set at 5 mm/min.

Nanopure water (pH 5.8) was used in most experiments as the sub-phase. CdCl<sub>2</sub> was added in experiments where sub-phase was adjusted by cationic species. Solution pH was controlled by 0.05 M phosphate buffer.



#### 2.4. Construction of monolayer films on the solid substrates

Details on how to manufacture ternary PDA biosensing films on the solid substrates are given elsewhere (Charych et al., 1996). In short, the molecules spread on the trough surface were compressed after the collapse point and transferred before the second steep rise of surface pressure. We studied the transfer at different surface pressure, and the results showed that the films obtained before first collapse exhibited low transfer rate and poor colour intensity. When the transfer was carried out at high surface pressure (in the realm of the second condensed phase), a high transfer rate could be achieved but films were quite resistant to colour change. For 5%GM1/5%SA-PDA/90%PDA film, transfer at the surface pressure of 18 mN/m was found to give the best results. The films were transferred to OTS (octadecyltrichlorosilane) coated glass slides using the vertical deposition technique. The dipping speed of film transfer was maintained at 5 mm/min. Three dips (two down and one up) were made to ensure the hydrophilic interface was exposed to solution. After completely drying in air, the films were irradiated by a hand held UV lamp to initiate polymerization of the PDA. The irradiation time was 1 min per side. To detect the response of cholera toxin on the film biosensor, a 40 ppm cholera toxin (from Sigma) solution in 200 mM NaCl and 50 mM Tris-base (pH 7.4) was used.

### 3. Results and discussion

#### 3.1. Isotherms of GM1/PDA mixed monolayers

The surface pressure-area isotherms for 100% PDA, 5% GM1/95% PDA, 20% GM1/80% PDA, 50% GM1/50% PDA and 100% GM1 on pure water are shown in Fig. 2. The characteristic peak feature was observed for 100% PDA and 5% GM1/95% PDA films, indicating a monolayer collapse occurred to these films. The steep rise of surface pressure before collapse is indicative of the condensed phase, where strong chain-chain

interactions hold the molecules in their close-packed arrangement as a result of compression. The 100% PDA film shows a limiting area of 25 Å<sup>2</sup> at a collapse pressure of 17.5 mN/m. The results point to a crystal-like closest packing of the PDA lipids, and are in generally good agreement with those published previously (Walsh and Lando, 1994a; Tieke et al., 1979). The collapsed film could be further compressed as seen in the second steep rise of surface pressure occurring in the small molecular area. The film collapsed at a surface pressure > 50 mN/m.

The 100% GM1 shows a very expanded isotherm on pure water, with first detectable surface pressure change occurred around 100 Å<sup>2</sup>. A very small phase transition shoulder was observed at the surface pressure of 17 mN/m and 60 Å<sup>2</sup> molecular area. This phase transition, reproducible in all isotherms of 100% GM1 regardless of compression speed, did not show time dependence when various evaporation time was investigated. Probst et al. ascribed the transition to a rearrangement of the polar head-group of GM1 that the sugar groups are oriented perpendicularly to the surface (Probst et al., 1984). After the phase transition, the GM1 compression curve arises rapidly and collapses at a molecular area of 38 Å<sup>2</sup>. This limiting molecular area, however, is smaller than the values reported by other authors (Maggio et al., 1978a; Beitingner et al., 1987; Parker, 1990; Perillo et al., 1993). Examination of possible material loss of GM1, which was conducted by monitoring the  $\pi$ -A isotherm at various evaporation time, shows no significant distinction in surface pressure and molecular area for isotherms between 5 min and 1 h evaporation. In addition, below 20 mN/m the GM1 film could be reversibly decompressed, suggesting that GM1 on the aqueous surface was in equilibrium with the sub-phase. The disagreement in GM1 isotherm, therefore, is likely due to the different experiment conditions such as material source, purification procedure and monolayer manipulation among individual labs, as suggested by Maggio and coworkers (Fidelio et al., 1991). Taking the bulk volume of the GM1 headgroup into consideration, a molecular area of 38 Å<sup>2</sup> is indeed smaller than the actual size. The area of the closest pack-

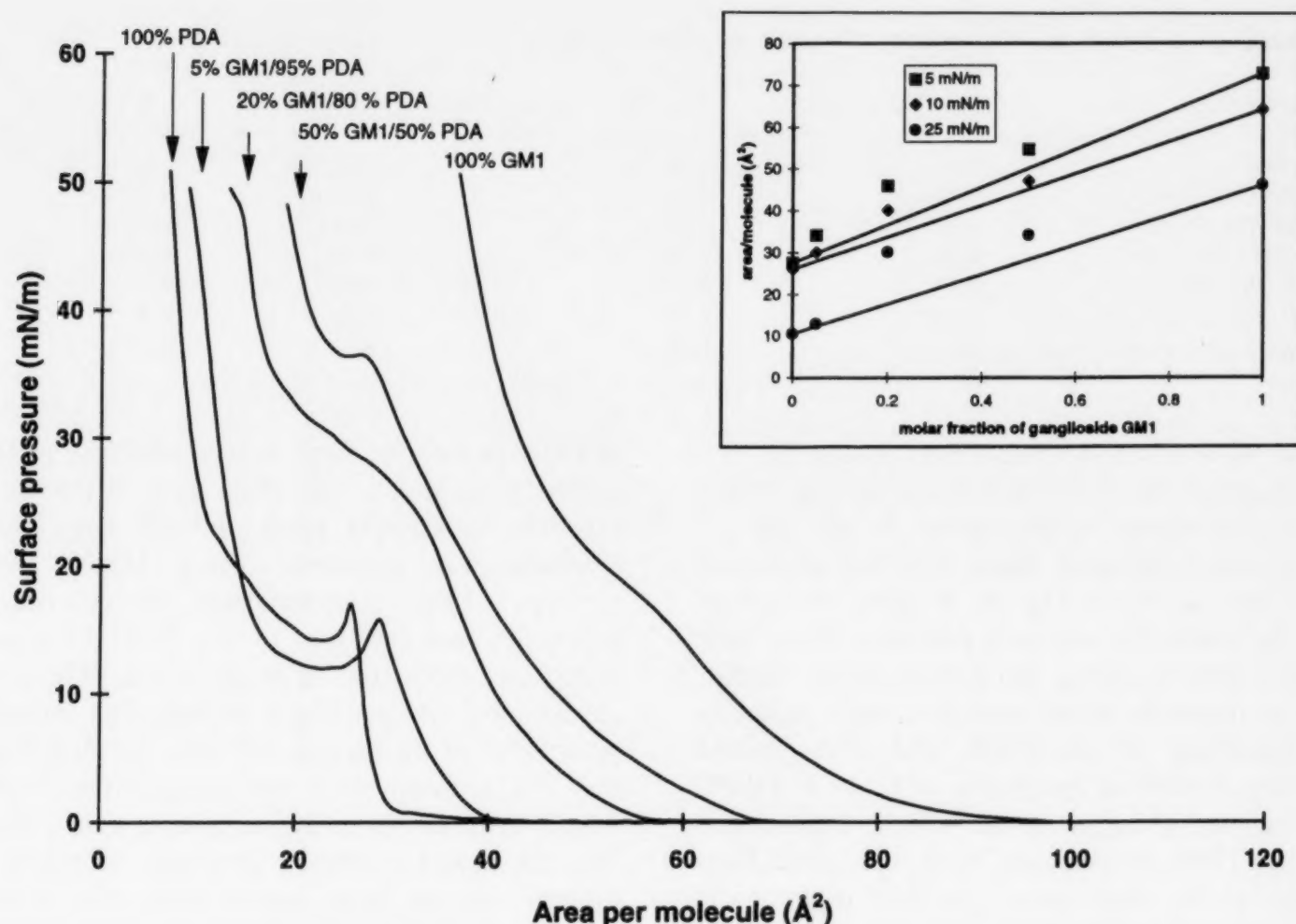


Fig. 2.  $\pi$ -A isotherms for monolayers of the pure and mixed components on water (pH 5.8) at 20°C. The insert is the plot of mean area/molecule for the mixed monolayers of PDA and GM1 at different surface pressures. The solid lines represent values calculated by the additivity rule. From top to bottom: 5 mN/m, 10 mN/m and 25 mN/m.

ing of ceramide is not enough to cover the area required by the polar group (Luckham et al., 1993). We speculate that the small molecular area in the condensed films may be due to the protrusion of the GM1 headgroup to the sub-phase in a staggered conformation.

In the mixed monolayers, the 5% GM1/95% PDA film preserved to a large extent the collapse curve as the 100% PDA's. As the mole fraction of GM1 increased to 20%, the peak feature of monomeric PDA disappeared from the isotherm, and a more classical phase transition curve was obtained. When the GM1 content was increased to 50% of the total molecules, the resulting isotherm differed greatly from PDA. The range of coexisting state for liquid and solid states was greatly reduced, while the expanded state looked very similar to pure GM1. Interestingly, the phase

transition point in 20% GM1/80% PDA and 50% GM1/50% PDA has higher surface pressure than the pure forms, similar to a positive azeotropic mixing type observed in biolipid studies (Birdi, 1989).

The behaviour of the mixed monolayers, particularly the film miscibility, can be analyzed by the additivity rule. For an 'ideal' mixed film involving two components where no interactions between the molecules are assumed, the following relationship can be applied: (Gaines, 1966)

$$A_{1,2} = N_1 A_1 + N_2 A_2 \quad (1)$$

where  $A_{1,2}$  is the molecular area of the mixed film,  $A_i$  is the molecular area of component  $i$  in pure form, and  $N_i$  is the mol fraction of compound  $i$  in the mixture. On the other hand, such 'ideal' behaviour might result as well from an interface



Table 1  
Properties and colorimetric response of GM1 biosensing monolayer assembly

Film composition	Initial absorbance	Monolayer transfer rate	CR in buffer	CR in analyte
100% PDA	0.052	0.94	0.02	0.02
5% GM1/95% PDA	0.049	0.89	0.03	0.03
20% GM1/80%PDA	0.018	0.34	0.03	0.04
5%SA-PDA/95%PDA	0.038	0.77	0.06	0.07
20% SA-PDA/80% PDA	0.032	0.62	0.14	0.15
5%GM1/5%SA-PDA/90% PDA	0.036	0.87	0.06	0.28
20%GM1/5%SA-PDA/75% PDA	0.014	0.33	0.10	0.13

formed by immiscible components. Using Eq. (1), we calculated the molecular areas for the mixed systems at surface pressures of 5, 10 and 25 mN/m, and compared them with the measured values (see insert in Fig. 2). Positive deviations from the additivity rule were obtained. Since both positive and negative deviations from ideality point to miscible behaviour, this result indicates the miscibility of the PDA and GM1 mixed monolayers. Similar behaviour of GM1 in DPPC was reported (Maggio et al., 1978b; Bianco and Maggio, 1989). In addition, since immiscible films collapse at the same surface pressure at which the film of the pure component collapses, varying the composition of an immiscible film would have no effect on the collapse pressure of that film. Along with the fact that GM1/PDA films studied in this work do not exhibit this type of behaviour, the results again point to a miscible, though not necessarily homogeneous, mixing between monomeric PDA and the functional molecule GM1 on the water surface.

### 3.2. Optimization of colorimetric response for GM1/PDA monolayer films

To evaluate the colorimetric response of the films, different concentration combinations of ligand (GM1) and PDA were tested. If too much ligand molecule was added (low concentration of polymerized lipid), the films were unstable and had high background. If the films had too much polymerized lipid molecule, they were too stable and the colour change would not occur. In the search for the GM1/PDA biosensor composition capable of displaying maximal response, a series

of PDA monolayer films were transferred to OTS coated glass slides. The films were evaluated by exposure to cholera toxin and the colorimetric response was measured using UV-Vis spectroscopy. Table 1 summarizes the colorimetric properties and response of the GM1 biosensing monolayer films studied in this work. The initial absorbance ( $A_{\text{init}}$ ), which reflects the maximal peak value of the films at 640 nm, is a function of the film transfer rate and composition. GM1, which does not provide chromatic functionality into the mixed assembly, generally decreases the intensity of the initial blue colour. The transfer rate, which is the ratio of the area decreased on the trough surface and the area of the substrate emerged into the sub-phase, indicates that the PDA films are highly transferable as compared to those of SA-PDA and GM1 molecules. The blue to red colorimetric response (CR) (Charych et al., 1993) shows that monolayer films exhibit low CR in buffer solution except when high content of GM1 or SA-PDA is used. For the optimal detection of cholera toxin, both SA-PDA and GM1 need be present in the films, otherwise the films are either too unstable or they do not change colour, depending on the concentration of all three components. The function of SA-PDA is thought to provide the metastable state of the films for biomolecular recognition through a stress-induced mechanism (Charych et al., 1996). A film consisting of 1%GM1/1% SA-PDA/98% PDA was also investigated, and the CR turned out to be low and it does not yield a useful colorimetric biosensor. Based on the above studies, the optimal colorimetric sensor was determined to be 5% GM1/5% SA-PDA/90% PDA.



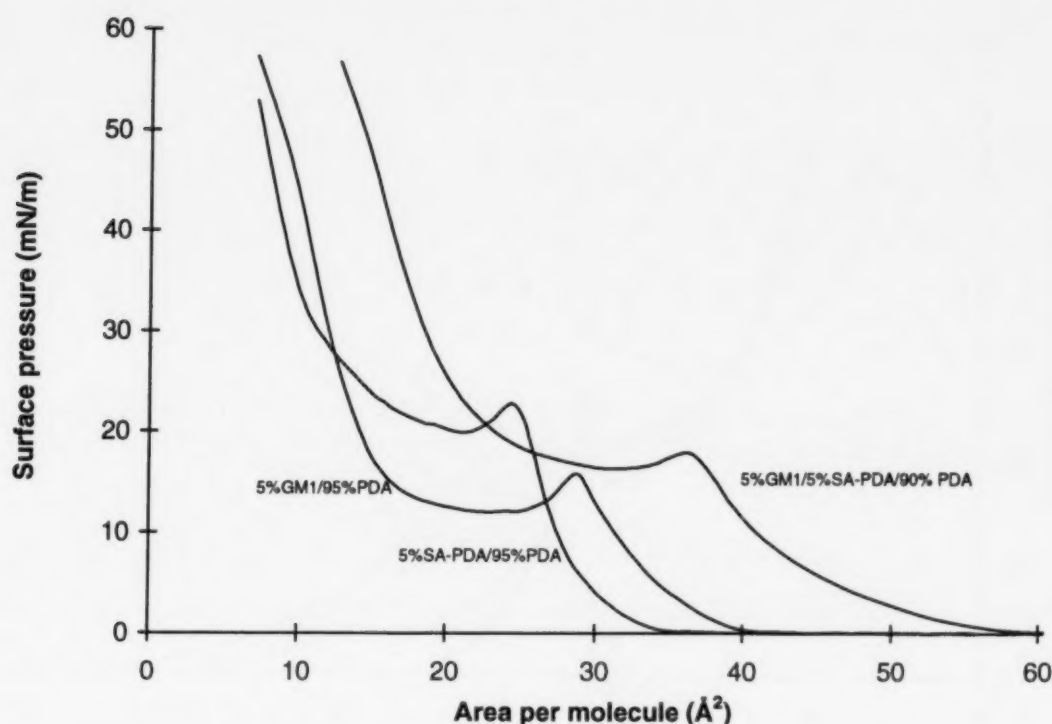


Fig. 3.  $\pi$ -A isotherms for monolayers containing SA-PDA on water (pH 5.8) at 20°C.

### 3.3. Isotherms of GM1/SA-PDA/PDA ternary mixed monolayers

Fig. 3 shows the isotherms of mixed films containing SA-PDA, the molecule responsible for promoting the chromatic transition of the cholera toxin biosensor. The slope of the isotherms in the condensed phase, which is a measure of the compressibility, indicates that the films are compressible. Peaks as well as plateaus in these isotherms were observed in the region of 17–21 mN/m. Compared to 100% PDA, 5% SA-PDA/95% PDA started to be compressed at a slightly higher surface molecular area, perhaps due to the large headgroup of SA-PDA. As for 5%GM1/5%SA-PDA/90%PDA, the shift was so significant that films started to be compressed around 60 Å<sup>2</sup>. The expanded region is much longer than in other systems, indicating a complicated compression mechanism for the ternary systems. It is worth noting that both 5%GM1/95% PDA and 5%GM1/5%SA-PDA/90%PDA showed very compressible isotherms while film condensation of pure GM1 was poor, as reflected by the large area under the  $\pi$ -A isotherm. This result implies that the PDA monolayer not only provides the necessary optical features for sensor design, but also

contributes to the mechanical and chemical environment for effective manipulation of the biological entities in the monolayer films.

Little is known about the monolayer structure after collapse. It has been suggested that collapse of the monolayer results in fluid-like media, where the disorder of the monolayer dominates the film structure (Walsh and Lando, 1994a; Day and Ringsdorf, 1978). We studied the monolayer transfer at different surface pressures, and the results suggest a different mechanism: (1) The collapsed films were highly transferable, indicating that some degree of ordered monolayer structure was preserved after the collapse; (2) The transferred films could be polymerized by UV irradiation. Considering the fact that polymerization of PDA requires strict spatial arrangement of the adjacent molecules (Wenzel and Atkinson, 1989; Deckert et al., 1995) and is sensitive to deposition conditions such as subphase composition and pH (Mino et al., 1992), we conclude that a highly ordered monolayer must be present after the collapse point. Fig. 2 shows that the PDA film can be compressed to 8 Å<sup>2</sup>, roughly one third of the normal limiting molecular area for a carboxylic lipid, pointing to a possibility of forming a trilayer of PDA after its first collapse. It is

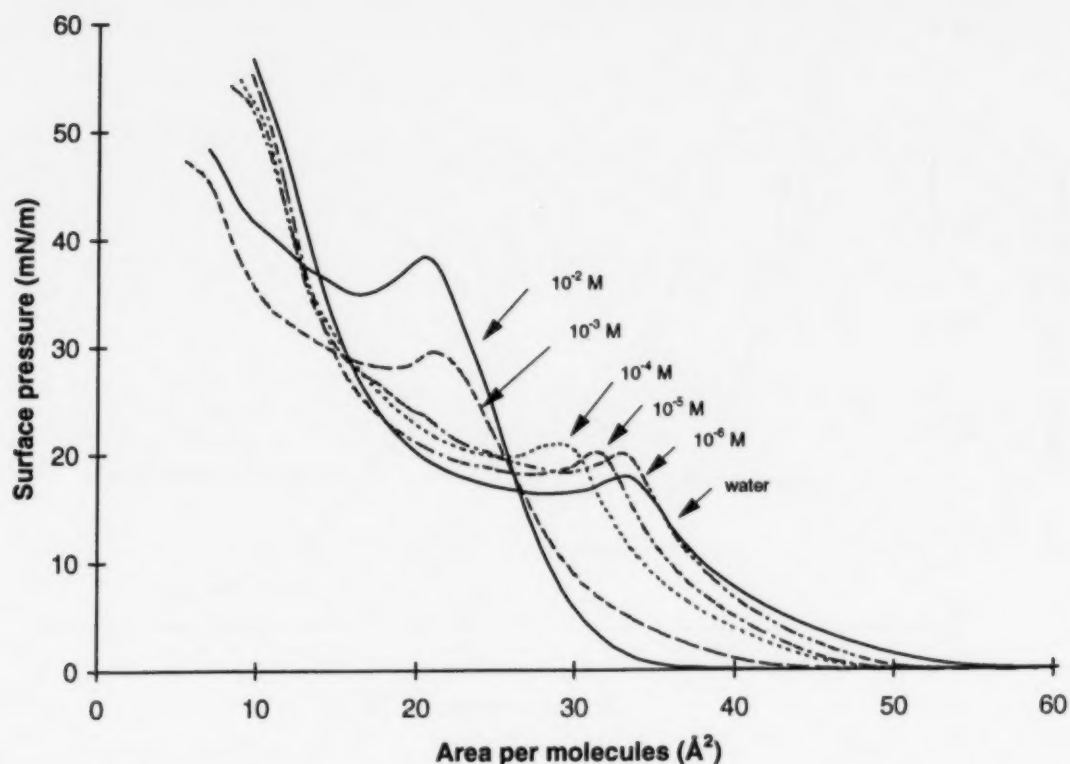


Fig. 4.  $\pi$ -A isotherms for 5%GM1/5%SA-PDA/90%PDA as a function of  $\text{Cd}^{2+}$  subphase concentration (pH 5.8) at 20°C. The subphase concentration of  $\text{Cd}^{2+}$  was adjusted by using  $\text{CdCl}_2 \cdot 2\text{H}_2\text{O}$ .

highly likely that the integrity of the two-dimensional array is maintained during the collapse process, since the collapse fragments atop the original monolayer show similar properties in terms of transferability and polymerization pattern. A similar mechanism has been suggested (Ries, 1973) to account for monolayer collapse of long chain fatty acids studied by EM. Further investigation in regards to film structure using surface characterization techniques will be needed for revealing structural information of monolayer collapse.

#### 3.4. Effect of subphase ionic content on ternary assembly

The ionic content of the aqueous subphase has significant impact on the properties of Langmuir monolayers. The presence of cationic species strengthens the electrostatic interactions of monolayers with anionic head-groups and consequently stabilizes the film Gaines, 1966. Fig. 4 shows the isotherms of 5%GM1/5%SA-PDA/90%PDA as a function of subphase concentration of  $\text{CdCl}_2$ . As the concentration of  $\text{Cd}^{2+}$  is increased, the ex-

panded phase shifts systematically toward the low molecular area, indicating that the monolayer is stabilized at high  $\text{Cd}^{2+}$  concentration. This behaviour results largely from the ionic interactions between  $\text{Cd}^{2+}$  and partially dissociated anionic carboxylate headgroup of PDA ( $\text{pK}_a \approx 5$ ), while acidic SA-PDA and GM1 ( $\text{pK}_a \approx 2.6$  for sialic acid in these molecules) certainly contribute to strengthen the effect. Further evidence for this mechanism of monolayer stabilization is seen in the increase in surface pressure as a function of higher ionic concentrations. Many divalent ions (Be, Mg, Ca, Ba, and Cd) have been shown to have an impact on the isotherms of PDA monomers through salt formation, which influences the packing of molecules on a basis of ion size and charge. No immiscible trend was observed for the ternary system of 5%GM1/5%SA-PDA/90%PDA on aqueous subphases containing up to 0.01 M  $\text{Cd}^{2+}$ , indicating that this mixed monolayer is relatively stable as respect to ionic content. When the  $\text{Cd}^{2+}$  was increased to 0.1 M, however, erratic behaviour of 5%GM1/5%SA-PDA/90%PDA monolayer was observed. This is possibly due to formation of aggregated domains

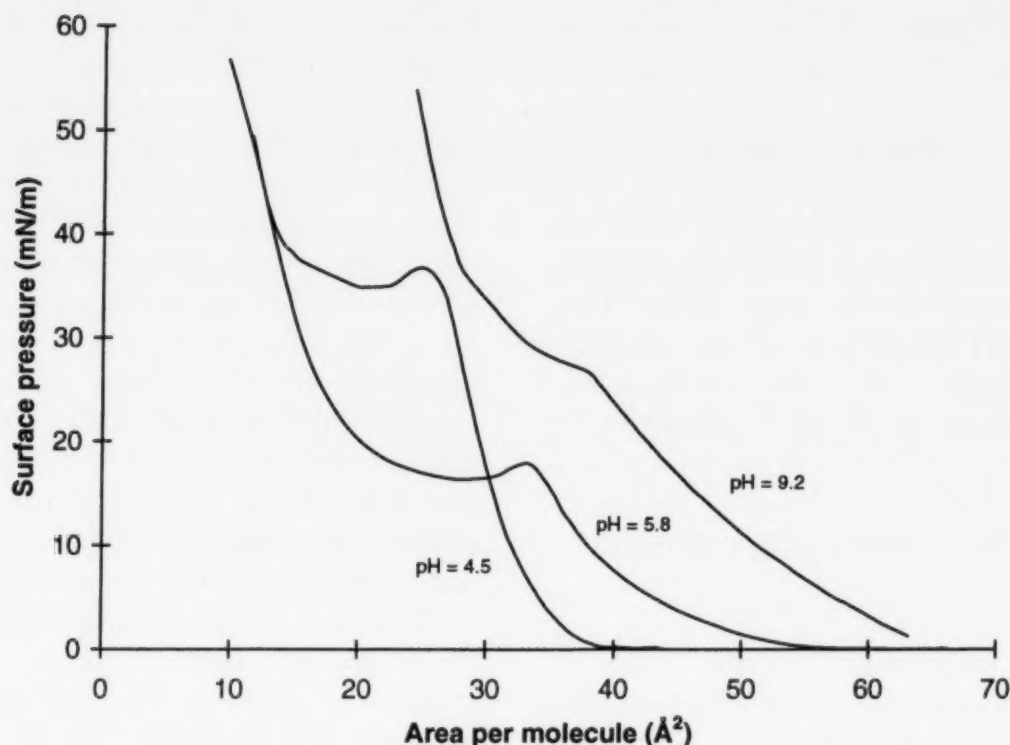


Fig. 5.  $\pi$ -A isotherms for 5% GM1/5% SA-PDA/90% PDA at pH 4.5, 5.8 and 9.2. The buffer was 0.05 M sodium phosphate, adjusted to the desired pH with phosphoric acid or NaOH.

as a result of different ability to interact with  $\text{Cd}^{2+}$  between sialic acid in SA-PDA and GM1 and carboxylic in PDA, or precipitation at high salt concentration.

It is worth noting that at low  $\text{Cd}^{2+}$  concentrations ( $\sim 10^{-4}$  M), the isotherms differ very little in the condensed phase region, indicating that low ionic content in subphase has no significant effect on the structure of the compact films. Increasing the concentration of  $\text{Cd}^{2+}$  above  $10^{-3}$  M resulted in a shift of molecular area in the condensed phase region (Fig. 4), pointing to some structural change in the compact monolayer. In order to explore the role of additives in the mixture for inducing such a structural change, an isotherm of pure PDA on  $10^{-2}$  M  $\text{Cd}^{2+}$  was measured. On the  $10^{-2}$  M  $\text{Cd}^{2+}$  subphase, a steep rise at low molecular area is seen in the isotherm of PDA. However, the slope of the isotherm within the compact region and the molecular area were essentially the same as on water. Such a result is consistent with an ordered film of PDA at high salt concentration, where the film characteristics are primarily dictated by the long hydrophobic segment of the molecules. Simi-

lar results were obtained for amine-based diacetylene (Walsh and Lando, 1994b). Therefore, the shift in Fig. 4 reflects a mixed electrostatic effect induced by differently dissociated individual components in the films, suggesting a lower stability of the ternary films as compared to the pure PDA films.

### 3.5. Effect of subphase pH on ternary assembly

For the acidic molecule PDA, an increase in pH results in the ionization of PDA molecules and consequently introduces substantial charge along the monolayer interface. Fig. 5 shows the isotherms of 5%GM1/5%SA-PDA/90%PDA at pH 4.5, 5.8 and 9.2. At high pH (pH 9.2), the film becomes very expanded as a result of electrostatic repulsion between the adjacent PDA molecules. Compression of such a film to form a monolayer was difficult. Additionally, distinct segments of individual molecules were observed, pointing to an immiscible trend in the mixed monolayer that tends to form segregated domains. Obviously, high charge density at the monolayer interface creates unfavourable interactions on the aqueous



surface. It can be expected that the addition of compounds such as GM1 (which is acidic) into the PDA mixture at this pH will be extremely unfavourable. The isotherm of the ternary system at low pH exhibits normal peak behaviour. The collapse pressure is significantly larger than at neutral pH, indicating a more stable film formed at low pH. Suppression of ionization of the PDA molecules at this pH contributes to the enhancement of film stability, which can consequently stabilize the incorporation of GM1 molecules in the PDA films.

### 3.6. Effect of subphase temperature on ternary assembly

An increase in temperature usually results in higher surface pressure, an enlargement of the expanded region and a shift in the phase transition point towards the low molecular area direction in  $\pi/A$  isotherms (Birdi, 1989). This effect stems from the higher flexibility of hydrocarbon tails of lipids at high temperature as a result of thermal agitation, and can be analyzed with the two-dimensional Clausius-Clapeyron equation (Birdi, 1989). Monolayer films containing PDA, however, typically experience film collapse during compression. Consequently, the evaluation of the subphase temperature effect has to take this phenomenon into consideration. Fig. 6 displays the temperature effect on the isotherms of 100% PDA, 5%SA-PDA/95%PDA, and 5%GM1/5%SA-PDA/90%PDA. With decrease in subphase temperature, the surface pressure increased and the isotherms' shape changed. Isotherms at low temperature exhibited more and more liquid-solid phase transition features, as indicated by the disappearance of the peak and occurrence of the smooth curve at the transition region. All the  $\pi$ -A isotherms obtained for the three monolayers display similar characteristics. The major difference between these figures is the position of collapse point, which is a function of film composition.

The anomalous thermal behaviour of 5%GM1/5%SA-PDA/90%PDA cannot be interpreted by a classical phase transition of thermodynamic effects. To account for such thermal anomalies, Cadenhead and Müller-Landau postulated a

mechanism that involves a conformational change at the interface (Cadenhead and Müller-Landau, 1974). Glazer suggested that the breakdown of intermolecular hydrogen bonds between polar head-groups provokes a reversal of temperature dependence (Glazer and Alexander, 1951). Loss of molecules at high temperature could be another explanation for the decrease in surface pressure. However, none of the above mechanisms seems applicable to this system. Material loss would appear unlikely since such a film loss should displace the entire isotherm to low area/molecule, and this did not happen. As diacetylene groups exhibit some degree of interactions with subphase water, we propose that these interactions, together with those at the hydrophobic portion when molecules are compressed to close-packed arrangement, induce the abnormal thermal behaviour. The diacetylene bonds interfere with the efficient packing and decreases the film fluidity on the aqueous surface, while the weak interactions between diacetylene and subphase water are broken down as the temperature increases. As a result, the tendency of film collapse is expected to be suppressed as the temperature is decreased. Therefore, at low temperature the chain mobility is balanced as to be comparable to that of fatty acids, leading to a classical phase transition to take place.

## 4. Conclusions

Monolayer properties of monosialoganglioside in binary and ternary mixed films have been studied by using LB technique. Though the GM1 molecule is difficult to compress into a monolayer, it forms miscible films with PDA, and the mixed films are highly transferable to solid substrates. When making a biosensitive film, it was found that 5% GM1/5% SA-PDA/90% PDA yielded the most sensitive film response to the target analyte cholera toxin. A higher concentration of the GM1 ligand molecule or SA-PDA promoter lipid results in a film with high background and consequently decreases the overall response.

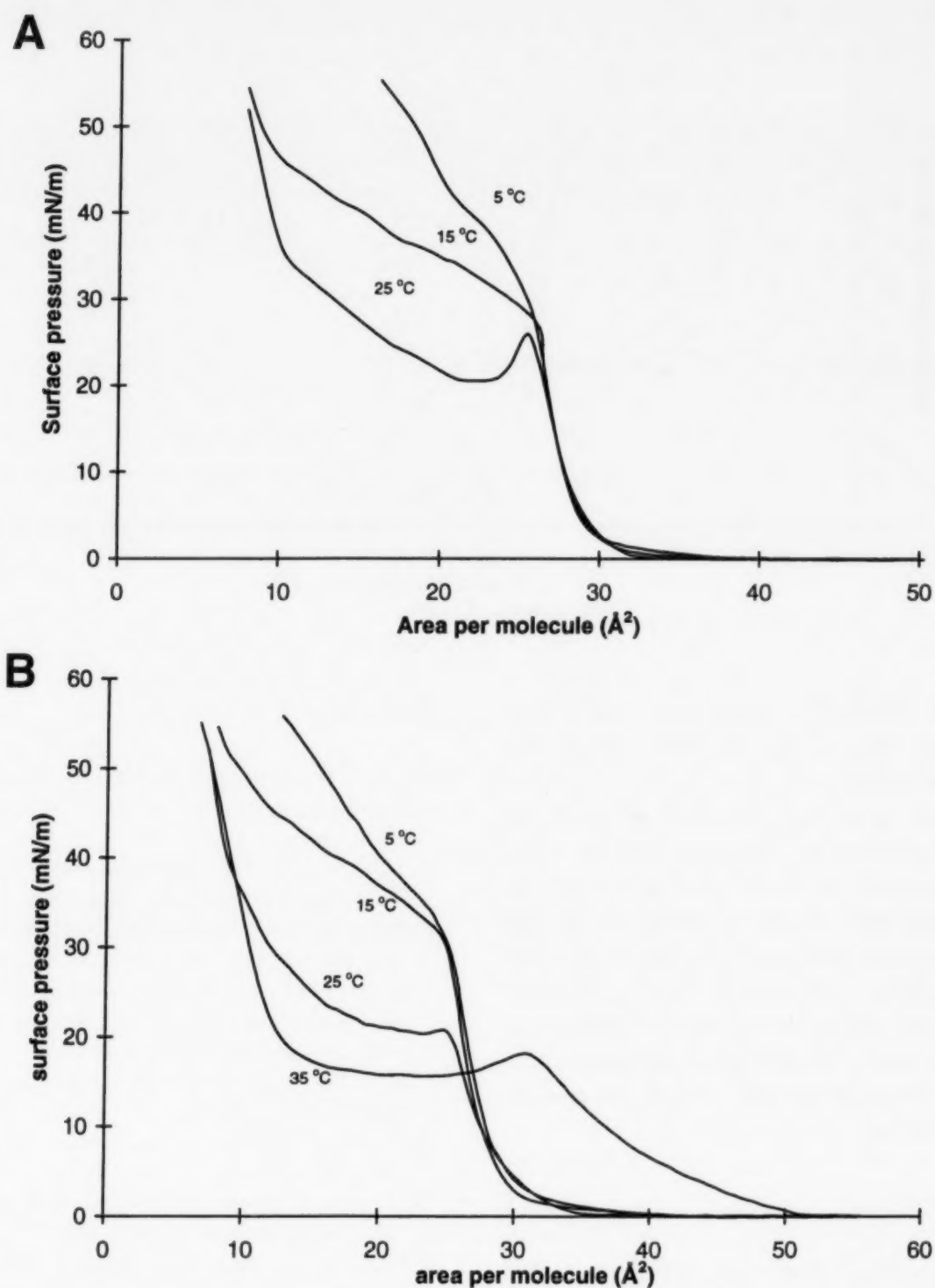


Fig. 6.  $\pi$ -A isotherms of monolayers containing PDA as a function of subphase temperature on  $10^{-4}$  M  $\text{Cd}^{2+}$ . (A) 100% PDA; (B) 5% SA-PDA/95% PDA; (C) 5% GM1/5% SA-PDA/90% PDA.

For the ternary monolayer films, the stability of mixed monolayers is influenced by: (1) the molecules contained in the monolayer itself, such as ligands molecules and promoter lipids; (2) the ionic strength and content of the aqueous subphase, (3) the pH of the subphase, and (4) the temperature of the subphase. The large headgroup

size of GM1 likely introduces a steric effect to the mixed systems resulting in a decrease in film stability. High ionic strength improves the interactions of the molecules. Acidification of the subphase could prove to be beneficial in terms of increasing miscibility of the mixed species. And contrary to the usual temperature effect on mono-

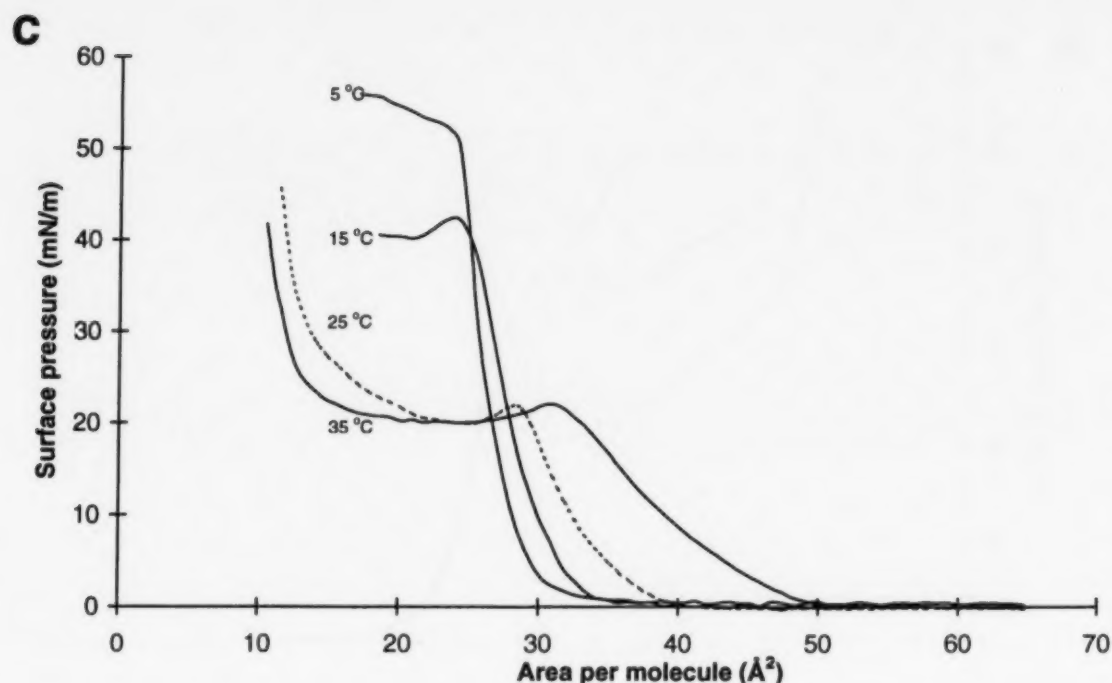


Fig. 6. (continued)

layer stability, 5%GM1/5%SA-PDA/90%PDA mixed monolayer shows high stability when the temperature is lowered.

The LB technique is a useful method to study the average properties of the monolayers. The information obtained helps in an understanding of the general features of the monolayers at the macroscopic scale. Detailed information regarding the multicomponent distribution and molecular interactions of the array, however, is difficult to obtain. Further study of mixed monolayers employing surface techniques with atomic resolution is currently underway.

#### Acknowledgements

This work was support by the Director, Office of Energy Research, Office of Basic Energy Sciences, Division of Materials Sciences, and the Division of Energy Biosciences of the US Department of Energy Contract No. DE-AC03-76SF0098. The work was also supported by the NSF Young Investigator Award (R.C.S.) and the Beckman Foundation Young Investigator Award (R.C.S.). We wish to thank Nathaniel David for critical reading of the manuscript, and Mark Alper for continued encouragement of this research program.

#### References

- Bianco, I.D., Maggio, B., 1989. *Colloids Surf.* 40, 249–260.
- Beitinger, H., Probst, W., Möbius, D., Rahmannm, H., 1987. *J. Biochem.* 102, 963–966.
- Birdi, K.S., 1989. *Lipid and Biopolymer Monolayers at Liquid Interfaces*. Plenum Press, New York.
- Cadenhead, D.A., Müller-Landau, F., 1974. *J. Colloid Interface Sci.* 49, 131–134.
- Charych, D., Cheng, Q., Reichert, A., Kuziemko, G., Stroh, M., Nagy, J.O., Spevak, W., Stevens, R.C., 1996. *Chemistry and Biology* 3, 113–120.
- Charych, D., Nagy, J.O., Spevak, W., Bednaeski, M.D., 1993. *Science* 261, 585–588.
- Day, D. and Ringsdorf, 1978. *J. Polym. Sci., Polym. Lett. Ed.*, 16, 205–210.
- Deckert, A.A., Horne, J.C., Valentine, B., Kiernan, L., Fallon, L., 1995. *Langmuir* 11, 643–649.
- Fidelio, G.D., Ariga, T., Maggio, B., 1991. *J. Biochem.* 110, 12–16.
- Fujita, K., Kimura, S., Imanishi, Y., Rump, E., Ringsdorf, H., 1994. *Langmuir* 10, 2731–2735.
- Gaines, G.L., 1966. *Insoluble Monolayers at Liquid-Gas Interface*. Interscience Publishers, New York, pp. 291–299.
- Glazer, J., Alexander, A.E., 1951. *Trans. Faraday Soc.* 47, 401–409.
- Luckham, P., Wood, J., Froggatt, S., Swart, R., 1993. *J. Colloid Interface. Sci.* 156, 164–172.
- Lukes, P.J., Petty, M.C., Yarwood, J., 1992. *Langmuir* 8, 3043–3050.
- Maggio, B., Cumar, F.A., Caputto, R., 1978a. *Biochem. J.* 171, 559–565.



- Maggio, B., Cumar, F.A., Caputto, R., 1978b. *Biochem. J.* 175, 1113–1118.
- Mino, N., Tamura, H., Ogawa, K., 1992. *Langmuir* 8, 594–598.
- Parker, J.L., 1990. *J. Colloid Interface. Sci.* 137, 571–576.
- Perillo, M.A., Polo, A., Guidotti, A., Costa, E., Maggio, B., 1993. *Chem. Phys. Lipids* 65, 225–238.
- Probst, W., Möbius, D., Rahmann, H., 1984. *Cell Mol. Neurobiol.* 4, 157–176.
- Ries, H.E. Jr., 1973. In: Hampel, C.A and Hawley, G.G. (Ed.), *Encyclopedia of Chemistry*, 3rd Ed. Van Nostrand Reinhold, New York, 696–700.
- Roberts, G., 1990. *Langmuir-Blodgett Films*, Plenum Press, New York.
- Spevak, W., 1984. Ph.D. Dissertation, University of California at Berkeley, CA.
- Svennerholm, L., 1994. *Life Sciences* 55, 2125–2134.
- Terrettaz, S., Stora, T., Duschl, C., Vogel, H., 1993. *Langmuir* 9, 1361–1369.
- Tieke, B., Lieser, G., Wegner, G., 1979. *J. Polym. Sci. Polym. Chem. Ed.* 17, 1631–1644.
- Tronin, A., Dubrovsky, T., De Nitti, C., Gussoni, A., Erokhin, V., Nicolini, C., 1994. *Thin Solid Films* 238, 127–132.
- Ulman, A., 1991. *An Introduction to Ultrathin Organic Films, from Langmuir-Blodgett to Self-Assembly*. Academic Press, New York.
- Walsh, S.P., Lando, J.B., 1994a. *Langmuir* 10, 246–251.
- Walsh, S.P., Lando, J.B., 1994b. *Langmuir* 10, 252–256.
- Wenzel, M., Atkinson, G.H., 1989. *J. Am. Chem. Soc.* 111, 6123–6127.



## Synthesis and nuclear magnetic resonance spectroscopic properties of some acetylenic tellura fatty acid esters

Marcel S.F. Lie Ken Jie \*, Sherman H. Chau

*Department of Chemistry, The University of Hong Kong, Pokfulam road, Hong Kong, Hong Kong*

Received 2 December 1996; received in revised form 26 March 1997; accepted 26 March 1997

### Abstract

Five positional isomers of acetylenic tellura stearate (1–5) have been synthesized by three different routes. The number of methylene groups located between the acetylenic system and the tellurium metal varies from 0 to 4. The  $^1\text{H}$  and  $^{13}\text{C}$  NMR spectroscopic properties have been studied. The tellurium atom induces strong deshielding effects on the adjacent methylene protons, which in combination with the deshielding effects of the acetylenic system allows most of the methylene groups between the tellurium and the triple bond to be identified by  $^1\text{H}$  NMR spectroscopic analysis. The tellurium causes a very strong shielding effect (ca.  $-27.1$  ppm) on the carbon shift of the adjacent  $\alpha$ -methylene carbon atom, but weak deshielding effects on the  $\beta$ - (ca.  $+2.6$  ppm) and  $\gamma$ - (ca.  $+2.3$  ppm) methylene carbon atoms. Carbon shifts of methylene carbon atoms, especially those which are located between the tellurium atom and the triple bond, are found very much upfield ( $\delta_{\text{C}}$  0.65–4.81) and in one case in the negative region ( $\delta_{\text{C}}$   $-17.95$ ) of the  $^{13}\text{C}$  NMR spectrum. Most of the signals of the carbon nuclei of these analogue have been identified and from the results of these analyses the number of methylene groups between the acetylenic system and the tellurium atom can be determined. © 1997 Elsevier Science Ireland Ltd.

**Keywords:** Acetylenic; NMR spectroscopy; Positional isomers; Synthesis; Unsaturated tellura; Stearate analogues

### 1. Introduction

We have reported the synthesis of a complete series of position isomers of methyl tellura laurate (Lie Ken Jie et al., 1991), long-chain methyl esters containing a tellurophene system (Lie Ken Jie and

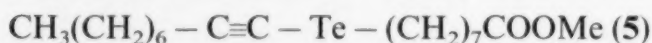
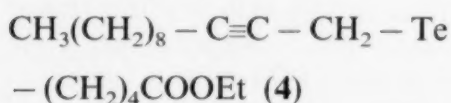
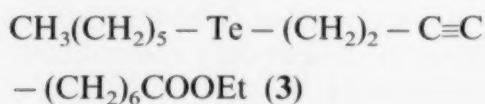
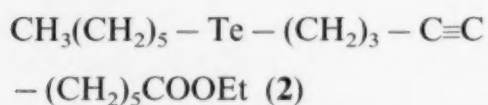
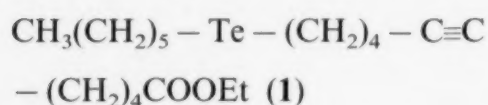
Chau, 1995a) and the dichloride derivatives of some methyl tellura laurates (Lie Ken Jie and Chau, 1995b), and have studied the nuclear magnetic resonance spectroscopic (NMR) and mass spectrometric properties of this class of fatty acid ester analogues (Lie Ken Jie and Chau, 1995c). Long-chain fatty acids containing a tellurium atom in the alkyl chain are shown to inhibit the process of  $\beta$ -oxidation of fatty acids in the my-

\* Corresponding author. Fax: +852 2517 0217; e-mail: hrsckj@hkucc.hku.hk



ocardium. Such long-chain fatty acids have been used to trap radiolabelled fatty acids in the heart tissues for myocardial imaging purposes (Knapp et al., 1979; Srivastava et al., 1987; Goodman and Knapp, 1982). There are only a few reported cases of unsaturated tellura fatty acids in the chemical literature. Knapp et al. have described the synthesis of unsaturated tellura fatty acid analogues containing an iodo-vinyl system, where the double bond is located at the end of the fatty acid chain (Knapp et al., 1984).

In our continuing effort to study the properties of long-chain fatty acids containing a hetero atom in the alkyl chain, we report in this paper the synthesis of five unsaturated tellura stearate ester analogues containing an acetylenic bond and a tellurium atom in defined positions of the alkyl chain (compounds 1–5).



One of the main objectives of this work is to study the effects of the tellurium atom and the acetylenic system on the shifts of the adjacent methylene group by NMR spectroscopy. For this reason the number of methylene groups between the acetylenic bond and the hetero atom (tellurium) in these fatty acid analogues is varied from 0 to 4.

## 2. Material and methods

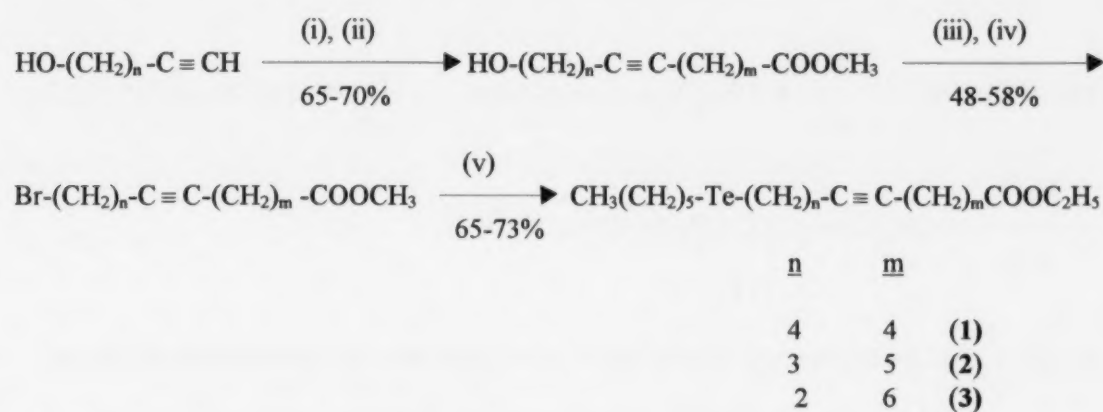
Infrared spectra were measured as neat samples on a Shimadzu model IR-470 spectrophotometer (Shimadzu, Kyoto, Japan). Nuclear magnetic resonance (NMR) spectra were recorded on a JEOL

GSX-270 fourier transformed NMR spectrometer (JEOL, Tokyo, Japan) at an operating frequency of 270 MHz for proton and 67.89 MHz for carbon nuclei from solutions in deuteriochloroform ( $\text{CDCl}_3$ ) with tetramethylsilane (TMS) as the internal reference standard. Chemical shifts are given in  $\delta_{\text{H}}$  and  $\delta_{\text{C}}$  values in ppm downfield from TMS ( $\delta_{\text{TMS}} = 0$ ). Solvents used in the synthesis were distilled and dried over sodium in benzophenone. 5-Hexyn-1-ol, 4-pentyn-1-ol, 3-butyln-1-ol, 5-bromopentanoic acid, 6-bromohexanoic acid and 8-bromooctanoic acid were purchased from Aldrich (St. Louis, MO).

### 2.1. General method for the preparation of di-, tri- and tetra-methylene interrupted acetylenic tellura fatty acid esters (1–3) as exemplified by the synthesis of ethyl 12-tellura-6-octadecynoate (1) (Scheme 1)

5-Hexyn-1-ol (13.2 g, 0.135 mol) was added to a suspension of lithamide [prepared from lithium (4.0 g, 0.57 mol), Fe(III) nitrate (0.5 g) and liquid ammonia (1 l)] in liquid ammonia and the reaction mixture was stirred for 1 h. 5-Bromopentanoic acid (23 g, 0.13 mol) in tetrahydrofuran (THF, 50  $\text{cm}^3$ ) was slowly added and the resulting mixture was stirred for 12 h. The ammonia was allowed to evaporate and dilute HCl (2 M, 200  $\text{cm}^3$ ) was added and the reaction mixture was extracted with diethyl ether (3  $\times$  100  $\text{cm}^3$ ). The ethereal extract was washed with water (2  $\times$  30  $\text{cm}^3$ ) and dried over anhydrous sodium sulfate. The filtrate was evaporated and the residue was refluxed with borontrifluoride-methanol complex (15%, w/w, 10  $\text{cm}^3$ ) and absolute methanol (100  $\text{cm}^3$ ) for 20 min. Water (150  $\text{cm}^3$ ) was added and the reaction mixture was extracted with petroleum ether (b.p. 60–80°C, 3  $\times$  50  $\text{cm}^3$ ). The petroleum extract was washed with water (30  $\text{cm}^3$ ) and dried. The filtrate was evaporated under reduced pressure and the residue was chromatographed (100 g silica) using a mixture of petroleum ether: diethyl ether (4:1, vol/vol) as eluent to give methyl 11-hydroxy-6-undecynoate (17.7 g, 65%) as an oil. Infrared analysis ( $\text{cm}^{-1}$ ) 3395, 1733, 1434, 1175, 1063;  $^1\text{H}$  NMR ( $\delta_{\text{H}}$ ) 1.4–1.8 (m, 8H,  $\text{CH}_2$ ), 2.0–2.4 (m, 6H, 2-H, 5-H and 8-H), 3.59 (s, 3H,

## Synthesis of di-, tri- and tetra-methylene interrupted acetylenic tellura fatty esters (1-3)



Reagents: (i)  $\text{LiNH}_2$ , ammonia,  $\text{Br}(\text{CH}_2)_m\text{COOH}$ ; (ii)  $\text{BF}_3/\text{MeOH}$ ; (iii) methanesulfonyl chloride, pyridine, dichloromethane; (iv)  $\text{LiBr}$ , acetone; (v)  $[\text{CH}_3(\text{CH}_2)_5\text{Te}]_2$ ,  $\text{NaBH}_4$ , ethanol.

Scheme 1.

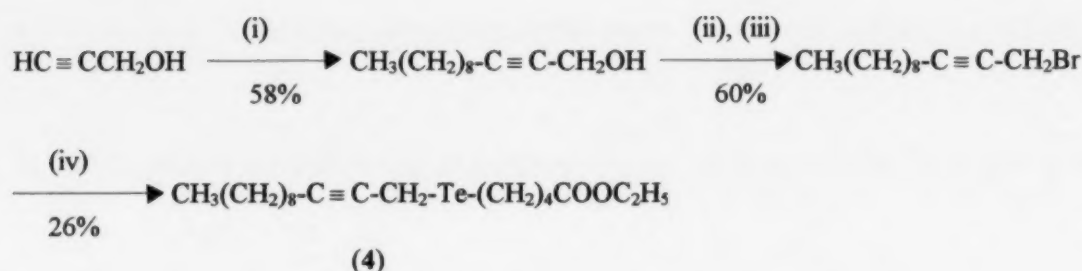
$\text{COOCH}_3$ ), 3.72 (t,  $J = 6.5$  Hz,  $\text{CH}_2\text{-OH}$ );  $^{13}\text{C}$  NMR ( $\delta_{\text{C}}$ ) 18.47 (C-5), 18.58 (C-8), 24.16 (C-3), 25.41 (C-9), 28.52, 29.01, 31.99 (C-10), 33.64 (C-2), 51.49 ( $\text{COOCH}_3$ ), 64.43 (C-11), 79.63 (C-6), 80.42 (C-7) and 174.11 (C-1).

A mixture of methyl 11-hydroxy-6-undecynoate (2.0 g, 9.4 mmol), methanesulfonyl chloride (2 g, 17.5 mmol), pyridine (5  $\text{cm}^3$ ) and dichloromethane (50  $\text{cm}^3$ ) was stirred at 0–5°C for 30 min and for a further 1 h at room temperature. The reaction mixture was successively washed with dilute HCl (2M, 30  $\text{cm}^3$ ), water (30  $\text{cm}^3$ ) and dried ( $\text{Na}_2\text{SO}_4$ ). The filtrate was evaporated and a solution of lithium bromide (1.5 g, 17 mmol) in acetone (25  $\text{cm}^3$ ) was added to the residue. The mixture was refluxed for 1 h and ice water (20  $\text{cm}^3$ ) was added to the cooled reaction mixture. The reaction mixture was extracted with petroleum ether (3  $\times$  30  $\text{cm}^3$ ). The petroleum extract was washed with water (30  $\text{cm}^3$ ) and dried ( $\text{Na}_2\text{SO}_4$ ). The filtrate was evaporated under reduced pressure and the residue was chromatographed on silica gel (40 g) using a mixture of petroleum ether: diethyl ether (9:1, vol/vol) as eluent to give methyl 11-bromo-6-undecynoate (1.5 g, 54%) as an oil. Infrared analysis ( $\text{cm}^{-1}$ ) 1734, 1432, 1332, 1251, 1174;  $^1\text{H}$  NMR ( $\delta_{\text{H}}$ ) 1.6–1.8 (m, 8H,  $\text{CH}_2$ ), 2.0–2.4 (m, 6H, 2-H, 5-H, 8-H), 3.44 (t,  $J = 6.4$  Hz,  $\text{CH}_2\text{Br}$ ) and 3.62 (s, 3H,

$\text{COOCH}_3$ );  $^{13}\text{C}$  NMR ( $\delta_{\text{C}}$ ) 17.99 (C-8), 18.47 (C-5), 24.92 (C-3), 27.52, 28.52, 31.85, 33.21 (C-11), 33.64 (C-2), 52.44 ( $\text{COOCH}_3$ ), 79.69 (C-6), 80.28 (C-7) and 173.87 (C-1); microanalysis: calc. for  $\text{C}_{12}\text{H}_{19}\text{O}_2\text{Br}$ , C, 52.37, H, 6.96, found C, 52.59 and H, 7.04.

A mixture of tellurium (powder, 1.0 g), sodium borohydride (0.2 g, 5.4 mmol) and dimethylformamide (DMF, 20  $\text{cm}^3$ ) was stirred at 80°C for 2 h under nitrogen. 1-Bromohexane (1.3 g, 7.6 mmol) in DMF (5  $\text{cm}^3$ ) was added and the reaction mixture was stirred for 2 h. Water (80  $\text{cm}^3$ ) was added and the reaction mixture was extracted with petroleum ether (3  $\times$  30  $\text{cm}^3$ ). The petroleum extract was evaporated under reduced pressure to give crude dihexylditelluride (1.55 g). Sodium borohydride (0.15 g, 4 mmol) and absolute ethanol (30  $\text{cm}^3$ ) were added to the crude dihexylditelluride and the mixture was stirred for 30 min at room temperature. The temperature of the reaction mixture was raised to 80°C and methyl 11-bromo-6-undecynoate (0.5 g, 1.8 mmol) in ethanol (5  $\text{cm}^3$ ) was added and the reaction mixture was stirred for 3 h. Water (50  $\text{cm}^3$ ) was then added to the cooled reaction mixture, which was extracted with diethyl ether (3  $\times$  30  $\text{cm}^3$ ). The ethereal extract was washed with water and dried ( $\text{Na}_2\text{SO}_4$ ). The filtrate was evaporated and the residue was chromatographed on a silica gel (50

## Synthesis of methylene-interrupted tellura-acetylenic fatty ester (4).



Reagents: (i)  $\text{LiNH}_2$ , ammonia, Fe(III) nitrate, 1-bromononane; (ii) methanesulfonyl chloride, pyridine,  $\text{CH}_2\text{Cl}_2$ ; (iii) LiBr, acetone; (iv)  $[\text{Te-(CH}_2)_4\text{COOCH}_3]_2$ ,  $\text{NaBH}_4$ , ethanol

Scheme 2.

g) column using a mixture of petroleum ether: diethyl ether (9:1, vol/vol) as eluent to give ethyl 12-tellura-6-octadecynoate (**1**, 0.55 g, 72%) as an oil.

### 2.2. Synthesis of the methylene-interrupted acetylenic tellura fatty acid ester (viz. ethyl 6-tellura-8-octadecynoate, **4**) (Scheme 2)

1-Bromo-2-decyne was prepared in 58% yield from 2-dodecyn-1-ol (obtained from the dilithio derivative of propargyl alcohol and 1-bromononane) by similar method as described for 11-bromo-6-undecynoate.

A mixture of tellurium (powder, 1.0 g), sodium borohydride (0.2 g, 5.4 mmol) and DMF (20  $\text{cm}^3$ ) was stirred at 80°C for 2 h under nitrogen. Methyl 5-bromopentanoate (1.5 g, 1.6 mmol) in DMF (5  $\text{cm}^3$ ) was added to the cooled reaction and the reaction mixture was stirred for 12 h at room temperature. Water (30  $\text{cm}^3$ ) was added and the reaction mixture was extracted with diethyl ether (3  $\times$  30  $\text{cm}^3$ ). The ethereal extract was washed with water (20  $\text{cm}^3$ ) and dried ( $\text{Na}_2\text{SO}_4$ ). The solvent was evaporated and the residue consisting of  $\text{CH}_3\text{OOC(CH}_2)_4\text{-Te-Te-(CH}_2)_4\text{COOCH}_3$  appeared as a red oily residue (1.8 g). A solution of sodium borohydride (0.15 g, 4 mmol) in ethanol (25  $\text{cm}^3$ ) was added to the red oily residue and the reaction mixture was stirred for 30 min. The reaction mixture was heated to 80°C and 1-bromo-2-dodecyne (1.0 g, 4.1 mmol) in ethanol (5

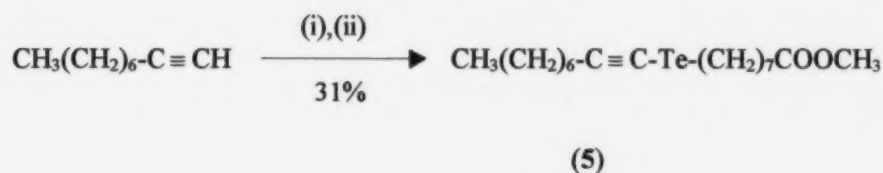
$\text{cm}^3$ ) was added and the mixture was stirred for 3 h. Water (100  $\text{cm}^3$ ) was added to the cooled reaction and the mixture was extracted with diethyl ether (3  $\times$  50  $\text{cm}^3$ ). The ethereal extract was washed with water (20  $\text{cm}^3$ ) and dried ( $\text{Na}_2\text{SO}_4$ ). The filtrate was evaporated and the residue was chromatographed on a silica gel (20 g) column using a mixture of petroleum ether: diethyl ether (9:1, vol/vol) as eluent to give ethyl 6-tellura-8-octadecynoate (**4**, 0.43 g, 26%) as an oil.

### 2.3. Synthesis of non-methylene interrupted acetylenic tellura fatty acid ester (viz. methyl 9-tellura-10-octadecynoate (**5**)) (Scheme 3)

*n*-Butyl lithium (2.5  $\text{cm}^3$ , 15% solution in *n*-hexane) was added to a solution of 1-nonyne (0.45 g, 3.6 mmol) in THF (15  $\text{cm}^3$ ) at 0°C under nitrogen and stirred for 15 min. Tellurium (powder, 0.3 g) was added and the reaction mixture was refluxed for 5 h. The reaction mixture was cooled to 0°C and a solution of methyl 8-bromooctanoate (0.45 g, 1.9 mmol) in THF (5  $\text{cm}^3$ ) was added. The reaction mixture was maintained at 0°C for 12 h. Water (40  $\text{cm}^3$ ) was then added and the reaction mixture was extracted with diethyl ether (3  $\times$  30  $\text{cm}^3$ ). The ethereal extract was washed with water (20  $\text{cm}^3$ ) and dried ( $\text{Na}_2\text{SO}_4$ ). The filtrate was evaporated and silica gel (20 g) chromatographic purification using a mixture of petroleum ether: diethyl ether (9:1, vol/vol) as eluent to give methyl 9-tellura-10-octadecynoate (**5**, 0.25 g, 31%).



## Synthesis of non-methylene interrupted acetylenic tellura fatty ester (5)



Reagents: (i) *n*-butyl lithium, THF, Te powder, reflux; (ii) methyl 8-bromooctanoate, THF.

Scheme 3.

### 3. Results and discussion

#### 3.1. Synthesis of acetylenic tellura fatty acid esters (1–5)

To incorporate 2–4 methylene groups between the tellurium atom and the acetylenic bond for the proposed acetylenic tellura analogues (1–3),  $\omega$ -alkyn-1-ols [ $\text{HO}(\text{CH}_2)_n\text{C}\equiv\text{CH}$ ,  $n = 2, 3$  or 4] were considered as the most suitable starting blocks (Scheme 1). Chain extension from the acetylenic end with esters of  $\omega$ -bromoalkanoic acids provided hydroxy-acetylenic acid intermediates (average yield of 65%). The hydroxy group of these intermediates was readily transformed to the bromide via the mesyloxy function using lithium bromide in acetone with an average yield of 53%. Subsequent reaction of the bromo-acetylenic ester intermediates with the corresponding sodium alkyltellurolate ( $\text{RTeNa}$ ) (from dialkylditelluride with sodium borohydride in ethanol) furnished the requisite ethyl acetylenic tellura fatty acid esters (1–3) (average 70% yield) (Scheme 1). Ethyl esters were obtained as the final products, due to the presence of a slight excess of sodium borohydride in ethanol employed during the final step of the synthesis sequence which caused the methyl ester group to be inter-esterified to the ethyl ester. In compounds 1–3 the tellurium atom occupied a position between the acetylenic bond and the terminal methyl group.

In the synthesis of the mono-methylene and the non-methylene interrupted acetylenic tellura fatty acid esters (compounds 4 and 5, respectively), the tellurium atom occupied a position between the acetylenic bond and the carboxylic ester group. This change in the synthesis strategy demon-

strated the versatile synthetic approach adopted in this work, which allowed the tellurium atom to be located at any pre-determined position of the alkyl chain of the fatty acid ester molecule. Compound 4 was prepared starting from commercially available propargyl alcohol, which was condensed via its dilithio derivative with 1-bromononane to give 2-dodecyn-1-ol. The latter was transformed to 1-bromo-2-decyne via the mesyloxy intermediate. 1-Bromo-2-decyne was subsequently coupled with the sodium tellurolate derived from methyl 5-bromopentanoate to give ethyl 6-tellura-8-octadecynoate (4) in 26% yield (Scheme 2). The yield of this last reaction was persistently low, as the formation of the ditelluride of the bromo-ester (methyl bromopentanoate) appeared to be a low-yielding reaction.

To prepare the non-methylene interrupted acetylenic tellura fatty acid ester (5), 1-lithium nonyne was reacted with tellurium metal in tetrahydrofuran (Dabdoub and Comasseto, 1988). The tellurium intermediate was subsequently reacted with methyl 8-bromooctanoate to yield the requisite product (methyl 9-tellura-10-octadecynoate, (5) in 31% yield. As no sodium borohydride and ethanol were involved in this reaction, the product obtained was the methyl ester derivative (Scheme 3).

#### 3.2. $^1\text{H}$ NMR properties of acetylenic tellura fatty acid esters (1–5)

The shift effects of an acetylenic system on the chemical shifts of the adjacent methylene protons are reported, the results of which showed that the acetylenic bond imparts a slight deshielding effect (given as a positive value) on the adjacent  $\alpha$ -,  $\beta$ -

Table 1  
Results of the  $^1\text{H}$ -NMR analysis of acetylenic tellura fatty acid esters (1–5)

Nucleus (protons)	Compound ( $\delta_{\text{H}}$ )				
	(1)	(2)	(3)	(4)	(5)
2-H	2.34(t) ( $J = 7.2$ )	2.32(t) ( $J = 7.2$ )	2.30(t) ( $J = 7.2$ )	2.34(t) ( $J = 7.2$ )	2.31(t) ( $J = 7.2$ )
3-H	a	a	a	a	a
4-H	a	a	a	a	a
5-H	2.10(m)	a	b	2.87(t) ( $J = 6.8$ )	b
6-H	—	2.10(m)	a	Te	a
7-H	—	—	2.10(m)	3.27(s)	a
8-H	2.10(m)	—	—	—	2.77(t) ( $J = 6.8$ )
9-H	a	2.10(m)	—	—	Te
10-H	a	2.10(m)	2.70(s)	2.10(m)	—
11-H	2.64 (t, $J = 6.8$ )	2.71(t) ( $J = 6.8$ )	2.70(s)	2.10(m)	—
12-H	Te	Te	Te	a	2.48(t) ( $J = 7.0$ )
13-H	2.64 (t, $J = 6.8$ )	2.63(t) ( $J = 6.8$ )	2.61(t) ( $J = 6.8$ )	b	a
14-H	a	a	a	b	a
15-H	b*	b	b	b	b
16-H	b	b	b	b	b
17-H	b	b	b	b	b
18-H	0.89(t) ( $J = 7.0$ )	0.89(t) ( $J = 7.0$ )	0.90(t) ( $J = 7.0$ )	0.90(t) ( $J = 7.0$ )	0.89(t) ( $J = 7.0$ )
Ethyl ester	1.25(t) 4.12(q)	1.25(t) 4.12(q)	1.25(t) 4.12(q)	1.25(t) 4.12(q)	—
Methyl ester	—	—	—	—	3.67(s)

a = 1.50–1.80; b = 1.20–1.40.

$\text{CH}_3(\text{CH}_2)_5\text{-Te-(CH}_2)_4\text{-C}\equiv\text{C-(CH}_2)_4\text{COOEt}$  (1)

$\text{CH}_3(\text{CH}_2)_5\text{-Te-(CH}_2)_3\text{-C}\equiv\text{C-(CH}_2)_5\text{COOEt}$  (2)

$\text{CH}_3(\text{CH}_2)_5\text{-Te-(CH}_2)_2\text{-C}\equiv\text{C-(CH}_2)_6\text{COOEt}$  (3)

$\text{CH}_3(\text{CH}_2)_8\text{-C}\equiv\text{C-CH}_2\text{-Te-(CH}_2)_4\text{COOEt}$  (4)

$\text{CH}_3(\text{CH}_2)_6\text{-C}\equiv\text{C-Te-(CH}_2)_7\text{COOMe}$  (5)

and  $\gamma$ -methylene protons of +0.82, +0.16 and +0.13 ppm, respectively (Frost and Gunstone, 1975). Such values (shift parameters) when added to a basic value (1.255) for the shift of unperturbed methylene protons would give a fairly accurate estimation of the proton shifts of a particular proton(s) under those effects. From our study of the  $^1\text{H}$  NMR properties of methyl telluraurates, the tellurium nucleus shows strong deshielding effects (positive values for the shift parameters) on the shifts of the adjacent methylene protons: +1.395, +0.495 and +0.145 ppm for the  $\alpha$ -,  $\beta$ - and  $\gamma$ -methylene protons, respectively (Lie Ken Jie et al., 1991). By taking the combined shift effect of the acetylenic system and that of the tellurium nucleus into consideration, the assignments of the various shifts of the adjacent methylene protons in the acetylenic tellura fatty acid esters could be readily

accomplished. The results of the  $^1\text{H}$  NMR chemical shifts of compounds 1–5 are summarized in Table 1.

The presence of four methylene groups between the acetylenic bond and the tellurium atom in the alkyl chain of compound 1 prevented the acetylenic system to exercising any additional shift effect on the methylene group adjacent to the tellurium atom and vice versa. As a result the shifts of the protons of the methylene groups (5-H, 8-H) adjacent to the acetylenic bond appeared at the anticipated region of the spectrum  $\delta_{\text{H}}$  2.10 (multiplet), while the shifts of the methylene protons adjacent to the tellurium atom (11-H, 13-H) appeared as a triplet at  $\delta_{\text{H}}$  2.64 (t,  $J = 6.8$  Hz). In the trimethylene-interrupted isomer (compound 2) the shifts of the methylene protons adjacent the tellurium atom were partially resolved into two overlapping triplets at  $\delta_{\text{H}}$  2.63



(13-*H*) and 2.71 (11-*H*) due to the  $\gamma$ -effect of the acetylenic system on the 11-*H* protons. However, the  $\gamma$ -effect from the tellurium on the methylene adjacent to the acetylenic bond was not obvious, as the signals for these protons were not further differentiated as they appeared unresolved in the region  $\delta_H$  2.10 (m) of the spectrum.

For compound **3** the shifts of the two methylene groups between the acetylenic bond and the tellurium atom were clearly being affected by these groups. The shifts of these protons appeared as a singlet at  $\delta_H$  2.70 (4H, 10-*H*, 11-*H*), which reflected the chemical equivalence of these protons. The shifts of the 13-*H* (methylene protons adjacent to the tellurium atom) and that of 7-*H* were found at  $\delta_H$  2.61 (triplet) and 2.10 (multiplet), respectively. Compound **4** could be readily differentiated from the other isomers from the singlet at  $\delta_H$  3.27, which was due to the shift of the protons of the methylene group between the acetylenic bond and the tellurium atom. A significant downfield effect from the acetylenic system on the other methylene group adjacent to the tellurium atom was also observed as the shifts of these protons (5-*H*) appeared at  $\delta_H$  2.87 (t). However, the tellurium atom appeared not to cause any significant deshielding effect on the protons of the remaining methylene group adjacent (10-*H*,  $\delta_H$  2.10) to the acetylenic bond.

In the analysis of compound **5**, where the acetylenic group and the tellurium atom are bonded together, the interaction of the metal and the acetylenic system caused the methylene protons adjacent to the acetylenic bond and that adjacent to the tellurium atom to be clearly resolved. The shifts of the 8-*H* and 12-*H* protons appeared as distinct triplets at  $\delta_H$  2.77 and 2.48, respectively. From this study of the  $^1H$  NMR properties of acetylenic tellura fatty acid esters, it was possible to characterise the non-methylene, mono- and di-methylene from the tri- and tetramethylene interrupted isomers from their  $^1H$  NMR spectral properties.

### 3.3. $^{13}C$ NMR properties of acetylenic tellura fatty acid esters (**1–5**)

In the study of  $^{13}C$  NMR properties of

acetylenic fatty esters, the shielding shift effects (given as negative values) of an acetylenic system on the carbon shifts of methylene groups have been determined as:  $-11.00$ ,  $-0.65$  and  $-0.80$  for the adjacent  $\alpha$ -,  $\beta$ - and  $\gamma$ -methylene carbon nuclei, respectively (Bus et al., 1976). We have also determined the effects of a tellurium atom on the shifts of the adjacent methylene carbon atoms as:  $-27.10$  (shielding),  $+2.62$  (deshielding) and  $+2.34$  (deshielding) for the  $\alpha$ -,  $\beta$ - and  $\gamma$ -methylene carbon nuclei, respectively (Lie Ken Jie et al., 1991). The shift value of an unperturbed methylene carbon atom was assumed at 29.75 ppm. Taking the combined effects of the acetylenic system and the tellurium nucleus into consideration, the assignments of the shifts of the various methylene carbon atoms were accomplished. The results of the  $^{13}C$  NMR chemical shifts of compound **1–5** are summarized in Table 2.

In compounds **1–4** the presence of less perturbed triple bond was readily confirmed by the signals in the region of  $\delta_C$  79–82 for the shifts of the acetylenic carbon atoms, but not in the case of compound **5** where the tellurium atom is bonded to the triple bond. The strong shielding effect of the acetylenic system on the adjacent methylene carbon atoms caused these carbon atoms to appear at  $\delta_C$  18–22, unless the nuclei were being further affected by the tellurium atom. The very strong shielding  $\alpha$ -effects exhibited by the tellurium atom caused many of the shifts of the adjacent methylene carbons to appear close to the zero value of the spectrum ( $\delta_C = 0$ , tetramethylsilane) and in one instance (compound **4**) the shift of one of the adjacent methylene carbons appeared in the negative range of the  $^{13}C$  NMR spectrum.

In compound **1** (a tetramethylene interrupted acetylenic tellura isomer) the combined effects of the tellurium and acetylenic system made it difficult to differentiate the shifts of the  $\beta$ -methylene carbon atoms (C-9 and C-10) as the shifts appeared at  $\delta_C$  31.35 and 31.45 for these two nuclei. However, in this narrow region of the spectrum, the signals at  $\delta_C$  31.27 and 31.75 could be assigned to the C-15 and C-16 carbon nuclei,



Table 2  
Results of the  $^{13}\text{C}$  NMR analysis of acetylenic tellura fatty acid esters (1–5)

Nucleus (carbon)	Compound ( $\delta_{\text{C}}$ )				
	(1)	(2)	(3)	(4)	(5)
C-1	173.87	173.30	173.63	173.60	174.06
C-2	33.67	34.02	34.35	33.72	34.08
C-3	24.20	24.54	24.89	27.34	24.92
C-4	28.20	28.41 <sup>a</sup>	28.77 <sup>a</sup>	31.57	29.12
C-5	18.53	28.76 <sup>a</sup>	28.50 <sup>a</sup>	4.81	28.58
C-6	79.91	18.66	28.68 <sup>a</sup>	Te	31.42
C-7	80.18	80.80	18.77	–17.95	31.50
C-8	18.15	79.20	80.93	82.99	8.90
C-9	31.45 <sup>a</sup>	21.07	81.04	78.23	Te
C-10	31.35 <sup>a</sup>	31.61	22.56	19.05	34.34
C-11	1.79	1.44	0.65	29.09 <sup>a</sup>	112.73
C-12	Te	Te	Te	28.97 <sup>a</sup>	21.02
C-13	2.79	2.95	3.11	29.27 <sup>a</sup>	28.82 <sup>a</sup>
C-14	32.29	32.26	32.34	29.56 <sup>a</sup>	28.82 <sup>a</sup>
C-15	31.27	31.26	31.23	29.23 <sup>a</sup>	29.12 <sup>a</sup>
C-16	31.75	31.75	31.75	31.93	31.77
C-17	22.59	22.56	22.69	22.70	22.64
C-18	14.03	14.00	14.00	14.00	14.06
Ethyl ester	14.30 60.25	14.28 60.28	14.27 60.11	14.30 60.20	—
Methyl ester	—	—	—	—	51.38

<sup>a</sup> Interchangeable.

$\text{CH}_3(\text{CH}_2)_5\text{-Te-(CH}_2)_4\text{-C}\equiv\text{C-(CH}_2)_4\text{COOEt}$  (1)

$\text{CH}_3(\text{CH}_2)_5\text{-Te-(CH}_2)_3\text{-C}\equiv\text{C-(CH}_2)_5\text{COOEt}$  (2)

$\text{CH}_3(\text{CH}_2)_5\text{-Te-(CH}_2)_2\text{-C}\equiv\text{C-(CH}_2)_6\text{COOEt}$  (3)

$\text{CH}_3(\text{CH}_2)_8\text{-C}\equiv\text{C-CH}_2\text{-Te-(CH}_2)_4\text{COOEt}$  (4)

$\text{CH}_3(\text{CH}_2)_6\text{-C}\equiv\text{C-Te-(CH}_2)_7\text{COOMe}$  (5)

respectively. The  $\alpha$ -methylene carbons to the acetylenic system and those adjacent to the tellurium atom were readily identified. In this isomer, where the acetylenic bond is located between the C-6/C-7 position of the fatty acid ester chain, the long range effect from the ethyl ester function on the shift of the acetylenic carbon atoms permitted the acetylenic carbon atoms to be resolved with the result that the shifts of the C-6 and C-7 carbon nuclei appeared at  $\delta_{\text{C}}$  79.91 and 80.18, respectively.

The carbon shifts of the methylene carbon atom(s) of the mono-, di- and tri-methylene interrupted acetylenic tellura isomers (compounds 2–4) were readily assigned. The effect of the tellurium atom on the shifts of the acetylenic system also allowed the acetylenic carbon atoms to be identified. Of interest was the large negative

shift value ( $\delta_{\text{C}}$  –17.95) observed for the shift of the methylene carbon atom (C-7) of compound 4, which is located between the acetylenic system and the tellurium atom.

In compound 5, where the tellurium atom is bonded to the acetylenic system, the shifts of the acetylenic carbon atoms were unique and appeared at  $\delta_{\text{C}}$  34.34 and 112.73 for C-10 and C-11, respectively. However, the shift of the methylene carbon atom adjacent to the tellurium nucleus (C-8) appeared much more downfield (at  $\delta_{\text{C}}$  8.90) than expected (at about  $\delta_{\text{C}}$  2.00–3.00 region) of this nucleus. Similarly the methylene carbon adjacent to the acetylene system (C-12) appeared at  $\delta_{\text{C}}$  21.02 instead of about  $\delta_{\text{C}}$  18.00 had there been no tellurium atom bonded to the triple bond system.

From the study of the NMR properties of these acetylenic tellura fatty acid esters, it was possible

to use this technique to identify each isomers as either the non-, mono-, di-, tri- or tetra-methylene interrupted isomer acetylenic tellura fatty ester analogue.

### Acknowledgements

The Lipid Research Fund, the Research Grants Committee of the University of Hong Kong and the Research Grant Council of Hong Kong provided financial assistance.

### References

- Bus, J., Sies, I., Lie Ken Jie, M.S.F., 1976. *Chem. Phys. Lipids* 17, 501–518.
- Dabdoub, M.J., Comasseto, J.V., 1988. *Organometallics* 7, 84–87.
- Frost, D.J., Gunstone, F.D., 1975. *Chem. Phys. Lipids* 15, 53–85.
- Goodman, M.M., Knapp, F.F., 1982. *J. Org. Chem.* 47, 3004–3006.
- Knapp, F.F., Ambrose, K.R., Callahan, A.P., Grigsby, R.A., Irgolic, K.J. 1979. *Radiopharm* 2, Proc Int Symp 101–108.
- Knapp, F.F., Srivastava, P.C., Callahan, A.P., Cunningham, E.B., Kabalka, G.W., Sastry, K.A.R., 1984. *J. Med. Chem.* 27, 57–63.
- Lie Ken Jie, M.S.F., Cheung, Y.K., Chau, S.H., Yan, B.F.Y., 1991. *J. Chem. Soc. Perkin Trans. 2*, 501–508.
- Lie Ken Jie, M.S.F., Chau, S.H., 1995. *J. Chem. Res. (S)*428, (M)2642–2657.
- Lie Ken Jie, M.S.F., Chau, S.H., 1995b. *Chem. Phys. Lipids* 78, 189–192.
- Lie Ken Jie, M.S.F., Chau, S.H., 1995c. *Biol. Mass. Spectrom.* 31, 115–117.
- Srivastava, P.C., Knapp, F.F., Kabalka, G.W., 1987. *Phosphorus Sulfur* 38, 49–58.





## Morphology of semisolid aqueous phosphatidylcholine dispersions, a freeze fracture electron microscopy study

Martin Brandl <sup>a,\*</sup>, Markus Drechsler <sup>b</sup>, Dieter Bachmann <sup>a,c</sup>, Kurt-Heinz Bauer <sup>a</sup>

<sup>a</sup> *Pharmazeutisches Institut, Pharmazeutische Technologie, Albert-Ludwigs-Universität Freiburg, 79104 Freiburg, Germany*

<sup>b</sup> *Kardiologisches Labor der Charité, Humboldt-Universität zu Berlin, 10117 Berlin, Germany*

<sup>c</sup> *Pastfach 652241, 22373 Hamburg, Germany*

Received 5 November 1996; received in revised form 25 March 1997; accepted 3 April 1997

### Abstract

Semisolid aqueous dispersions of soy phosphatidylcholine (PC) with high PC mass fractions between 0.35 and 0.6 were prepared using a high-pressure homogeniser. Their morphologies were investigated by freeze fracture transmission electron microscopy (FF-TEM) with regard to the quantity of water present. With all lipid/buffer ratios studied, vesicular structures in dense packing were seen on FF-TEM micrographs. PC ratios of up to 0.45 yielded small, unilamellar vesicles which were uniform in size. Matrices of higher lipid/buffer-ratios (0.45–0.6) also contained these small unilamellar vesicles plus an increasing fraction of more heterogeneous large multivesicular or multilamellar vesicles. Apparently, organisation of PC into small, homogeneous and unilamellar vesicles is not limited to ‘classical’ liposome dispersions, i.e. dilute lipid dispersions (< 300 mM), but can also be achieved in more concentrated lipid dispersions of PC fractions of up to 0.45 (600 mM) when lipid swelling is exerted under high mechanical stress conditions. © 1997 Elsevier Science Ireland Ltd.

**Keywords:** Phospholipid; Phosphatidylcholine; Liposome; Vesicle; Electron microscopy; Freeze fracture

### 1. Introduction

The structure of phosphatidylcholine (PC) crystals and mesomorphic transitions occurring upon contact with water have been studied since the thirties, employing light microscopy, small angle X-ray scattering and later on neutron scattering and NMR techniques: PC-dihydrate can be obtained by crystallisation from water-containing

*Abbreviations:* FF-TEM, freeze fracture transmission electron microscopy; MLV, multilamellar vesicle; MVV, multivesicular vesicle; PC, phosphatidylcholine; SPC, soy phosphatidylcholine; SUV, small unilamellar vesicle.

\* Corresponding author. Tel.: + 49 761 2036330; fax: + 49 761 2036366; e-mail: brandlma@sun2.ruf.uni-freiburg.de

media (Yang et al., 1988). In the crystals PC molecules are arranged in lamellar structure with strong hydrogen bonding of the polar regions (Pearson and Pascher, 1979). The crystals show thermotropic and lyotropic mesomorphism. For reviews (Luzzati et al., 1968; Sackmann, 1974; Small, 1986; Cevc and Marsh, 1987; Borovyagin and Sabelnikov, 1989). Structures formed upon hydration with a limited amount of water are birefringent liquid crystals of (multi-) layered structure as revealed by X-ray analysis (Baer et al., 1941; Small, 1967). Isoelectric lipids show limited swelling whereas lipids with a net charge swell without limitation (Gulik-Krzywicki et al., 1969). Water uptake expands the gap between the bimolecular leaflets. At a certain mixing ratio, swelling of specimens reaches a maximum as derived from interlamellar repeat distances. At this particular mixing ratio, occurrence of water droplets embedded in the lamellar (neat) lipid phase first was observed light microscopically by Small (1967). Small thus defined this mixing ratio as the boundary between monophasic and biphasic state. A detailed interpretation of the different levels of the swelling of lipids based on neutron scattering and NMR is given by Klose (Klose et al., 1986 and Klose et al., 1988). For a review on maximum hydration and structural dimensions of lipid multilayers Rand and Parsegian (1989).

Liposomes, i.e. closed vesicles forming if lipid(s) are dispersed in excess aqueous medium, were extensively studied over the past decades. The vast majority of investigations deals with dispersions of relatively low lipid concentrations of not more than 300 mM or 25% (m/m). It is well established that application of mechanical stress reduces size as well as lamellarity of vesicles (Brandl, 1996). Various preparation methods utilise this effect, such as ultrasonication (Huang, 1969), extrusion through membrane filters (Hope et al., 1986; Jousma et al., 1987; Schneider et al., 1994) or high-pressure homogenisation. Furthermore, solid lipids can be transferred into small unilamellar liposomes by appropriate homogenisers in a single step (Brandl et al., 1990).

The morphology of more concentrated phospholipid dispersions (> 300 mM), however, has not been studied systematically. Besides the above

mentioned light microscopic and a number of X-ray studies, little information on their morphology is available in the literature (Cevc and Marsh, 1987; Rand and Parsegian, 1989).

The aim of the present study was to prepare highly concentrated aqueous phosphatidylcholine dispersions, i.e. mixtures of PC mass fractions between 0.35 and 0.6 by applying different levels of mechanical stress, and to elucidate the morphology of the obtained dispersions by freeze fracture transmission electron microscopy (FF-TEM). It has previously been observed that particular high-pressure homogenisers can process highly viscous material (Brandl et al., 1993), and thus appear suitable to achieve 'forced hydration' of lipids in a controlled manner. A preliminary report of this work has been presented before (Brandl et al., 1996a,b).

## 2. Materials and methods

Preparation of concentrated phosphatidylcholine dispersions with increasing PC contents ranging from 35 to 60% has been performed in analogy with the one-step technique for preparation of liposomes (Brandl et al., 1990, 1993). In brief: dry powdered lipids were mixed with aqueous medium and this coarse dispersion was directly fed into a lab-scale high-pressure homogeniser (Gaulin Micron Lab 40, APV Homogeniser, Lübeck, Germany). The lipids used were highly purified phosphatidylcholine fractions from soy beans (Lipoid SPC, Lipoid GmbH, Ludwigshafen, Germany or Phospholipon 100, Nattermann Phospholipid GmbH, Köln, Germany). The buffer was isotonic phosphate buffered saline with a pH of 7.4. The homogenisation conditions were 70 MPa and 10 homogenisation cycles. These conditions previously had been found ideal (Brandl et al., 1990, 1993).

Preparation of specimens for electron microscopy: small pieces of the lipid paste were mounted on a gold specimen holder (Baltec, Balzers, Liechtenstein) and quick-frozen by plunging into liquid ethane cooled to 77–100 K using liquid nitrogen. After a few seconds the sample was transferred onto a specimen table immersed



in liquid nitrogen until insertion into the pre-cooled freeze fracture unit (BAF 301, Baltec, Balzers, Liechtenstein). Fracturing was carried out at 173 K and between  $3.5 \times 10^{-6}$  Pa and  $1.4 \times 10^{-5}$  Pa. The fractured faces were etched for 30 s at 173 K. Subsequently, the etched surface was vacuum deposited unidirectionally with platinum/carbon (2 nm) and carbon (30 nm) at an angle of 40–45°. The obtained replica was floated off in ethanol/water or ethanol/chloroform mixtures. Lipid traces were removed by repeated flushing. Specimens were visualised on a Philips EM400 transmission electron microscope or a Zeiss CEM 902, both operated at 80 kV high tension. At least three different freeze fracture replica of two separate lipid preparations were examined for each lipid/buffer ratio.

### 3. Results

Firstly, for reasons of comparison, PC was allowed to swell in buffer under low mechanical stress conditions, i.e. stirring by a magnetic stirrer for 2 h. In Fig. 1 micrographs of freeze fracture replica are given of such a preparation with PC/buffer ratio of 0.40: 0.60. The micrograph Fig. 1(a) gives an overview of the structures: more or less hemispherical fracture faces can be seen all over the image. The size distribution is quite heterogeneous with diameters ranging from below 0.1  $\mu\text{m}$  up to some ten micrometers. Step-like fractures through single lamellae are observed. Fig. 1(b) displays a cross fracture through a large vesicle with hundreds of concentric lamellae, separated by narrow spaces.

Secondly, samples of identical PC/buffer ratio (0.40:0.60) were prepared employing high mechanical stress conditions (high-pressure homogenisation). The corresponding freeze-fracture images are given in Fig. 2. The overall appearance of the specimen is totally different: very small, round fracture faces are seen almost exclusively with diameters below 100 nm and much more homogeneous appearance (Fig. 2(a)). Only a minute proportion of very large vesicles in the micrometer range can be observed. An example of such a large vesicle is depicted in

Fig. 2(b). Here the structure underneath the etched surface can also be distinguished: the interior of the large vesicle consists of hundreds of round, quite small fracture faces. Apparently the large vesicle is tightly filled with numerous small vesicles, it represents a multivesicular vesicle (MVV). In these preparations cross fractures through lamellae cannot be observed which indicates the absence of oligo- or multilamellar vesicles.

Almost identical observations were made with high-pressure homogenised samples of slightly lower and slightly higher PC contents (0.35 and 0.45 mass ratio respectively, Figs. 3 and 4 respectively). Mostly small, uniform and smooth fracture faces were found and few very large vesicles. When comparing the structures of 35, 40 and 45% dispersions, the proportion of very large vesicles seems to increase slightly with increasing lipid content. These large vesicles were all found to be filled with small vesicles when exhibiting their interior.

With further increased PC content of 0.50 mass ratio, a dramatic change in the structures is found (Fig. 5): besides areas with predominantly small uniform vesicles, a considerable fraction of larger vesicles can be distinguished. Furthermore, these large vesicles do not exhibit multivesicular inner structures rather than concentric lamellar packing. Also some plane-parallel stacks of lamellar sheets are seen (Fig. 5(a) and (b)).

With PC/buffer mixtures of even higher PC proportion of 0.60, freeze fracture images (Fig. 6(a) and (b)) reveal similar types of structures: firstly, small uniform fracture faces, secondly large vesicles with cross fractures of concentric lamellae and thirdly lamellar stacks. A difference in the proportion of these three elements between matrices of 0.50 and 0.60 PC mass ratio could not be found.

For comparison, solid crystalline PC was freeze fractured and examined, which exhibit a lamellar crystal structure of undisturbed plane-parallel organisation within the dimension detectable by FF-TEM, i.e. several microns (Fig. 7), comparable to those published by Daemer et al., 1970.



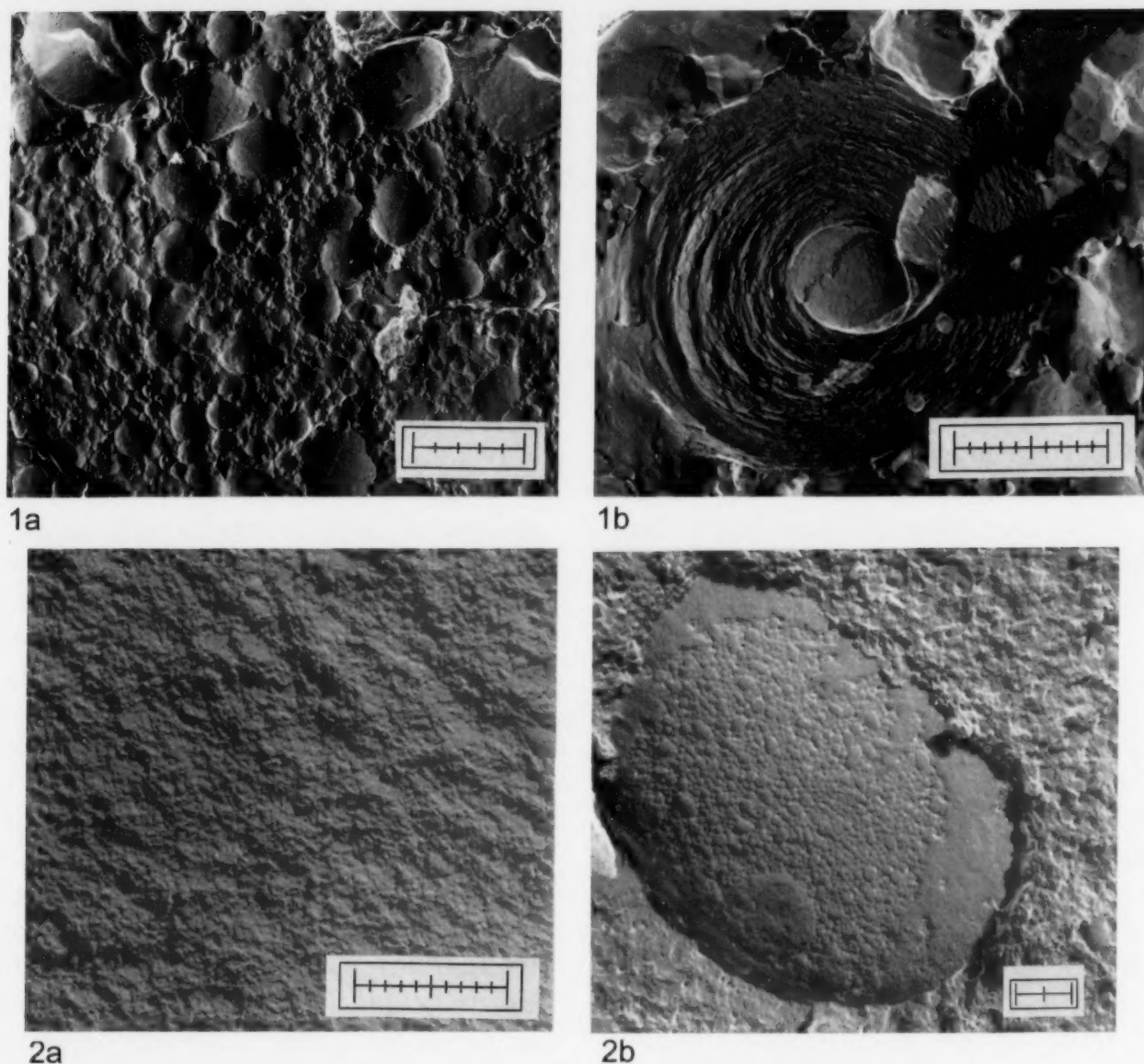


Fig. 1. FF-TEM micrograph of 40% soy phosphatidylcholine (SPC) dispersion in buffer, prepared by gentle agitation using a magnetic stirrer. (a) Heterogeneous vesicles of broad size distribution up to several microns in dense packing; bar is 5  $\mu\text{m}$  in total. (b) Cross fracture through large vesicle with multiple concentric lamellae (multilamellar vesicle, MLV) embedded in lipid matrix; bar is 1  $\mu\text{m}$  in total.

Fig. 2. FF-TEM micrograph of 40% SPC dispersion in buffer, prepared under high mechanical stress conditions by high-pressure homogenisation at  $10 \times 70$  Mpa. (a) Homogeneous, uniform small vesicles in the size range below 100 nm in dense packing; bar is 1  $\mu\text{m}$  in total. (b) Fracture through a very large vesicle filled with numerous small vesicles (multivesicular vesicle, MVV), embedded in matrix of small vesicles; bar is 200 nm in total.

#### 4. Discussion

Visualisation of semisolid PC dispersions by freeze-fracture transmission electron microscopy revealed one typical morphology for all lipid/buffer ratios studied (0.35–0.6): a matrix of tightly packed vesicles with almost no space between them. The sizes and morphologies of the vesicles, however, varied widely with lipid content and preparation conditions:

When prepared by using low mechanical stress (magnetic stirring) pastes of PC fractions of 0.40 exhibited a heterogeneous vesicle population with diameters ranging from below 0.1 to some 10  $\mu\text{m}$  and with uni- to multi-lamellar walls. Cross fractured vesicles showed up to hundreds of concentric lamellae. The 'onion' structure is typical for multilamellar vesicles (MLVs) and comparable to those typically found in 'classical', handshaken liposome dispersions (Guiot et al., 1980). The

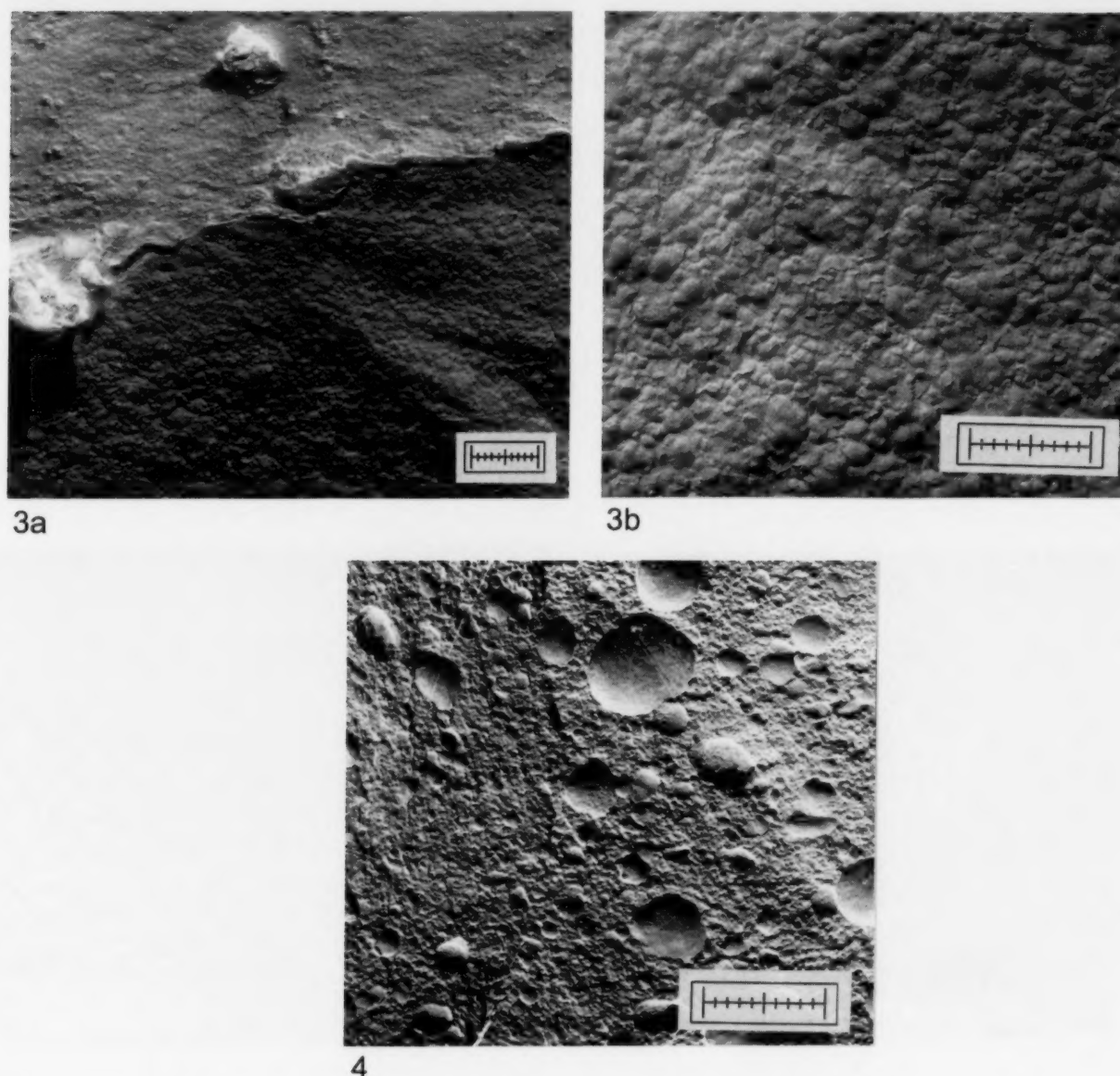


Fig. 3. FF-TEM micrograph of 35% SPC dispersion in buffer, prepared by high-pressure homogenisation at  $10 \times 70$  Mpa. (a) Fracture plane (lower part of the image) and surface (upper part) of a matrix of homogeneous, uniform small vesicles in the size range below 100 nm; bar is 1  $\mu$ m in total. (b) Enlarged sector of the fracture plane of (a); bar is 1  $\mu$ m in total.

Fig. 4. FF-TEM micrograph of 45% SPC dispersion in buffer, prepared by high-pressure homogenisation at  $10 \times 70$  Mpa. Matrix of predominantly small vesicles with embedded large vesicles in the micrometer-range partly exhibiting golf-ball-like surfaces due to filling with small vesicles (multivesicular vesicles, MVV); bar is 1  $\mu$ m in total.

only difference is that the vesicles formed at the high phospholipid concentrations appear closely packed and no space between the vesicles can be seen. The absence of regions of extended plane-parallel lamellar organisation (Daemer et al., 1970) indicates that no unswollen, crystalline lipid remains.

Preparations obtained by lipid swelling under high mechanical stress conditions (high pressure homogenisation) can be classified into two groups. The first group of lipid concentrations

between 35 and 45% has a highly homogenous appearance and consists of densely packed vesicles of small and uniform size ( $< 100$  nm in diameter). Only a minute proportion of large vesicles tightly filled with small vesicles, i.e. multivesicular vesicles (MVV) is found. No cross fractures displaying concentric lamellae can be seen. It is thus assumed that the vesicles are unilamellar.

In the second group with higher lipid contents of 50 and 60% of PC, more heterogeneous struc-



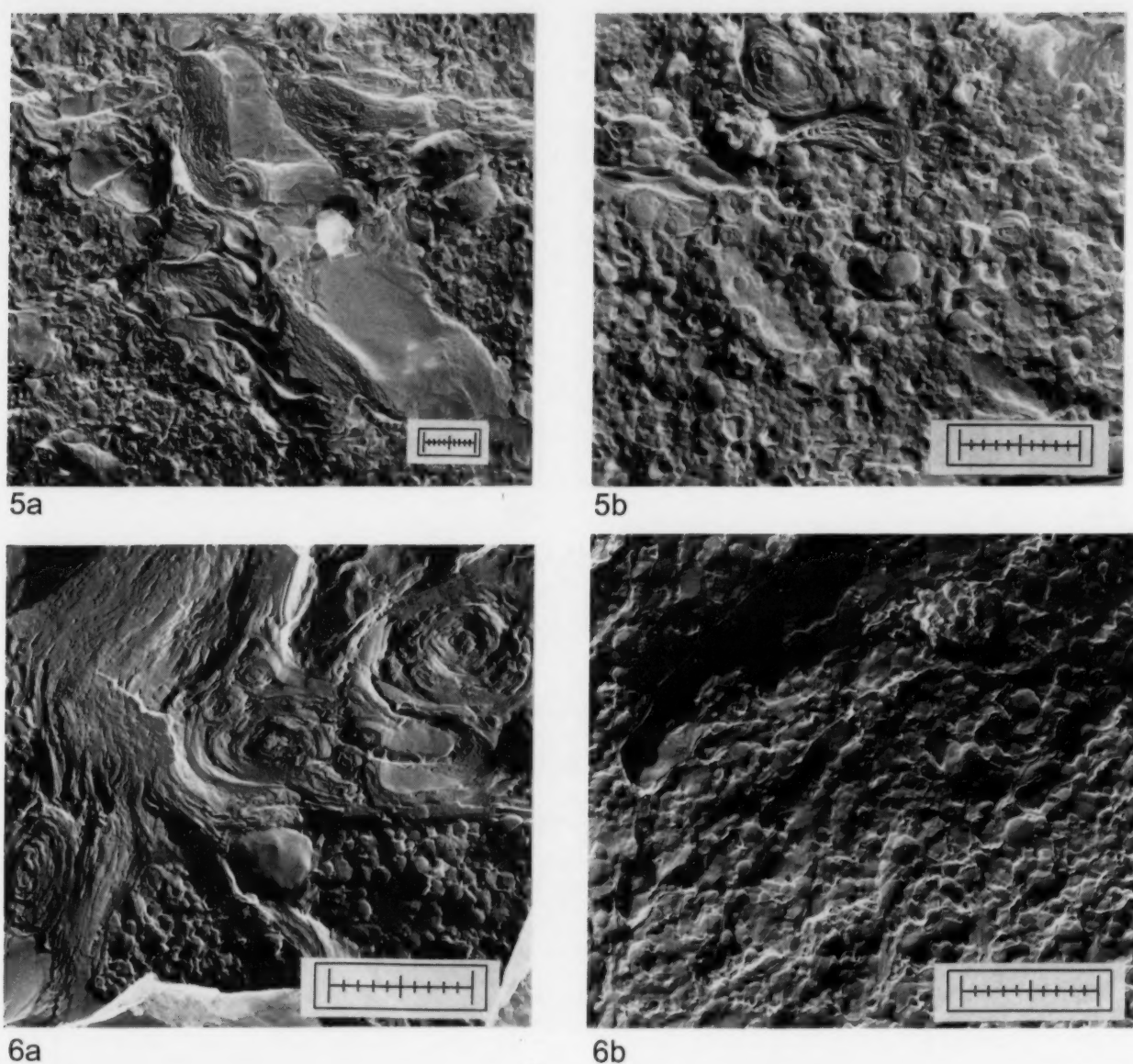


Fig. 5. FF-TEM micrograph of 50% SPC dispersion in buffer, prepared by high-pressure homogenisation at  $10 \times 70$  Mpa. (a) Matrix of small uniform vesicles with embedded (deformed) large multilamellar vesicles (MLV) and plane-parallel stacks of lamellae; bar is  $1 \mu\text{m}$  in total. (b) Enlarged sector of (a); bar is  $1 \mu\text{m}$  in total.

Fig. 6. FF-TEM micrograph of 60% SPC dispersion in buffer, prepared by high-pressure homogenisation at  $10 \times 70$  Mpa. (a) matrix composed of small uniform vesicles and stacks of lamellae with embedded (deformed) large multilamellar vesicles (MLV); bar is  $1 \mu\text{m}$  in total. (b) Sector displaying matrix predominantly composed of small uniform vesicles; bar is  $1 \mu\text{m}$  in total.

tures are seen even after high-pressure homogenisation. Besides small uniform and unilamellar vesicles, large multilamellar vesicles and stacks of lamellae turn up. Some of the lamellar stacks can be assigned to deformed multilamellar vesicles. In other cases it is difficult, however, to distinguish between parts of very large closed vesicular systems and remainders of PC crystals. From light microscopic observations and X-ray analysis of highly concentrated PC dispersions, which had been allowed to swell under low mechanical stress

conditions, Small (1967) concluded that PC contents of more than 55% yield monophasic preparations of neat or lamellar character. In the literature different data on hydration capacities are found (Rand and Parsegian, 1989). All these data, however, refer to dispersions which were allowed to swell under low mechanical stress conditions whereas here forced hydration (high-pressure homogenisation) was used. Klose et al. (1988) demonstrated that the extended planar sheets of the lamellar phase near the boundary



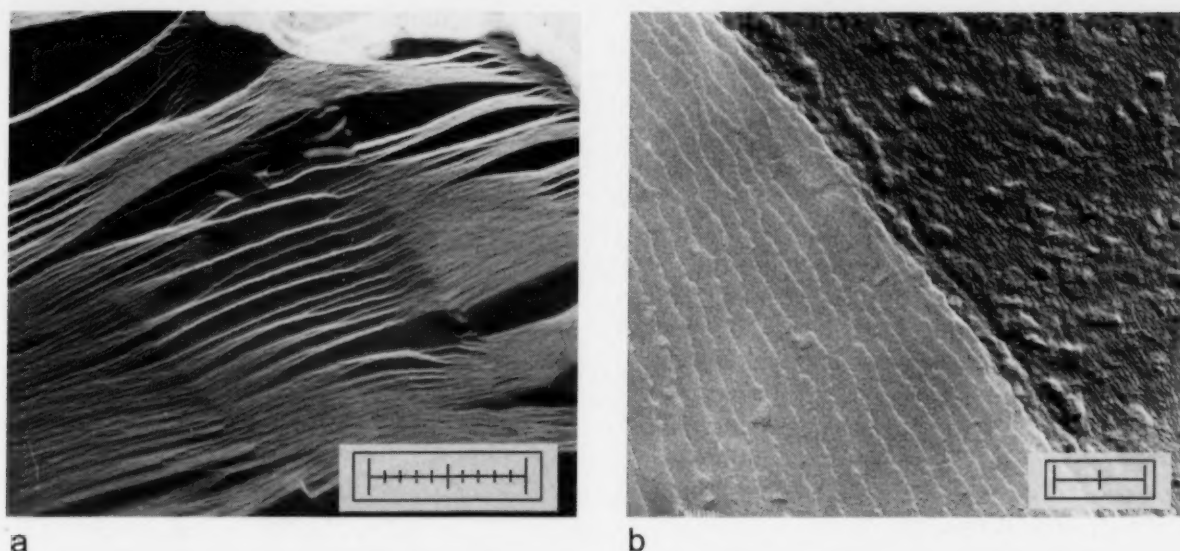


Fig. 7. FF-TEM micrograph of crystalline SPC. (a) Fracture face of SPC crystallite exhibiting plane-parallel lamellar orientation; bar is 1  $\mu\text{m}$  in total. (b) as a) but fractured at different angle; bar is 200 nm in total.

between mono- and biphasic show local defects such as vesicle-like structures and spheroidal water cores. Klose observed this after hydration by back and forward centrifugation and found that the repeat distances measured by X-ray diffraction were influenced by this. In the 50 and 60% dispersions studied here, apparently these structural 'defects' are enhanced: a considerable proportion of the PC is arranged in the form of small unilamellar vesicles due to homogenisation. Limitation of free water seems to prevent complete reorganisation of the dispersion, some proportion remaining in the form of stacks of planar lamellar sheets or large multilamellar vesicles respectively. FF-TEM cannot quantify lamellar sheets of unswollen, partly or completely swollen lipid. Although characterisation of the concentrated lipid dispersions so far is by no means exhaustive and information from FF-TEM will have to be complemented by small angle X-ray scattering, NMR and other techniques it can be concluded: highly concentrated lipid dispersions (PC mass fractions between 0.35 and 0.60) adopt vesicular structures upon swelling, analogous to dilute liposome dispersions. Size and lamellarity of the vesicles depend on lipid concentration as well as on intensity of mechanical stress exerted during swelling. Upon gentle agitation, very heterogeneous disper-

sions of uni- to multilamellar vesicles in a broad size distribution are formed, whereas after high-pressure homogenisation the pastes predominantly consist of homogeneous small and unilamellar vesicles as long as lipid concentrations do not exceed 45%. Above 45% large multilamellar vesicles (MLVs) and planar lamellar stacks extending to a range of several 10  $\mu\text{m}$  are found as well as small unilamellar vesicles (SUVs).

The pastes consisting of vesicles in dense packing might have a potential as drug carrier systems. They may be used as an implantable depot formulation for controlled release of drugs in locoregional or systemic therapy (Brandl et al., 1996b).

#### Acknowledgements

We should like to thank Dr A. Bauer-Brandl and Professor Dr R. Schubert, University of Freiburg, for helpful discussions during the preparation of the manuscript and Günther Kopp and Eva Schill-Wendt for excellent technical support in the photographic workshop. Donations of lipid samples by Lipoid GmbH, Nattermann Phospholipid GmbH and financial support by Deutsche Forschungsgemeinschaft (grant for M.D. within SFB 60) are gratefully acknowledged.

## References

- Baer, S., Palmer, X., Schmitt, X., 1941. X-ray diffraction studies on nerve lipids. *J. Cell. Comp. Physiol.* 17, 355–367.
- Borovyagin, V.L., Sabelnikov, A.G., 1989. Lipid polymorphism of model and cellular membranes as revealed by electron microscopy. *Electron. Microsc. Rev.* 2, 75–115.
- Brandl, M., Bachmann, D., Drechsler, M., Bauer, K.H., 1990. Liposome preparation by a new high pressure homogenizer Gaulin Micron Lab 40. *Drug Dev. Ind. Pharm.* 16, 2167–2191.
- Brandl, M., Bachmann, D., Drechsler, M., Bauer, K.H., 1993. Liposome preparation using high-pressure homogenizers. In: Gregoriadis, G., (Ed.), *Liposome Technology* 2nd ed. vol. 1, CRC Press, Boca Raton, pp. 49–65.
- Brandl, M., Bachmann, D., Reszka, R., Drechsler, M., 1996a. Unilamellar Liposomal Preparations with High Active Substance Content, PCT/DE95/01062 (WO 96/05808).
- Brandl, M., 1996. From myelin figures to small, unilamellar vesicles: how mechanical stress influences the formation of liposomes. *Polymorfi* 12–15.
- Brandl, M., Drechsler, M., Bachmann, D., Bauer, K.H., 1996b. Three-dimensional networks of liposomes: Preparation and electron microscopical characterization. *Proceed. Intern. Symp. Control. Rel. Bioact. Mater.* 23, 25–26.
- Cevc, G. and Marsh, D., 1987. *Phospholipid Bilayers. Physical Principles and Models*, John Wiley and Sons, New York.
- Daemer, D.W., Leonard, R., Tardieu, A., Branton, D., 1970. Lamellar and hexagonal lipid phases visualized by freeze-etching. *Biochim. Biophys. Acta* 219, 47–60.
- Guiot, P., Baudhuin, P., Gotfredsen, C., 1980. Morphological characterization of liposome suspensions by stereological analysis of freeze-fracture replicas from spray-frozen samples. *J. Microsc.* 120, 159–174.
- Gulik-Krzywicki, T., Tardieu, A., Luzzati, V., 1969. The Smectic Phase of Lipid-Water Systems: Properties Related to the Nature of the Lipid and to the Presence of Net Electrical Charges. *Mol. Cryst. Liquid Cryst.* 8, 285–291.
- Hope, M.J., Bally, M.B., Mayer, L.D., Janoff, A.S., Cullis, P.R., 1986. Generation of multilamellar and unilamellar phospholipid vesicles. *Chem. Phys. Lipids* 40, 89–107.
- Huang, C., 1969. Studies on phosphatidylcholine vesicles formation and physical characteristics. *Biochemistry* 8, 344–352.
- Jousma, H., Talsma, H., Spies, F., Joosten, J.G.H., Junginger, H.E., Crommelin, D.J.A., 1987. Characterization of liposomes. The influence of extrusion of multilamellar vesicles through polycarbonate membranes on particle size, particle size distribution and number of bilayers. *Int. J. Pharm.* 35, 263–274.
- Klose, G., Brückner, S., Bezzabotnov, V.Y.U., Borbely, S., Ostanevich, Y.U.M., 1986. Hydration and swelling of the total lipid fraction of egg yolk and the influence of some additives studied by small-angle neutron scattering. *Chem. Phys. Lipids* 41, 293–307.
- Klose, G., König, B., Meyer, H.W., Schulze, G., Degovics, G., 1988. Small-angle X-ray scattering and electron microscopy of crude dispersions of swelling lipids and the influence of the morphology on the repeat distance. *Chem. Phys. Lipids* 47, 225–234.
- Luzzati, V., Gulik-Krzywicki, T., Tardieu, A., 1968. Polymorphism of Lecithins. *Nature* 218, 1031–1034.
- Pearson, R.H., Pascher, I., 1979. The molecular structure of lecithin hydrate. *Nature* 281, 499–501.
- Rand, R.P., Parsegian, V.A., 1989. Hydration forces between phospholipid bilayers. *Biochim. Biophys. Acta* 988, 351–376.
- Sackmann, E., 1974. Flüssig-kristalline Zustände in künstlichen und biologischen Membranen. *Ber. Bunsenges.* 78, 929–941.
- Schneider, T., Sachse, A., Rößling, G., Brandl, M., 1994. Large-scale production of liposomes of defined size by a new continuous high pressure extrusion device. *Drug. Dev. Ind. Pharm.* 20, 2787–2807.
- Small, D.M., 1967. Phase equilibria and structure of dry and hydrated egg lecithin. *J. Lipid Res.* 8, 551–557.
- Small, D.M., 1986. Phospholipids. In: *Handbook of Lipid Research*, Plenum Press, New York pp. 475–522.
- Yang, C.P., Wiener, M.C., Nagle, J.F., 1988. New phases of DPPC/water mixtures. *Biochim. Biophys. Acta* 945, 101–104.

## Plastoquinol and $\alpha$ -tocopherol quinol are more active than ubiquinol and $\alpha$ -tocopherol in inhibition of lipid peroxidation

Jerzy Kruk, Małgorzata Jemioła-Rzemińska, Kazimierz Strzałka \*

*Department of Plant Physiology and Biochemistry, The Jan Zurzycki Institute of Molecular Biology, Jagiellonian University,  
Al. Mickiewicza 3, 31–120 Kraków, Poland*

Received 13 January 1997; received in revised form 1 April 1997; accepted 3 April 1997

### Abstract

Comparative studies of antioxidant activities of such natural prenyllipids as plastoquinol-9 (PQH<sub>2</sub>-9),  $\alpha$ -tocopherol quinol ( $\alpha$ -TQH<sub>2</sub>), ubiquinol-10 (UQH<sub>2</sub>-10) and  $\alpha$ -tocopherol ( $\alpha$ -T) in egg yolk lecithin liposomes have been performed. The investigated compounds showed oxidation under molecular oxygen in the order UQH<sub>2</sub>-10 >  $\alpha$ -TQH<sub>2</sub> > PQH<sub>2</sub>-9 >  $\alpha$ -T. The corresponding second order rate constants have been determined in Tris buffer (pH = 6.5) and were 0.413, 0.268, 0.154 and 0.022 M<sup>-1</sup>/s, respectively. The inhibition order of Fe<sup>2+</sup>-H<sub>2</sub>O<sub>2</sub>-induced lipid peroxidation, corrected for the amount of prenyllipids oxidized during the initiation period, was  $\alpha$ -TQH<sub>2</sub> > PQH<sub>2</sub>-9 >  $\alpha$ -T > UQH<sub>2</sub>-10 for 5 mol% of the antioxidants content in liposomes. The radicals formed in the initiation phase of the reaction caused oxidation of 27.5–33%  $\alpha$ -T, 40–64% UQH<sub>2</sub>-10, 42–85% PQH<sub>2</sub>-9 and 43–80%  $\alpha$ -TQH<sub>2</sub>, depending on the antioxidant concentration in liposomes (5–1 mol%, respectively) which reflects approximately their reactivity against radicals derived from the Fenton reaction. The antioxidant activity of the investigated prenylquinols, in relation to the activity of  $\alpha$ -T, in natural membranes is discussed. © 1997 Elsevier Science Ireland Ltd.

**Keywords:** Plastoquinol;  $\alpha$ -Tocopherol quinol; Ubiquinol;  $\alpha$ -Tocopherol; Antioxidant activity; Lipid peroxidation; Liposome

### 1. Introduction

Apart from the well established role of plastoquinol-9 (PQH<sub>2</sub>-9) and ubiquinol-10 (UQH<sub>2</sub>-10)

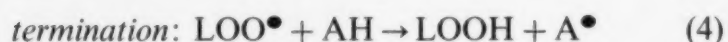
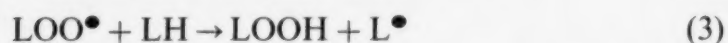
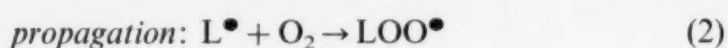
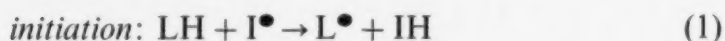
as hydrogen carriers in the photosynthetic (Rich and Moss, 1987) and respiratory (Gutman, 1980) electron transport chains, respectively, there is increasing evidence accumulating of their additional function as antioxidants (Frei et al., 1990; Kruk et al., 1994; Mukai et al., 1993; Stocker et al., 1991; Yamamoto et al., 1990) similar to that

\* Corresponding author: Tel.: +48 12 341305 ext. 237; fax: +48 12 336907; e-mail: strzalka@mol.uj.edu.pl



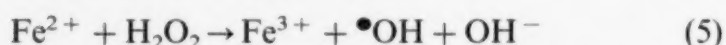
of  $\alpha$ -tocopherol ( $\alpha$ -T). The occurrence of  $\alpha$ -tocopherol quinol ( $\alpha$ -TQH<sub>2</sub>) in thylakoid and mitochondrial membranes whose function is hitherto not fully explained may be also connected with its antioxidant action in these systems as suggest some preliminary experiments (Bindoli et al., 1985; Kruk et al., 1994).

Lipid peroxidation is an autocatalytic chain reaction induced by a free radical initiator (I<sup>•</sup>), proceeding in the following steps (Vigo-Pelfrey, 1990):



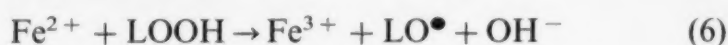
where LH, I<sup>•</sup> and L<sup>•</sup> and LOO<sup>•</sup> and AH are polyunsaturated fatty acid, initiator, the fatty acid alkyl and peroxy radicals, and antioxidant molecule, respectively.  $\alpha$ -T is the best known example of natural lipid soluble antioxidants (Machlin, 1980). The reduction of peroxy radicals by an antioxidant molecule Eq. (4) is the key reaction accounting for the inhibitory effect of antioxidants in lipid peroxidation.

In model systems, Fe<sup>2+</sup> salts were widely used for initiation of lipid peroxidation (Fujii et al., 1991; Fukuzawa et al., 1988a,b; Gutteridge, 1984; Liebler et al., 1986) giving in Fenton-type reaction with H<sub>2</sub>O<sub>2</sub> reactive hydroxyl radicals (and OH) which could be effective peroxidation initiators (Halliwell and Gutteridge, 1990):



Although the hydroxyl radical formed in this reaction is a very reactive species, it is a very short-lived radical which reacts with most organic compounds at nearly diffusion-controlled rates (Halliwell and Gutteridge, 1990). This reactivity makes little probable migration of <sup>•</sup>OH from the site of generation to the hydrophobic membrane compartments where the lipid peroxidation must be initiated. The other possibility could be site-specific, generation of <sup>•</sup>OH radicals at the site where they could immediately react with the target molecule, e.g. at the membrane surface

(Halliwell and Gutteridge, 1990). It was also proposed (Schaich and Borg, 1988) that the Fenton reaction Eq. (4) could also occur in the lipid phase of the membrane. The alternative initiators, suggested in Fenton reactions are complexes between oxygen and different valence state of iron (Halliwell and Gutteridge, 1990; Minotti and Aust, 1987), such as ferryl ion (FeO<sub>2</sub><sup>+</sup> or FeOH<sup>3+</sup>), the perferryl ion (Fe<sup>2+</sup>-O<sub>2</sub> or Fe<sup>3+</sup>-O<sub>2</sub><sup>•</sup>) and a ferrous-dioxygen-ferric complex (Fe<sup>2+</sup>-O<sub>2</sub>-Fe<sup>3+</sup>). In the absence of H<sub>2</sub>O<sub>2</sub>, Fe<sup>2+</sup> ions may also induce lipid peroxidation by reaction with traces of peroxides present originally in lipids or formed during the propagation step Eq. (3) of the peroxidation reaction:



The considerably lower concentration of lipid peroxides than those of H<sub>2</sub>O<sub>2</sub> usually used in the experiments is partially compensated by about 20 times higher reaction rate constant of the Eq. (6) than of the Eq. (5) (Halliwell and Gutteridge, 1990). Therefore, the rate of formation of the initiating radicals is probably of the same order in both cases.

Although there have been some studies performed on PQH<sub>2</sub>-9 and  $\alpha$ -TQH<sub>2</sub> as lipid antioxidants (Bindoli et al., 1985; Kruk et al., 1994; Mukai et al., 1992), mainly in solution, and on UQH<sub>2</sub>-10 in different systems (Beyer, 1990; Cabrini et al., 1991; Frei et al., 1990; Kagan et al., 1990; Mukai et al., 1992, 1993; Stocker et al., 1991; Yamamoto et al., 1990), so far there was no report on the antioxidant activity of these prenylquinols during Fe<sup>2+</sup>-induced lipid peroxidation of liposome membranes. Although the widely used system of peroxidation initiation with the azo-compounds enables calculation of peroxidation inhibition rate constants (Barclay et al., 1984), it gives much lower peroxidation rate than the Fenton system and therefore longer measurements time is required, during which considerable oxidation of such labile compounds as prenylquinols may take place. Moreover, the lipid soluble azoinitiator (AMVN) may perturb the liposome bilayer structure and change the antioxi-

dants localization or mobility within the membrane.

We have determined the inhibitory effect of the natural prenylquinols, in comparison to  $\alpha$ -T, on  $\text{Fe}^{2+}$ - $\text{H}_2\text{O}_2$ -induced lipid peroxidation of egg yolk lecithin liposomes at different antioxidant concentration, measuring oxygen uptake during this process. The prenyllipids concentration during the peroxidation reaction was followed directly by their fluorescence intensity (Kruk et al., 1993, 1994). Since quinols are known to oxidize under molecular oxygen, this reaction was measured for the compounds used in our study, and the reaction rate constants of prenyllipids auto-oxidation were determined. These data were used for the correction of oxygen uptake during the lipid peroxidation reaction.

## 2. Materials and methods

Ubiquinone-10 and plastoquinone-9 were a kind gift from Hoffmann-La Roche (Switzerland). They were purified by TLC on silica gel plates (Merck) using chloroform as an eluent.  $\alpha$ -Tocopherol quinone was prepared and purified according to Kruk (1988). The prenylquinols were obtained by reduction of the corresponding quinones with  $\text{NaBH}_4$  in methanol. The  $\alpha$ -T was from Merck and egg yolk lecithin (EYL), type V-E, was purchased from Sigma. The EYL preparation used for our studies was partially oxidized, having absorbance ratio  $A_{233}/A_{215} = 0.73$  in ethanol, which corresponds to approximately 1% of peroxides (Bergelson, 1980). Such increased content of lipid peroxides should promote  $\text{Fe}^{2+}$ -LOOH catalyzed lipid peroxidation. Small unilamellar liposomes were prepared by injection of ethanol solutions of an antioxidant and EYL into 10 mM Tris buffer (pH = 6.5) under continuous stirring. The final EYL concentration was 0.5 mM, ethanol concentration of 1.25% and antioxidants content in liposomes of 1, 3 or 5 mol%. All the measurements and liposome preparation were performed at 25°C. Lipid peroxidation was measured by monitoring oxygen uptake using Clark-type electrode (Hansatech), assuming an oxygen concentration of 253  $\mu\text{M}$  in the initial reaction

mixture at 25°C. Prenylquinols and  $\alpha$ -T concentration was measured fluorimetrically, on Perkin-Elmer LS-50 fluorimeter, using excitation at 290 nm and emission at 370 nm for UQH<sub>2</sub>-10 or 330 nm for the other compounds. We have found no changes in the fluorescence background level during the peroxidation reaction of the control sample containing no antioxidant, which could interfere with the antioxidant fluorescence. The total sample volume was 1 ml for oxygen uptake measurements and 2 ml for fluorescence measurements. Ferrous ammonium-sulphate (Aldrich) stock solution, because of its instability, was prepared directly before the measurements, in nitrogen saturated water. The lipid peroxidation reaction was started by addition of  $\text{H}_2\text{O}_2$  and  $\text{Fe}(\text{NH}_4)_2(\text{SO}_4)_2$  stock solutions to the preformed liposomes to a final concentration of 50  $\mu\text{M}$   $\text{Fe}^{2+}$  and 100  $\mu\text{M}$   $\text{H}_2\text{O}_2$ .

## 3. Results and discussion

Table 1 shows changes in the prenyllipids (AH) level in liposome membranes after the first 15 min of the measurement. The only possible reason for the prenyllipids concentration decrease is their oxidation under molecular oxygen, since the samples did not contain any initiators of the lipid peroxidation reaction. The average oxidation rates demonstrate that  $\alpha$ -T autoxidation is negligible, whereas UQH<sub>2</sub>-10 is most easily oxidized and the rates changed in the order  $\text{UQH}_2\text{-10} > \alpha\text{-TQH}_2 > \text{PQH}_2\text{-9} > \alpha\text{-T}$ . For the determination of the second order rate constants of the reaction ( $v = k[\text{O}_2][\text{AH}]$ ) the initial AH concentrations, reaction rates ( $\Delta\text{AH}$ ) and oxygen concentration (253  $\mu\text{M}$ ) were taken. The  $k$  values given in Table 1 are the average of the  $k$  values calculated for different initial AH concentrations (1, 3 and 5 mol%). The oxidation rates of the prenyllipids ( $\Delta[\text{AH}]_{15 \text{ min}}\%$ ) are similar for their different content in liposomes. This indicates that the possible differences in the localization of prenyllipids within the liposome bilayer at their different content (Jemioła-Rzemińska et al., 1996; Kruk et al., 1992) have no influence on the prenyllipids autoxidation rates. The obtained rate constants are



Table 1

Rates of prenyllipids (AH) in liposome membranes and the second order rate constants ( $k$ ) of the reaction determined from the fluorescence intensity changes of the prenylquinols

Antioxidant [content in mol%]	$\Delta[AH]_{15\text{min}}$ (%)	$\Delta[AH]_{15\text{min}}$ (%) (average)	$\Delta[AH](\mu\text{M}/\text{min})$	$k(\text{M}^{-1}/\text{s})$
PQH <sub>2</sub> -9 [1]	$4.4 \pm 1.0$	$3.5 \pm 0.6$	0.014	0.154
PQH <sub>2</sub> -9 [3]	$3.0 \pm 0.7$		0.03	
PQH <sub>2</sub> -9 [5]	$3.3 \pm 0.1$		0.055	
$\alpha$ -TQH <sub>2</sub> [1]	$5.6 \pm 0.5$	$6.1 \pm 0.9$	0.018	0.268
$\alpha$ -TQH <sub>2</sub> [3]	$5.3 \pm 1.6$		0.053	
$\alpha$ -TQH <sub>2</sub> [5]	$7.4 \pm 0.7$		0.124	
$\alpha$ -T [1]	$0.8 \pm 0.3$	$0.5 \pm 0.3$	0.002	0.022
$\alpha$ -T [3]	$0.3 \pm 0.1$		0.003	
$\alpha$ -T [5]	$0.5 \pm 0.4$		0.008	
UQH <sub>2</sub> -10 [1]	$10.8 \pm 0.9$	$9.4 \pm 2.7$	0.036	0.413
UQH <sub>2</sub> -10 [3]	$7.6 \pm 2.3$		0.076	
UQH <sub>2</sub> -10 [5]	$9.9 \pm 4.9$		0.165	

comparable with those determined for UQH<sub>2</sub>-1 ( $1.5 \text{ M}^{-1}/\text{s}$ , pH 7.5) (Sugioka et al., 1988) and UQH<sub>2</sub>-0 ( $1.32 \text{ M}^{-1}/\text{s}$ , pH 7.3) (Cadenas et al., 1977) in aqueous systems.  $\alpha$ -Tocopherol practically does not undergo autoxidation. Since the autoxidation of prenylquinols is pH dependent and is considerably faster at alkaline pH (29), so the observed reaction rates in our case (pH = 6.5) are expected to be higher at physiological pH (7.4) and temperatures. Even though the rate constants are relatively low, the autoxidation of prenylquinols decreases their concentration and this effect should be taken into account in studies of peroxidation inhibition reactions, especially during long-lasting reactions, such as those with the azoinitiators. The oxidized prenylquinols (prenylquinones), in contrast to  $\alpha$ -tocopherol, could be easily rereduced in natural membranes: plastoquinone by photosystem II in thylakoid membranes (Rich and Moss, 1987); ubiquinone by NADH-ubiquinone reductase or succinate-ubiquinone reductase in mitochondrial membranes (Gutman, 1980) and  $\alpha$ -tocopherol quinone both in thylakoid (Kruk and Strzałka, 1995) and mitochondrial (Bindoli et al., 1985) membranes by unidentified enzymes.

Changes in the AH concentration during  $\text{Fe}^{2+}$ - $\text{H}_2\text{O}_2$ -induced lipid peroxidation of EYL liposomes are biphasic (Fig. 1). The first, fast phase

taking about 30–40 s and a following, slow phase correspond to similar changes in oxygen consumption during the peroxidation reaction (Fig. 2). During the fast phase, the formation of hydroxyl radicals takes place Eq. (5) and probably of other active radicals which initiate lipid peroxidation and oxidize the prenyllipids. The hydroxyl

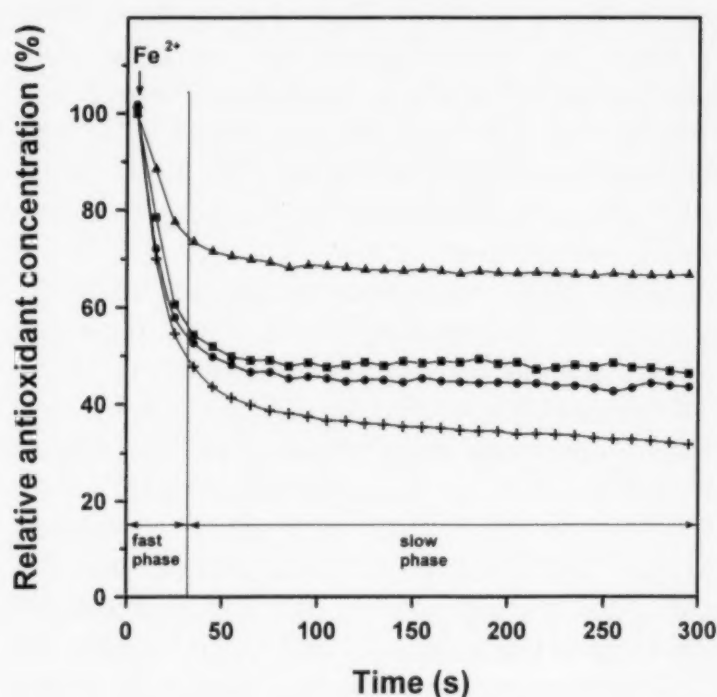


Fig. 1. Prenyllipids concentration changes in EYL liposomes during  $\text{Fe}^{2+}$ - $\text{H}_2\text{O}_2$ -induced lipid peroxidation. The antioxidants initial concentrations were 3 mol% in liposomes ( $15 \mu\text{M}$  in solution);  $\blacktriangle$ :  $\alpha$ -T,  $\blacksquare$ : UQH<sub>2</sub>-10,  $\bullet$ : PQH<sub>2</sub>-9,  $+$ :  $\alpha$ -TQH<sub>2</sub>



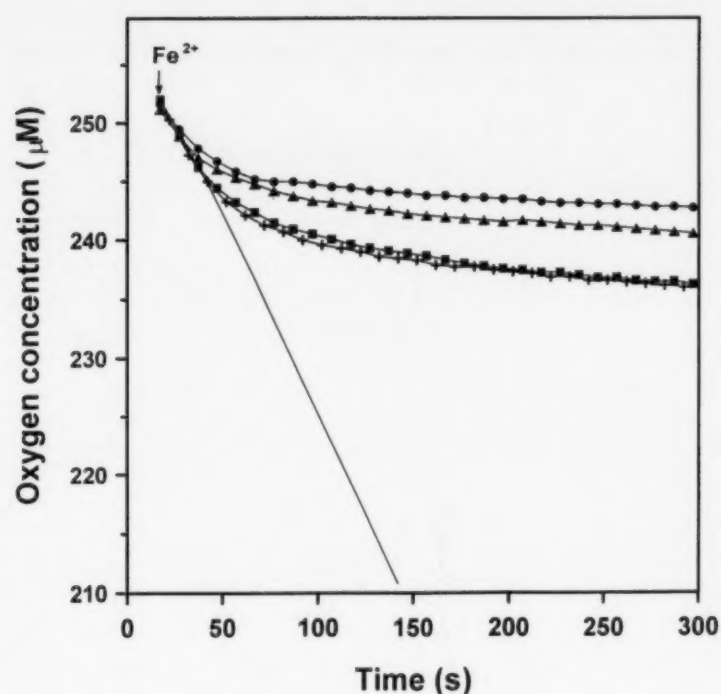


Fig. 2. Oxygen concentration changes during  $\text{Fe}^{2+}$ - $\text{H}_2\text{O}_2$ -induced lipid peroxidation of EYL liposomes (—), and liposomes containing 3 mol% of  $\alpha$ -T ( $\blacktriangle$ ),  $\text{PQH}_2$ -9 ( $\bullet$ ),  $\alpha$ - $\text{TQH}_2$  (+) or  $\text{UQH}_2$ -10 ( $\blacksquare$ ).

radicals are formed in the Fenton reaction only within the first 30 s of the reaction (Minotti and Aust, 1987). Therefore, their formation is probably negligible in the slow phase. The oxidation of AH during the fast phase followed the single exponential decay with  $k$  values in the range of  $11\text{--}13 \times 10^{-2} \text{ s}^{-1}$  and without any pronounced AH concentration dependence. The relative reactivity of the investigated compounds against radicals which initiate peroxidation in our system (mainly hydroxyl radicals), can be inferred from the relative AH amount oxidized after the fast phase of the reaction which changed in the order  $\alpha$ - $\text{TQH}_2 > \text{PQH}_2$ -9  $>$   $\text{UQH}_2$ -10  $>$   $\alpha$ -T (Table 2) for 3 and 5 mol% of the antioxidants content in liposomes. This order is probably a measure of the prenyllipids antioxidants activity against hydroxyl radicals formed in the fast phase of the peroxidation reaction. During the slow phase, where  $\text{Fe}^{2+}$ - $\text{LOOH}$ -induced lipid peroxidation Eq. (6) dominates, AH consumption was relatively low (Table 2) and was caused by oxidation of AH molecules by the lipid peroxy radicals (chain breaking reaction, Eq. (4)) and slow AH autooxidation. We have not observed any direct

AH oxidation by  $\text{Fe}^{3+}$  ions (data not shown) which are formed in the Fenton reaction. As can be seen from Fig. 2, there is a pronounced inhibitory effect of all the investigated antioxidants on oxygen consumption during lipid peroxidation of EYL liposomes, which is the consequence of peroxy radicals reduction by antioxidants Eq. (4) and breaking the chain reaction. The oxygen uptake rate is similar for 3 and 5 mol% of a given AH (Table 3) but at 1 mol%, apart from  $\alpha$ -T, is strongly increased, probably by the high degree of AH oxidation in these samples (Table 2). To compare the inhibitory effects of the investigated antioxidants, we have to also take into account the oxygen consumption associated with AH oxidation in the slow phase and due to AH autooxidation (assuming  $\text{O}_2$ :AH stoichiometry of 1:1) and the amount of the antioxidant left after the fast phase ( $1 - 100/\Delta[\text{AH}]_{\text{FP}}[\%]$ ). The corrections for AH oxidation is shown in brackets (Table 3, column 3) and the peroxidation inhibition coefficients calculated for the initial AH concentration from the formula:  $(100/v)/(1 - \Delta[\text{AH}]_{\text{FP}}[\%]/100)$  are shown in Fig. 3. The corrected inhibition coefficients are the highest for  $\alpha$ - $\text{TQH}_2$  and  $\text{PQH}_2$ -9 for 3 and 5 mol%. The considerably lower values for 1 mol% might be connected with a low antioxi-

Table 2

Concentration changes of prenyllipids (AH) after the fast phase of  $\text{Fe}^{2+}$ - $\text{H}_2\text{O}_2$ -induced lipid peroxidation ( $\Delta[\text{AH}]_{\text{FP}}$ ) of EYL liposomes and rates of AH oxidation during the slow phase ( $\Delta[\text{AH}]_{\text{SP}}$ )

Antioxidant [content in mol%]	$\Delta[\text{AH}]_{\text{FP}}$ (%)	$\Delta[\text{AH}]_{\text{SP}}$ ( $\mu\text{M}$ AH/min)
$\text{PQH}_2$ -9 [1]	85	$\sim 0.01$
$\text{PQH}_2$ -9 [3]	53	0.08
$\text{PQH}_2$ -9 [5]	42	0.23
$\alpha$ - $\text{TQH}_2$ [1]	80	$\sim 0.02$
$\alpha$ - $\text{TQH}_2$ [3]	60	0.23
$\alpha$ - $\text{TQH}_2$ [5]	43	0.58
$\alpha$ -T [1]	33	$\sim 0$
$\alpha$ -T [3]	30	0.09
$\alpha$ -T [5]	27	0.13
$\text{UQH}_2$ -10 [1]	64	$\sim 0$
$\text{UQH}_2$ -10 [3]	52	0.09
$\text{UQH}_2$ -10 [5]	40	0.40

Table 3

Oxygen concentration changes during the slow phase of  $\text{Fe}^{2+}$ - $\text{H}_2\text{O}_2$ -induced lipid peroxidation of EYL liposomes, the relative rates ( $v$ ) and ratios of the reaction rates with and without prenyllipids ( $100/v$ )

Antioxidant [content in mol%]	$\Delta[\text{O}_2]$ ( $\mu\text{M O}_2/\text{min}$ )	Relative rate ( $v$ )	Inhibition ratio ( $100/v$ )
—	$16.0 \pm 2.3$	100	1
PQH <sub>2</sub> -9 [1]	$4.8 \pm 0.9$	30	3.331
PQH <sub>2</sub> -9 [3]	$0.81 \pm 0.02$	5	19.8 (22.8)
PQH <sub>2</sub> -9 [5]	$0.87 \pm 0.30$	5.4	18.5 (30.2)
$\alpha$ -TQH <sub>2</sub> [1]	$5.61 \pm 0.11$	35	2.85
$\alpha$ -TQH <sub>2</sub> [3]	$1.16 \pm 0.20$	7.2	13.8 (18.2)
$\alpha$ -TQH <sub>2</sub> [5]	$1.08 \pm 0.12$	6.7	14.8 (63.2)
$\alpha$ -T [1]	$0.91 \pm 0.08$	5.7	17.6
$\alpha$ -T [3]	$0.90 \pm 0.11$	5.6	17.8 (19.8)
$\alpha$ -T [5]	$0.65 \pm 0.10$	4.0	24.6 (31.8)
UQH <sub>2</sub> -10 [1]	$4.12 \pm 0.34$	25.7	3.9
UQH <sub>2</sub> -10 [3]	$1.18 \pm 0.15$	7.4	13.6 (15.8)
UQH <sub>2</sub> -10 [5]	$1.39 \pm 0.13$	8.7	11.5 (24.2)

The values in brackets were calculated taking into account oxygen consumption by prenyllipids in the slow phase and due to their autoxidation.

dant content after the fast phase (0.15 mol% for PQH<sub>2</sub>-9, 0.2 mol% for  $\alpha$ -TQH<sub>2</sub> and 0.36 mol% for UQH<sub>2</sub>-10) for the effective lipid peroxidation inhibition. The calculated inhibition coefficients presented in Fig. 3 are reflecting the antioxidant activity of the prenyllipids against lipid peroxidation derived peroxy radicals (Eq. (4)).

It should be also considered if the semiquinone forms of the investigated prenyllipids, formed in

the Eq. (4), could act as pro-oxidants, i.e. stimulate the lipid peroxidation, for example by decomposition of lipid peroxides, as in the case of  $\text{Fe}^{2+}$  ions Eq. (6). However, it was found (Porter et al., 1995) that the reaction rate constants of the pro-oxidant reactions of  $\alpha$ -T are several orders of magnitude lower than the  $k$  value of its antioxidant reaction (Eq. (4)). Similar relations can be expected for the prenyllipids investigated in our system.

Our results show that in the determination of the inhibitory effects of labile compounds such as prenylquinols on lipid peroxidation, it is important to examine all the possible side reactions, e.g. the reaction of peroxidation initiators with the antioxidants, which may strongly influence their concentrations. In the case of azoinitiators, there is a constant rate of initiator production during the peroxidation reaction. This reaction constantly changes the level of antioxidants which is not due to the termination reaction by the antioxidants as it was recently shown by Koga and Terao, 1996 where the rate of tocopherol loss in dimyristoyl phosphatidylcholine liposomes was similar as in soyabean phosphatidylcholine liposomes in the course of AAPH-initiated peroxida-

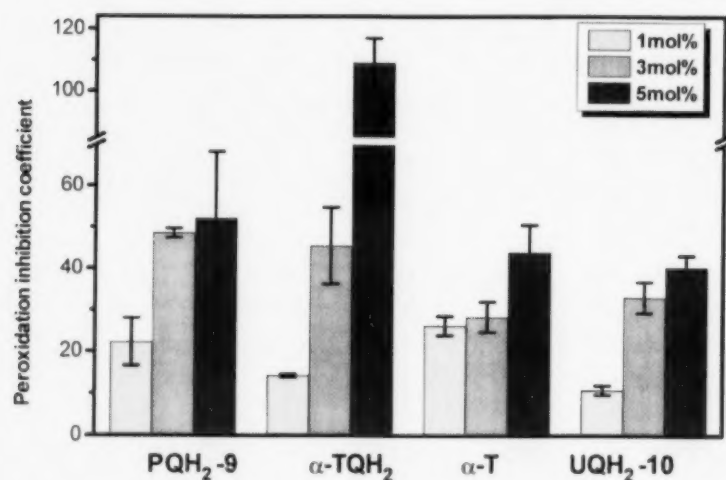


Fig. 3. Peroxidation inhibition coefficients of prenyllipids (AH) in EYL liposomes calculated for the initial prenyllipids concentration:  $(100/v)/(1-\Delta[\text{AH}]_{\text{FP}}[\%]/100)$ .

tion reaction. Although our initiation system is not as well defined as that of the azoinitiators, it also gives in the slow phase of the reaction continuous initiating system ( $\text{Fe}^{2+} + \text{LOOH} \rightarrow \text{Fe}^{3+} + \text{LO}^\bullet + \text{OH}$ ) which is evident from the approximately constant antioxidants and oxygen concentration changes during the slow phase (Figs. 1 and 2).

Considering the function of the investigated prenylquinols as antioxidants in natural membranes we have to take into account the relative proportions of UQH<sub>2</sub>-10 and  $\alpha$ -T in mitochondrial membranes (Mellors and Tappel, 1966) whose molar ratio is about 10 and PQH<sub>2</sub>-9 and  $\alpha$ -T ratio in thylakoid membranes (Lichtenthaler et al., 1981) which is about 2. This suggests that the contribution of PQH<sub>2</sub>-9 and UQH<sub>2</sub>-10 in preventing membrane lipid peroxidation may be even higher than that of  $\alpha$ -T. The recent finding (Hundal et al., 1995) of inhibition of lipid peroxidation by PQH<sub>2</sub>-9 in chloroplast thylakoid membranes during strong illumination may support the significant antioxidant function of PQH<sub>2</sub>-9 in natural membranes.

### Acknowledgements

This work was supported by Committee for Scientific Research (KBN) grant 6 6075 92 03 and 6 PO4A 009 10.

### References

- Barclay, L.R.C., Locke, S.J., MacNeil, J.M., VanKessel, J., Burton, G.W., Ingold, K.U., 1984. Autooxidation of micelles and model membranes. Quantitative kinetic measurements can be made by using either water-soluble or lipid-soluble chain-breaking antioxidants. *J. Am. Chem. Soc.* 106, 2479–2481.
- Bergelson, L.D., 1980. *Lipid Biochemical Preparations*, Elsevier, Amsterdam-New York-Oxford.
- Beyer, R.E., 1990. The participation of coenzyme Q in free radical production and antioxidation. *Free Radic. Biol. Med.* 8, 545–565.
- Bindoli, A., Valente, M., Cavallini, L., 1985. Inhibition of lipid peroxidation by  $\alpha$ -tocopherolquinone and  $\alpha$ -tocopherolhydroquinone. *Biochem. Int.* 10, 753–761.
- Cabrini, L., Stefanelli, C., Fiorentini, D., Landi, L., 1991. Ubiquinol prevents  $\alpha$ -tocopherol consumption during liposome peroxidation. *Biochem. Int.* 23, 743–749.
- Cadenas, E., Boveris, A., Iannigan, C., Stoppani, A.O.M., 1977. Production of superoxide radicals and hydrogen peroxide by NADH-ubiquinone reductase and ubiquinol-cytochrome c reductase from beef-heart mitochondria. *Arch. Biochem. Biophys.* 180, 248–257.
- Frei, B., Kim, M.C., Ames, B.N., 1990. Ubiquinol-10 is an effective lipid-soluble antioxidant at physiological concentrations. *Proc. Natl. Acad. Sci. USA* 87, 4879–4883.
- Fujii, T., Hiramoto, Y., Terao, J., Fukuzawa, K., 1991. Site-specific mechanisms of initiation by chelated iron and inhibition by  $\alpha$ -tocopherol of lipid peroxide-dependent lipid peroxidation in charged micelles. *Arch. Biochem. Biophys.* 284, 120–126.
- Fukuzawa, K., Kishikawa, K., Tadokoro, T., Tokumura, A., Tsukatani, H., Gebicki, J.M., 1988a. The effect of  $\alpha$ -tocopherol on site-specific lipid peroxidation induced by iron in charged micelles. *Arch. Biochem. Biophys.* 260, 153–160.
- Fukuzawa, K., Tadokoro, T., Kishikawa, K., Mukai, K., Gebicki, J.M., 1988b. Site-specific induction of lipid peroxidation by iron in charged micelles. *Arch. Biochem. Biophys.* 260, 146–152.
- Gutman, M., 1980. Electron flux through the mitochondrial ubiquinone. *Biochim. Biophys. Acta* 594, 53–84.
- Gutteridge, J.M.C., 1984. Ferrous ion-EDTA-stimulated phospholipid peroxidation. A reaction changing from alkoxyl-radical- to hydroxyl-radical-dependent initiation. *Biochem. J.* 224, 697–701.
- Halliwell, B., Gutteridge, J.M.C., 1990. Role of free radicals and catalytic metal ions in human disease: an overview. *Methods Enzymol.* 186B, 1–83.
- Hundal, T., Forsmark-Andree, P., Ernster, L., Andersson, B., 1995. Antioxidant activity of reduced plastoquinone in chloroplast thylakoid membranes. *Arch. Biochem. Biophys.* 324, 117–122.
- Jemioła-Rzemińska, M., Kruk, J., Skowronek, M., Strzałka, K., 1996. Location of ubiquinone homologues in liposome membranes studied by fluorescence anisotropy of diphenyl-hexatriene and trimethylammonium-diphenyl-hexatriene. *Chem. Phys. Lipids*, 55–63.
- Kagan, V.E., Serbinowa, E.A., Koynova, G.M., Kitanova, S.A., Tyurin, V.A., Stoytchev, T.S., Quinn, P.J., Packer, L., 1990. Antioxidant action of ubiquinol homologues with different isopenoid chain length in biomembranes. *Free Radic. Biol. Med.* 9, 117–126.
- Koga, T., Terao, J., 1996. Antioxidant behaviors of vitamin E analogues in unilamellar vesicles. *Biosci. Biotech. Biochem.* 60, 1043–1045.
- Kruk, J., 1988. Charge-transfer complexes of plastoquinone and  $\alpha$ -tocopherol quinone in vitro. *Biophys. Chem.* 30, 143–149.
- Kruk, J., Schmid, G.H., Strzałka, K., 1994. Antioxidant properties of plastoquinol and other biological prenylquinols in liposomes and solution. *Free Radic. Res.* 21, 409–416.



- Kruk, J., Strzałka, K., 1995. Occurrence and function of  $\alpha$ -tocopherol quinone in plants. *J. Plant Physiol.* 145, 405–409.
- Kruk, J., Strzałka, K., Leblanc, R.M., 1992. Monolayer study of plastoquinones,  $\alpha$ -tocopherolquinone, their hydroquinone forms and their interaction with monogalactosyldiacylglycerol. Charge-transfer complexes in a mixed monolayer. *Biochim. Biophys. Acta* 1112, 19–26.
- Kruk, J., Strzałka, K., Leblanc, R.M., 1993. Fluorescence properties of plastoquinol, ubiquinol and  $\alpha$ -tocopherol quinol in solution and liposome membranes. *J. Photochem. Photobiol.* 19, 33–38.
- Lichtenthaler, H.K., Prenzel, U., Douce, R., Joyard, J., 1981. Localization of prenylquinones in the envelope of spinach chloroplasts. *Biochim. Biophys. Acta* 641, 99–105.
- Liebler, D.C., Kling, D.S., Reed, D.J., 1986. Antioxidant protection of phospholipid bilayers by  $\alpha$ -tocopherol. *J. Biol. Chem.* 261, 12114–12119.
- Machlin, L., 1980. *Vitamin E: A Comprehensive Treatise*, Marcel Dekker, New York.
- Mellors, A., Tappel, A.L., 1966. The inhibition of mitochondrial peroxidation by ubiquinone and ubiquinol. *J. Biol. Chem.* 241, 4353–4356.
- Minotti, G., Aust, S.D., 1987. The requirement for iron (III) in the initiation of lipid peroxidation by iron (II) and hydrogen peroxide. *J. Biol. Chem.* 262, 1098–1104.
- Mukai, K., Itoh, S., Morimoto, H., 1992. Stopped-flow kinetic study of Vitamin E regeneration reaction with biological hydroquinones (reduced forms of ubiquinone, vitamin K, and tocopherolquinone) in solution. *J. Biol. Chem.* 267, 22277–22281.
- Mukai, K., Morimoto, H., Kikuchi, S., Nagaoka, S., 1993. Kinetic study of free-radical-scavenging action of biological hydroquinones (reduced forms of ubiquinone, vitamin K and tocopherol quinone) in solution. *Biochim. Biophys. Acta* 1157, 313–317.
- Porter, N.A., Caldwell, S.E., Mills, K.A., 1995. Mechanism of free radical oxidation of unsaturated lipids. *Lipids* 30, 277–290.
- Rich, P.R., Moss, D.A., 1987. The reactions of quinones in higher plant photosynthesis. In: Barber, J., (Ed.), *The Light Reactions*, Elsevier Science B.V., pp. 421–445.
- Schaich, K.M., Borg, D.C., 1988. Fenton reactions in lipid phases. *Lipids* 23, 570–579.
- Stocker, R., Bowry, V.W., Frei, B., 1991. Ubiquinol-10 protects human low density lipoprotein more efficiently against lipid peroxidation than does  $\alpha$ -tocopherol. *Proc. Natl. Acad. Sci., USA* 88, 1646–1650.
- Sugioka, K., Nakano, M., Totsune-Nakano, H., Minakami, H., Tero-Kubota, S., Ikegami, Y., 1988. Mechanism of  $O_2$ — generation in reduction and oxidation cycle of ubiquinones in a model of mitochondrial electron transport systems. *Biochim. Biophys. Acta* 936, 377–385.
- Vigo-Pelfrey, C., 1990. *Membrane Lipid Oxidation*, vol. 1. CRC Press, Boca Raton, Florida.
- Yamamoto, Y., Komuro, E., Niki, E., 1990. Antioxidant activity of ubiquinol in solution and phosphatidylcholine liposome. *J. Nutr. Sci. Vitaminol.* 36, 505–511.

## Increased levels of lipid oxidation products in low density lipoproteins of patients suffering from rheumatoid arthritis

Wolfgang Jira <sup>a,\*</sup>, Gerhard Spiteller <sup>a</sup>, Andreas Richter <sup>b</sup>

<sup>a</sup> *Lehrstuhl für Organische Chemie I, Universität Bayreuth, NW I, Universitätsstraße 30, 95440 Bayreuth, Germany*

<sup>b</sup> *Klinikum Bayreuth, Orthopädische Klinik, Preuschwitzer Str. 101, 95445 Bayreuth, Germany*

Received 16 December 1996; received in revised form 18 March 1997; accepted 23 April 1997

### Abstract

9-Hydroxy-10,12-octadecadienoic acid (9-HODE) and 13-hydroxy-9,11-octadecadienoic acid (13-HODE) are accumulated in the low density lipoproteins of patients suffering from rheumatoid arthritis for a factor of 20–50 compared to healthy individuals of the same age. Both acids, derived by lipid peroxidation of linoleic acid, induce the release of interleukin 1 $\beta$ . The latter induces bone degeneration. The genesis of 9- and 13-HODE seems therefore to be an important factor in the development and progression of rheuma; in addition 9-HODE was reported to be a stimulus of inflammation, comparable to leukotrienes. © 1997 Elsevier Science Ireland Ltd.

**Keywords:** Hydroxy fatty acids;  $\alpha$ -hydroxyaldehydes; LDL; Rheuma; Aging

### 1. Introduction

Lipidperoxidation products of arachidonic acid, e.g. prostaglandines (Bergström and Sjövall, 1957; Bergström et al., 1962), thromboxanes (Hamberg et al., 1975), prostacyclines (Moncada et al., 1976, 1978) and leukotrienes (Borgeat and Samuelsson, 1979; Murphy et al., 1979; Oerning et al., 1980) are well known potent physiological active compounds in humans and animals. Jasmonic acid,

derived by lipid peroxidation of linolenic acid is a comparable potent active compound in plants (Vick and Zimmerman, 1987). In contrast only very little is known about the physiological role of lipid peroxidation products of linoleic acid: Moch et al. (Moch et al., 1990) recognized that 9-Hydroxy-10,12-octadecadienoic (9-HODE), derived by lipid peroxidation of linoleic acid followed by enzymic reduction, has comparable inflammatory potency to leukotrienes. Ku et al. (Ku et al., 1992) reported, that 9-HODE and the isomeric 13-hydroxy-9,11-octadecadienoic acid (13-HODE), but also cholesteryl-9-HODE induce the release of interleukin 1 $\beta$  from macrophages.

\* Tel.: +49 0921 552680; fax: +49 0921 552671; e-mail: gerhard.spiteller@uni-bayreuth.de

Comparing the lipid peroxidation products of myocardial infarcted tissue of a porcine heart with the surrounding non infarcted tissue of the same heart we recognized that the content of 9-HODE was increased for a factor of about 20 (Dudda et al., 1996).

9- and 13-HODE are also main lipid peroxidation products observed after injury of tissue. Hereby hydroxy acids of linoleic acid outweighed those of arachidonic acid for a factor of four, indicating a major involvement of linoleic acid in the LPO process (Herold and Spiteller, 1996). This observation stimulated us to investigate samples of patients suffering from other diseases in which increased amounts of lipid peroxidation products were reported by measurement of thiobarbituric acid reactive substances (TBARS). One of these diseases is rheumatism.

Lunec et al. (Lunec et al., 1981) found increased concentrations of conjugated dienes and fluorescent lipid peroxidation products in the serum and synovial fluid of patients with inflammatory joint diseases. By measuring MDA with the thiobarbituric acid test Muus et al. (Muus et al., 1979) detected, that the MDA concentration in the plasma correlates with disease activity. Selley et al. (Selley et al., 1992) found 4-hydroxy-2-nonenal in plasma and synovial fluid of patients with rheumatoid arthritis (RA) and osteoarthritis. In addition a loss of vitamin E in synovial fluid of rheumatic patients was observed (Fairburn et al., 1993). We report in this paper on the observation of a strong increase of 9- and 13-HODE and enhanced levels of aldehydic compounds in the LDL of patients suffering from RA.

## 2. Materials and methods

### 2.1. Materials

*N*-Methyl-*N*-trimethylsilyltrifluoroacetamide (MSTFA) was obtained from Machery and Nagel (Düren, Germany). All other chemicals were purchased from Fluka (Neu Ulm, Germany). Solvents were distilled before use.

### 2.2. Methods

Blood samples of healthy individuals were obtained from the red cross blood service in Bayreuth. Samples of patients suffering from RA were provided from the hospital in Bayreuth. All patients (with exception of patient no. 8) showed typical signs of RA, considering the revised criteria from the American Rheumatism Association (Arnett et al., 1988). All blood samples were taken after fasting over night in the morning.

The different kinds of lipoproteins (VLDL, LDL and HDL) were precipitated from 10 ml of human blood serum following a method of Leiss et al. (Leiss et al., 1979). Since conjugated compounds are sensitive to further oxidation all processing steps were carried out in an argon atmosphere. The lipoproteins were lyophilized, the residues were weighted (about 50 mg) and dissolved in 200 ml TRIS/HCl-buffer (pH 7.4). Protection against oxidation was achieved by addition of 200 µl of a BHT solution (2% in methanol) and 3.75 ml of a EDTA-Na<sub>2</sub> solution (1% in bidistilled water).

The lipoprotein solution was divided in two parts for determination of (1) LOOHs and LOHs and (2) 2-hydroxyaldehydes, malondialdehyde and glyoxal.

#### 2.2.1. Investigation of LOOHs and LOHs by determination as hydroxy fatty acid methyl esters

6-hydroxyheptadecanoic acid (for quantification of the monohydroxy fatty acids) was used as internal standard. The lipid extraction followed the method of Bligh and Dyer (Bligh and Dyer, 1959). Chloroform was removed under reduced pressure. The samples were processed in exactly the same manner as described previously (Jira et al., 1996).

#### 2.2.2. Investigation of plasmalogen epoxides, 2-hydroxyaldehydes, glyoxal and MDA by determination as pentafluorobenzyloxime derivatives

Aldehydic LPO products were captured as pentafluorobenzyloximes (Loidl-Stahlhofen and Spiteller, 1994; Van Kuijk et al., 1986; Siakotos et al., 1988). Quantification of  $\alpha$ -hydroxyaldehydes



was achieved by addition of 1-hydroxy-2-tridecanone as internal standard. Quantification of glyoxal and MDA was carried out by addition of acetylacetone as internal standard. PFBO derivatives were extracted with chloroform and separated by thin layer chromatography (CH–EE 9:1; detection:  $UV_{254\text{ nm}}$  and spraying with 10% ethanolic AMPA) using 1-hydroxy-2-tridecanone-PFBO ( $R_f = 0.3$ ) and MDA-(PFBO)<sub>2</sub> ( $R_f = 0.5$ ) for detection of the corresponding zones. The area containing the indicated compounds was scraped off, eluted with chloroform and dried under reduced pressure. The samples were trimethylsilylated with MSTFA and analyzed by GC–MS. Quantification of MDA and glyoxal was achieved by mass spectrometry ion tracing, using the M-197 ion in comparison to those of the internal standard. Quantification of 2-hydroxyaldehydes was achieved by mass spectrometry ion tracing, using the M-15 fragment.

### 3. Results

Most of the LOOHs produced during lipid peroxidation (LPO) of LDL are reduced enzymically to their hydroxy derivatives under catalysis by glutathione-dependent peroxidases (Lehmann et al., 1992). Thus determination of LOOHs and LOHs is required to obtain a true picture of the amount of LPO. This is achieved when the total content of LOOHs and LOHs is determined together by reduction of the mixture of hydroperoxides by catalytic hydrogenation (Nikkari et al., 1995), which not only reduces the hydroperoxyl-groups but also hydrogenates the double bonds. In addition this procedure excludes the risk of further lipid oxidation during the workup procedure.

Analysis of the free hydroxy fatty acids was achieved by sample processing omitting the hydrolysis step. The content of both esterified and free hydroxy fatty acids was determined with a second sample after hydrolysis. The samples were transformed into their methylesters and were separated from the bulk of accompanying fatty esters by column chromatography. After derivatization with MSTFA, the trimethylsilylated monohy-

droxy fatty acids were analyzed by GC and GC–MS. The ion currents of the typical  $\alpha$ -cleavage products of these compounds were quantified by comparing the area of the selected  $\alpha$ -cleavage fragment ions with those of the standard compound added to the sample at the beginning of the workup procedure.

About 90% of the total amount of hydroxy fatty acids found in LDL were free fatty acids. This indicates the involvement of phospholipases in a previous reaction step.

Monohydroxy acids derived from linoleic or oleic acid were detected in about three to five times higher amounts than those of arachidonic acid. A reason therefore could be the increased ability of arachidonic acid oxidation products to undergo secondary and tertiary peroxidation reactions. These reactions are facilitated since arachidonic acid possesses three bisallylically activated methylene groups in contrast to linoleic acid with only one bisallylically activated  $CH_2$  group (Mlakar and Spiteller, 1994; Tamura et al., 1991; Rubbo et al., 1994).

As reported recently the amounts of different hydroxy acids, e.g. 9-hydroxy octadecanoic acid (derived from 9-LOOH) in LDL of healthy volunteers increase with age (Jira et al., 1996). Therefore comparison of the content of 9-HODE in rheuma patients with that of healthy individuals of the same age is required. Even young RA patients showed significantly enhanced levels of 9-LOH compared to healthy people of the same

Table 1  
Content of 9-LOH in LDL samples of healthy volunteers

	age	sex	9-LOH $\mu\text{g/g}$ LDL
1	22	m	0.5
2	24	m	0.6
3	25	m	0.5
4	39	f	0.8
5	44	f	0.3
6	54	f	0.9
7	56	m	1.8
8	60	m	1.1
9	64	m	2.3
10	66	f	3.1
11	68	f	12.2

Table 2  
Content of 9-LOH in LDL and important clinical data of patients suffering from rheumatoid arthritis

	Age	Sex	9-LOH $\mu\text{g/g}$ LDL	LDL mg/dl	HDL mg/dl	Triglycerides mg/dl	Cholesterol mg/dl	Diagnosis	Activity of disease	Medication
1	20	f	13.4	156	77	80	221	rheumatoid arthritis	2	NSAID (occasional), azulfidine, DMARD
2	29	f	23.7	—	—	60	202	rheumatoid arthritis	3	NSAID (occasional)
3	33	f	47	181	63	151	275	rheumatoid arthritis	3	NSAID
4	46	f	15.9	185	74	64	272	rheumatoid arthritis	2	prednisone, cortisone
5	49	f	46.1	189	49	88	256	rheumatoid arthritis	3	NSAID, subbreum, cortisone
6	49	m	56	167	32	300	259	rheumatoid arthritis	3	NSAID, methotrexate, corti- son
7	51	f	22.7	99	42	124	166	rheumatoid arthritis	2-3	NSAID, imurek, cortisone
8	55	m	4.6	142	46	167	221	beginning rheumatoid arthritis	0-1	NSAID (occasional)
9	59	f	21.8	121	56	172	211	rheumatoid arthritis	2	NSAID, subbreum, cortisone
10	63	f	26.4	233	56	105	310	rheumatoid arthritis	3	NSAID, azulfidine
11	67	f	36.7	195	49	113	267	seronegative rheumatoid arthritis	2-3	NSAID, methotrexate, corti- son

Scale of activity: 0 = no signs of disease; 1 = moderate, a few joints stricken; 2 = inflammation at a few joints; 3 = strong inflammation at a few joints; 4 = strong inflammation at many joints.

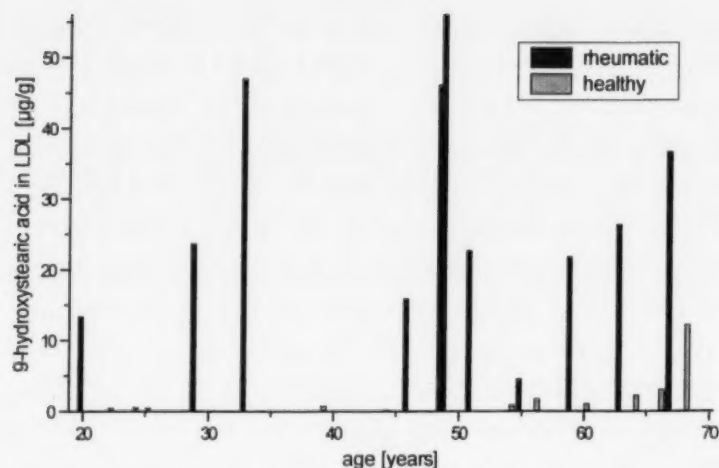


Fig. 1. Content of 9-LOH in LDL of healthy individuals and patients suffering from RA.

age group. Table 1 shows ages, sex and content of derived 9-hydroxyoctadecanoic acid of healthy volunteers.

Table 2 shows ages, sex, content of derived 9-hydroxyoctadecanoic acid, LDL, HDL, cholesterol, triglycerides and diagnosis of RA patients.

The values obtained from patients and healthy volunteers are arranged with increasing age, the age (in years) is indicated at the *x*-axis of the diagram (Fig. 1).

Determination of  $\alpha$ -hydroxyaldehydes was achieved by addition of pentafluorobenzylhydroxylamine-hydrochloride to the lipoprotein-solution, causing immediate trapping of  $\alpha$ -hydroxyaldehydes and plasmalogenepoxides by formation of pentafluorobenzylloximes. Main product of short chain  $\alpha$ -hydroxyaldehydes is 2-hydroxyheptanal, derived by direct decomposition of 13-hydroperoxy-9,11-octadecadienoic acid (13-HPODE) and 15-hydroperoxy-5,8,11,13-eicosatetraenoic acid (15-HPETE) (Loidl-Stahlhofen and Spiteller, 1994; Mlakar and Spiteller, 1996). The short chain  $\alpha$ -hydroxyaldehyde 2-hydroxyheptanal was found in nearly equal amounts as the long chain  $\alpha$ -hydroxyaldehyde 2-hydroxyhexadecanal in healthy volunteers. A comparison of the content of 2-hydroxyheptanal and 2-hydroxyhexadecanal (average value) in LDL of a group of healthy volunteers with patients suffering from RA showed enhanced levels of these aldehydic com-

pounds in rheumatic volunteers. Hereby 2-hydroxyhexadecanal increased at a higher rate in LDL of RA patients than 2-hydroxyheptanal in comparison to healthy individuals of the same age group. Fig. 2 shows the content of 2-hydroxyheptanal and 2-hydroxyhexadecanal (average value of 11 volunteers each) in LDL of healthy people (average age 47.5 years) and patients suffering from RA (average age 47.4 years).

A typical degradation product of hydroperoxides of polyunsaturated fatty acids is MDA (Esterbauer and Cheeseman, 1990; Dahle et al., 1962; Janero, 1990; Esterbauer, 1982; Grosch, 1987). It is commonly used for the measurement of LPO with the thiobarbituric acid test. But it is also able to form a (bis)-PFBO derivative (Loidl-Stahlhofen and Spiteller, 1994; Mlakar and Spiteller, 1996) as well as glyoxal. (Bis)-PFBO derivatives of both compounds were quantified using the (bis)-PFBO derivative of acetylacetone as internal standard. Glyoxal and MDA were found in higher amounts in LDL of patients suffering from RA than in volunteers of the same age. The amount of MDA in LDL of RA patients increased for a factor of three to four in comparison to healthy volunteers. In Fig. 3 the content of glyoxal and MDA in LDL of healthy and RA patients is shown.

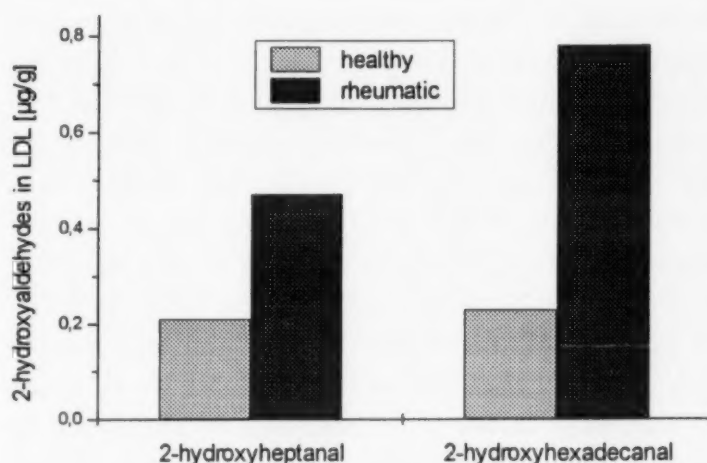


Fig. 2. Content of 2-hydroxyheptanal and 2-hydroxyhexadecanal in LDL of healthy volunteers and patients suffering from RA.



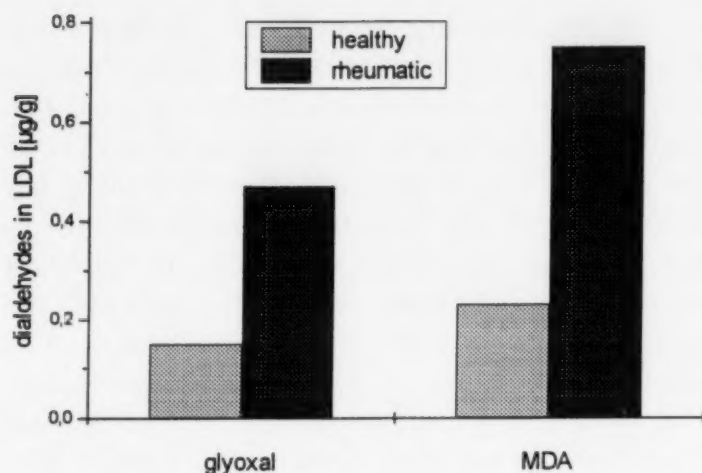


Fig. 3. Content of glyoxal and MDA in LDL of healthy and patients suffering from RA.

#### 4. Discussion

Reactive oxygen species (ROS) play an important role in the pathology of a wide range of inflammatory diseases (Blake and Lunec, 1990). The involvement of these ROS in the pathogenesis of human rheumatoid diseases is based on the work of McCord (McCord, 1974) who showed that the decreased viscosity of synovial fluid from the joints of patients with RA could also be produced by exposing synovial fluid of hyaluronate (the glycosaminoglycan responsible for most of the synovial fluid viscosity) to a superoxidegenerating system *in vitro*. The lipid peroxidation in the blood of rheumatic patients was usually determined by measuring MDA with the thiobarbituric acid test. Linoleic acid hydroperoxides are transformed only to a very small amount to MDA. They therefore escape determination with this method. In addition MDA determination with the TBA-test requires heating of the samples up to 100°C. At this temperature precursor molecules may decompose to MDA, leading to high MDA levels. Indeed the determination of MDA as (bis)-PFBO-derivative in LDL of healthy volunteers and patients suffering from RA showed, that the content of MDA is much lower (for a factor of about 30) in comparison to the content of 9-HODE. In addition the differences in the amount of 9-HODE between rheumatic and healthy people are for a factor of 10 higher than that of MDA. Therefore the deter-

mination of 9-HODE seems to be a more reliable and better parameter for LPO in LDL than determination of MDA. The primary LPO products of linoleic acid, the most abundant unsaturated fatty acids in human LDL are 9- and 13-HPODE. Their reduction products, 9- and 13-hydroxystearic acid were detected in highly raised amounts in LDL of patients suffering from RA in comparison to healthy people of the same age group. This increase can not be caused by intake of NSAID, since these drugs are known to be inhibitors of lipoxygenase (Sircar et al., 1983) and decrease the level of reactive oxygen species (Mueller-Peddinghaus and Wurl, 1987) and TBARS (Bilodeau et al., 1995)—thus their intake rather results in a decrease of 9-LOH than in an increase.

The investigated 55 year old patient with a beginning RA showed an enhanced level of hydroxy acids in LDL compared to healthy individuals. Of course the level is much lower than in the other RA patients suffering from an acute stage of the disease. This fact could be of diagnostic importance since no suited parameter for the diagnosis of rheumatism is known until now. Hydroxy acids derived from arachidonic acid were detected in a three to five fold lower amount in comparison to hydroxy acids derived from linoleic acid. This observation might be caused by the lower amount of arachidonic acid in comparison to linoleic acid in the LDL particle and the higher ability of LOOHs derived from arachidonic acid to undergo secondary and tertiary peroxidation reactions due to the presence of three bisallylically activated methylene groups in arachidonic acid compared to only one in linoleic acid. Hydroxy acids are the most abundant primary LPO products in LDL. Their precursor molecules, the hydroperoxy fatty acids show cytotoxic activities: LOOHs react with plasmalogens by formation of plasmalogenepoxides (Scheick and Spiteller, 1993), which decompose to long chain  $\alpha$ -hydroxyaldehydes. These  $\alpha$ -hydroxyaldehydes stimulate the oxidative burst reaction in macrophages (Heinle et al., 1996). These compounds were found in our investigation in enhanced levels in LDL of RA patients in comparison to healthy individuals of the same age group.

Hydroperoxy fatty acids also decompose to reactive aldehydes like glyoxal, MDA or 4-hydroxynonenal. Glyoxal and MDA were also found in increased amounts in LDL of RA patients (for a factor of three to four), whereas 4-HNE was not detected, probably caused by the high reactivity of this substance. 4-HNE can react with nucleophils in a Michael addition *in vivo*. It must be emphasized that LOOHs are not detoxified completely by reduction: The corresponding hydroxy fatty acids have cytotoxic and chemoattractant activities: Nakao et al. (Nakao et al., 1982) demonstrated, that the lipoxygenase products 12- and 15-hydroxyeicosatetraenoic acid stimulate the rat aortic smooth muscle cell migration *in vitro*. 5- and 12-HETE are chemoattractants for human mononuclear leukocytes. They are chemotactic for neutrophils (Goetzl et al., 1977; Goetzl and Pickett, 1980). In addition Moch et al. (Moch et al., 1990) reported that 9-hydroxy-10,12-octadecadienoic acid is an equal strong proinflammatory mediator as leucotrienes. Ku et al. (Ku et al., 1992) showed that this compound, but also the 13 isomer, induces the release of interleukin 1 $\beta$  from macrophages. Gallwitz et al. (Gallwitz et al., 1993) showed that 5-lipoxygenase metabolites, e.g. 5-HETE stimulates isolated osteoclasts to resorb bone *in vitro*. Also interleukin 1 is a potent and powerful stimulator of bone resorption *in vitro* (Gowen and Mundy, 1986). This fact seems remarkable since bone resorption is a characteristic indication for a rheumatic disease. Therefore the strong increase of 9- and 13-HODE in rheumatic LDL might be involved in the pathology and joint destruction of this disease.

## 5. Abbreviations

13-HODE, 13-hydroxy-9,11-octadecadienoic acid; 13-HPODE, 13-hydroperoxy-9,11-octadecadienoic acid; 15-HPETE, 15-hydroperoxy-5,8,11,13-eicosatetraenoic acid; 9-HODE, 9-hydroxy-10,12-octadecadienoic acid; 9-LOH, 9-hydroxy octadecanoic acid; 9-LOOH, 9-hydroperoxy octadecanoic acid; AMPA, ammoniummolybdatophosphorus acid; BHT, butylated hydroxytoluene; CH cyclohexane; DMARD, disease-modifying anti-

rheumatic drugs; EDTA, ethylene diamine tetraacetic acid; EE, ethylacetate; GC, gas chromatography; HDL, high density lipoproteins; HETE, hydroxy eicosatetraenoic acid; LDL, low density lipoproteins; LOH, hydroxy octadecanoic acid; LOOH, hydroperoxy octadecanoic acid; LPO, lipid peroxidation; MDA, malondialdehyde; MS, mass spectrometry; MSTFA, *N*-methyl-*N*-trimethylsilyltrifluoroacetamide; NSAID, non-steroidal anti-inflammatory drugs; PFBO, pentafluorobenzyl-oxime; PUFAs, polyunsaturated fatty acids; RA, rheumatoid arthritis; TBA, thiobarbituric acid; TBARS, thiobarbituric acid reactive substances; TRIS, tris-(hydroxymethyl)-aminomethane; VLDL, very low density lipoproteins

## References

- Arnett, F.C., Edworthy, S.M., Bloch, D.A., McShane, D.J., Fries, J.F., Cooper, N.S., Healey, L.A., Kaplan, S.R., Liang, M.H., Luthra, H.S., Medsger, T.A., Mitchell, D.M., Neustadt, D.H., Pinals, R.S., Schaller, J.G., Sharp, J.T., Wilder, R.L., Hunder, G.G., 1988. The American Rheumatism Association 1987 revised criteria for the classification of rheumatoid arthritis. *Arthritis and rheumatism* 31, 315–324.
- Bergström, S., Sjövall, J., 1957. The isolation of prostaglandine. *Acta Chem. Scand.* 11, 1086.
- Bergström, S., Ryhage, R., Samuelsson, B., Sjövall, J., 1962. The structure of prostaglandin E, F1 and F2. *Acta Chem. Scand.* 16, 501–502.
- Bilodeau, J.F., Wang, M., Chung, F.L., Castonguay, A., 1995. Effects of nonsteroidal antiinflammatory drugs on oxidative pathways in A/J mice. *Free Radical Biol. Med.* 18 (1), 47–54.
- Blake, D.R., Lunec, J., 1990. In: Cohen, R.D., Alberti, K.G.M.M., Lewis, B., Denman, A.M. (Eds.), *The Metabolic and Molecular Basis of Acquired Disease*, vol. 20, Bailliere Tindall Limited, London, pp. 189–212.
- Bligh, E.G., Dyer, W.J., 1959. A rapid method of total lipid extraction and purification. *Can. J. Biochem. Physiol.* 37, 911–917.
- Borgeat, P., Samuelsson, B., 1979. Arachidonic acid metabolism in polymorphonuclear leukocytes. III. Effects of ionophore A23187. *Proc. Natl. Acad. Sci. U.S.A.* 76 (5), 2148–2152.
- Dahle, L.K., Hill, E.G., Holman, R.T., 1962. The thiobarbituric acid reaction and the autoxidation of polyunsaturated fatty acid methyl esters. *Arch. Biochem. Biophys.* 98, 253–261.
- Dudda, A., Spiteller, G., Kobelt, F., 1996. Lipid oxidation products in ischemic porcine heart tissue. *Chem. Phys. Lipids* 82, 39–51.



- Esterbauer, H., 1982. Aldehydic products of lipid peroxidation Free Radicals. In: McBrien, D.C.H., Slater, T.F. (Eds.) Lipid Peroxidation Cancer, Proceedings of N.F.C.R., 1st Cancer Symposium, 1981, Academic Press, London, pp. 101–128.
- Esterbauer, H., Cheeseman, K.H., 1990. Determination of aldehydic lipid peroxidation products: malonaldehyde and 4-hydroxynonenal. *Methods Enzymol.* 186, 407–421.
- Fairburn, K., Groorveld, M., Ward, R.J., et al., 1993.  $\alpha$ -Tocopherol, lipids and lipoproteins in knee-joint synovial fluid and serum from patients with inflammatory joint diseases. *Clin. Sci.* 83, 657–664.
- Gallwitz, W.F., Mundy, G.R., Lee, C.H., Qiao, M., Roodman, G.D., Raftery, M., Gaskell, S.J., Bonewald, L.F., 1993. 5-Lipoxygenase metabolites of arachidonic acid stimulation isolated osteoclasts to resorb calcified matrices. *J. Biol. Chem.* 268 (14), 10087–10094.
- Goetzl, E.J., Pickett, W.C., 1980. The human PMN leukocyte chemotactic activity of complex hydroxy-eicosatetraenoic acids (HETEs). *J. Immunol.* 125, 1789–1791.
- Goetzl, E.J., Woods, J.M., Gorman, R.R., 1977. Stimulation of human eosinophil and neutrophil polymorphonuclear leukocyte chemotaxis and random migration by 12-L-hydroxy-5,8,10,14-eicosatetraenoic acid. *J. Clin. Invest.* 59, 179–183.
- Gowen, M., Mundy, G.R., 1986. Actions of recombinant interleukin 1, interleukin 2, and interferon- $\gamma$  on bone resorption in vitro. *J. Immunol.* 136 (7), 2478–2482.
- Grosch, W., 1987. Reactions of hydroperoxides. In: Chan, H.W.-S. (Ed.), Products of low molecular weight Autoxid. Unsaturated Lipids, Academic Press London, pp. 95–139.
- Hamberg, M., Svenson, J., Samuelsson, B., 1975. Thromboxanes. New group of biologically active compounds derived from prostaglandin endoperoxides. *Proc. Natl. Acad. Sci. U.S.A.* 72 (8), 2994–2998.
- Heinle, H., Gugeler, N., Felde, R., Spiteller, G., 1996. Oxidation of plasmalogens produce highly effective modulators of macrophage function, *Free Rad. Biol.*, in press.
- Herold, M., Spiteller, G., 1996. Enzymic production of hydroperoxides of unsaturated fatty acids by injury of mammalian cells. *Chem. Phys. Lipids* 79 (2), 113–121.
- Janero, D.R., 1990. Malondialdehyde and thiobarbituric acid-reactivity as diagnostic indexes of lipid peroxidation and peroxidative tissue injury. *Free Radical Biol. Med.* 9 (6), 515–540.
- Jira, W., Spiteller, G., Schramm, A., 1996. Increase in hydroxy fatty acids in human low density lipoproteins with age. *Chem. Phys. Lipids* 84, 165–173.
- Ku, G., Thomas, C.E., Akeson, A.L., Jackson, R.L., 1992. Induction of interleukin 1 $\beta$  expression from human peripheral blood monocyte-derived macrophages by 9-hydroxy-octadecadienoic acid. *J. Biol. Chem.* 267 (20), 14183–14188.
- Lehmann, W.A., Stephan, M., Fürstenberger, G., 1992. Profiling assay for lipoxygenase products of linoleic and arachidonic acid by gas chromatography-mass spectrometry. *Anal. Biochem.* 204 (1), 158–170.
- Leiss, O., Murawski, U., Egge, H., 1979. The microanalysis of serum lipoprotein lipids. *J. Clin. Chem. Clin. Biochem.* 17, 619–625.
- Loidl-Stahlhofen, A., Spiteller, G., 1994.  $\alpha$ -Hydroxyaldehydes, products of lipid peroxidation. *Biochim. Biophys. Acta* 1211 (2), 156–160.
- Lunec, J., Halloran, S.P., White, A.G., Dormandy, T.L., 1981. Free-radical oxidation (peroxidation) products in serum and synovial fluid in rheumatoid arthritis. *Journal of Rheumatology* 8 (2), 233–245.
- McCord, J.M., 1974. Free radicals and inflammation. Protection of synovial fluid by superoxide dismutase. *Science* 185 (4150), 529–531.
- Mlakar, A., Spiteller, G., 1994. Reinvestigation of lipid peroxidation of linolenic acid. *Biochim. Biophys. Acta* 1214 (2), 209–220.
- Mlakar, A., Spiteller, G., 1996. Previously unknown aldehydic lipid peroxidation compounds of arachidonic acid. *Chem. Phys. Lipids* 79 (1), 47–53.
- Moch, D., Schewe, T., Kuehn, H., Schmidt, D., Buntrock, P., 1990. The linoleic acid metabolite 9*De*-hydroxy-10,12(E,Z)-octadecadienoic acid is a strong proinflammatory mediator in an experimental wound healing model of the rat. *Biomed. Biochim. Acta* 49, 201–207.
- Moncada, S., Gryglewski, R., Bunting, S., Vane, J.R., 1976. An enzyme isolated from arteries transforms prostaglandin endoperoxides to an unstable substance that inhibits platelet aggregation. *Nature (London)* 263 (5579), 663–665.
- Moncada, S., Korb, R., Bunting, S., Vane, J.R., 1978. Prostacyclin is a circulating hormone. *Nature (London)* 273 (5665), 767–768.
- Mueller-Peddinghaus, R., Wurl, M., 1987. The amplified chemiluminescence test to characterize antirheumatic drugs as oxygen radical scavengers. *Biochem. Pharmacol.* 36 (7), 1125–1132.
- Murphy, R.C., Hammarstroem, S., Samuelsson, B., 1979. Leukotriene C: A slow-reacting substance from murine mastocytoma cells. *Proc. Natl. Acad. Sci. U.S.A.* 76 (9), 4275–4279.
- Muus, P., Bonta, I.L., Den Ouden, S.A., 1979. Plasma levels of malondialdehyde, a product of cyclo-oxygenase-dependent and independent lipid peroxidation in rheumatoid arthritis: A correlation with disease activity. *Prostaglandins Med.* 2 (1), 63–65.
- Nakao, J., Ooyama, T., Ito, H., Chang, W.C., Murota, S., 1982. Comparative effect of lipoxygenase products of arachidonic acid on rat aortic smooth muscle cell migration. *Atherosclerosis* 44 (3), 339–342.
- Nikkari, T., Malo-Ranta, U., Hiltunen, T., Jaakkola, O., Ylä-Herttuala, S., 1995. Monitoring of lipoprotein oxidation by gas chromatographic analysis of hydroxy fatty acids. *J. Lipid Res.* 36, 200–207.
- Oerling, L., Hammarstroem, S., Samuelsson, B., 1980. Leukotriene D: A slow reacting substance for rat basophilic leukemia cells. *Proc. Natl. Acad. Sci. U.S.A.* 77 (4), 2014–2017.




- Rubbo, H., Radi, R., Trujillo, M., Telleri, R., Kalyanaraman, B., Barnes, S., Kirk, M., Freeman, B.A., 1994. Nitric oxide regulation of superoxide and peroxynitrite-dependent lipid peroxidation. Formation of novel nitrogen-containing oxidized lipid derivatives. *J. Biol. Chem.* 269 (42), 26066–26075.
- Scheick, C., Spiteller, G., 1993. Formation of enol ether epoxides by reaction of (9S,10E,12Z)-hydroperoxyoctadecadienoic acid with plasmalogens. *Liebigs Ann. Chem.* 12, 1245–1248.
- Selley, M.L., Bourne, D.J., Bartlett, M.R., Tymms, K.E., Brook, A.S., Duffield, A.M., Ardlie, N.G., 1992. Occurrence of (E)-4-hydroxy-2-nonenal in plasma and synovial fluid of patients with rheumatoid arthritis and osteoarthritis. *Ann. Rheumatic Dis.* 51 (4), 481–484.
- Siakotos, A.N., Bray, R., Dratz, E., van Kuijk, F.J.G.M., Sevanian, A., Koppang, N., 1988. 4-Hydroxynonenal: a specific indicator for canine neuronal-retinal ceroidosis. *American Journal of Medical Genetics Supplement.* 5, 171–181.
- Sircar, J.C., Schwender, C.F., Johnson, E.A., 1983. Soybean lipoxygenase inhibition by nonsteroidal antiinflammatory drugs. *Prostaglandins* 25 (3), 393–396.
- Tamura, H., Kitta, K., Shibamoto, T., 1991. Formation of reactive aldehydes from fatty acids in a iron(2+)/hydrogen peroxide oxidation system. *J. Agric. Food Chem.* 39 (3), 439–442.
- Van Kuijk, F.J.G.M., Thomas, D.W., Stephens, R.J., Dratz, E.A., 1986. Occurrence of 4-hydroxyalkenals in rat tissues determined as pentafluorobenzyl oxime derivatives by gas chromatography–mass spectrometry. *Biochem. Biophys. Res. Commun.* 139 (1), 144–149.
- Vick, B.A., Zimmerman, D.C., 1987. Oxidative systems for modification of fatty acids: the lipoxygenase pathway. In: Stumpf, P.K. (Ed.), *Biochem. Plants*, vol. 9. Academic Press, Orlando FL, pp. 53–90.



## Interested in Associative Learning?

OPAL is the answer! Open Programs for Associative Learning is an interactive system using computer technology and hypermedia principles to present a revolutionary approach to learning and teaching. OPAL modules provide the tools for intuitive and associative learning. By browsing freely the User can create his/her own knowledge trail.

### OPAL Modules available:



OPAL Module 1	Neural Communication
OPAL Module 2	Calcium as a Messenger
OPAL Module 3	Immune Cells
OPAL Module 4	Endocrine Cells
OPAL Module 5	Autonomic Nervous System
OPAL Module 6	Brain Aging
OPAL Module 7	Cell Structure
OPAL Module 8	Pain: Basic Science

#### Options

- Easy to use
- In-depth information
- Interactive animations and simulations
- Knowledge evaluation through electronic questionnaire

**Seeing is believing....**

**so log into the OPAL Website today!**

**<http://www.elsevier.com/locate/opal>**

**<http://www.elsevier.nl/locate/opal>**

**check out the OPAL Website for information on and demos of the OPAL Modules.**





# The Language of Shape

## The Role of Curvature in Condensed Matter: Physics, Chemistry and Biology

By S. Hyde, S. Andersson, K. Larsson, Z. Blum, T. Landh,  
S. Lidin and B.W. Ninham



ELSEVIER  
SCIENCE

This book develops the thesis that structure and function in a variety of condensed systems - from the atomic assemblies in inorganic frameworks and organic molecules, through molecular self-assemblies to proteins - can be unified when curvature and surface geometry are taken together with molecular shape and forces. An astonishing variety of synthetic and biological assemblies can be accurately modelled and understood in terms of hyperbolic surfaces, whose richness and beauty are only now being revealed by applied mathematicians, physicists, chemists and crystallographers. These surfaces, often close to periodic minimal surfaces, weave and twist through space, carving out interconnected labyrinths whose range of topologies and symmetries challenge the imaginative powers.

The book offers an overview of these structures and structural transformations, convincingly demonstrating their ubiquity in covalent frameworks from zeolites used for cracking oil and pollution control to enzymes and structural proteins, thermotropic and lyotropic bicontinuous mesophases formed by surfactants, detergents and lipids, synthetic block copolymer and protein networks, as well as biological cell assemblies, from muscles to membranes in prokaryotic and eukaryotic cells. The relation between structure and function is analysed in terms of the previously neglected "hidden variables" of curvature and topology. Thus, the catalytic activity of zeolites and enzymes, the superior material properties of interpenetrating networks in microstructured polymer composites, the transport requirements in cells, the transmission of nerve signals and the folding of DNA can be more easily understood in the light of this.

The text is liberally sprinkled with figures and colour plates, making it accessible to both the beginning graduate student and researchers in condensed matter physics and chemistry, mineralogists, crystallographers and biologists.

### Contents:

Preface.

1. The Mathematics of Curvature.
  2. The Lessons of Chemistry.  
Inorganic Chemistry: From the discrete lattice of crystal symmetry to the continuous manifolds of differential geometry. Organic Chemistry: The shape of molecules.
  3. Molecular Forces and Self-Assembly.
  4. Beyond Flatland. The Geometric Forms due to Self-Assembly.
  5. Lipid Self-Assembly and Function in Biological Systems.  
Self-association of lipids in an aqueous environment. Cell membranes.
  6. Folding and Function in Proteins and DNA.
  7. Cytomembranes and Cubic Membrane Systems Revisited.
  8. Some Miscellaneous Speculations. Templating. Supra self-assembly.
- Index.

©1997 396 pages Hardbound  
Price: NLG 370.00 (US\$231.25)  
ISBN 0-444-81538-4

To order please contact the Customer Support Department at the Regional Sales Office nearest you:

#### New York

Elsevier Science

Fax: (+1) 212-633-3680

E-mail: usinfo-f@elsevier.com

#### Amsterdam

Elsevier Science

Fax: (+31) 20-485-3432

E-mail: nlinfo-f@elsevier.nl

#### Tokyo

Elsevier Science

Fax: (+81) 3-5561-5047

E-mail: info@elsevier.co.jp

#### Singapore

Elsevier Science

Fax: (+65) 337-2230

E-mail: asiainfo@elsevier.com.sg

The currencies as stated with this information are definitive. *Dutch Guilder (NLG)* prices apply to customers *within Europe and Japan* only.

*US dollar (\$)* prices apply to all customers residing *outside Europe and Japan*. Prices are subject to change without prior notice. If you are a resident of the European Union you should either state your Value Added Tax (VAT) number or add the relevant VAT percentage applicable in your country to the total amount.

For a full description and contents of this and other Elsevier products please go to the Elsevier Science Catalogue on Internet  
Americas and Pacific Rim:  
<http://www.elsevier.com>  
Rest of World:  
<http://www.elsevier.nl>

## INFORMATION FOR AUTHORS

### Submission of Manuscripts

The original and two copies, typed double-spaced with 4-cm margins, should be sent (i) *from Europe to*: Professor F. Paltauf, Institut für Biochemie und Lebensmittelchemie, Technische Universität Graz, Petersgasse 12, A 8010 Graz, Austria, and (ii) *from other parts of the world to*: Professor H.H.O. Schmid, The Hormel Institute, University of Minnesota, 801 16th Avenue N.E., Austin, MN 55912, USA.

A submission letter should always accompany the submitted paper providing the following information:

- The full name and address of the corresponding author (including telephone and fax numbers, and e-mail addresses).
- Any known changes of address within a period of six months after submission of the paper.
- The full title of the submitted paper.
- The names and addresses of at least three suitable potential reviewers. If there are compelling reasons for excluding some individuals as potential reviewers, these can be mentioned. However, choice of reviewers is at the editors' discretion.

### Electronic Manuscripts

Electronic manuscripts have the advantage that there is no need for the rekeying of text, thereby avoiding the possibility of introducing errors and resulting in reliable and fast delivery of proofs.

For the initial submission of manuscripts for consideration, hardcopies are sufficient. After *final acceptance*, your disk plus two final and exactly matching printed versions should be submitted together. Double density (DD) or high density (HD) diskettes (3½ or 5¼ inch) are acceptable. It is important that the file saved is in the native format of the wordprocessor program used. Please do not save your text as ASCII or similar as this will cause all special formatting codes to be lost. Label the disk with the name of the computer and wordprocessing package used, your name, and the name of the file on the disk. Further information may be obtained from the Publisher.

### Organization of Manuscripts

(a) *Title page*. The title should be concise, descriptive and informative. The names of the authors should be followed by their addresses and indicated by corresponding letters. Changes in address should be indicated by footnotes. The author(s) to whom correspondence and proofs should be sent should be indicated, giving a full address (including fax number and e-mail address). Authors are requested to select a maximum of six key words and to present them on the title page of the typescript. These key words will be used for indexing and abstracting. Indicate also if the paper is a "Review" or "Short Communication".

(b) *Abstract*. An abstract not exceeding 150 words should summarize the objectives, procedures, results and conclusions of the research. It should be typed on a separate page and will appear at the beginning of the article.

(c) *Presentation of material*. The text should be concise and organized in the conventional manner. An *Introduction* should state the purpose of the work in the context of current knowledge. *Experimental Procedures* should be brief but sufficiently detailed to allow for potential repetition of the work by others. *Results* may include tables and figures, and a *Discussion* should primarily deal with the interpretation of the results. When appropriate, especially in Short Communications, *Results* and *Discussion* sections may be combined.

(d) *Acknowledgements*. Financial support, technical assistance, and other help or advice should be acknowledged in a separate paragraph at the end of the text.

### References

1. Quote references in the text by first author's name and year (in parenthesis). For two authors quote both names; for three or more authors, quote first author's name, *et al.*

2. At the end of the article, list references alphabetically by first author; include all authors' names, followed by initials and include full titles of publications.

*Examples of references:* (a) *to Journal articles*: Hupfer, B. and Ringsdorf, H. (1983) Spreading and polymerization behavior of diacetylene phospholipids at the gas-water interface. *Chem. Phys. Lipids* 33, 263–282. (b) *to books*: Dahlén, G. (1990) Clinical significance of Lp[a] lipoprotein, in: Berg, K., Rettersöl, N. and Refsum, F. (Eds.), *From Phenotype to Gene in Common Disorders*, Munksgaard, Copenhagen, pp. 163–178. The names of the journals should be abbreviated according to the list of serial title word abbreviations (ISDS, Paris, 1985. ISBN 2-904938-02-8). Unpublished results should not be listed in the References section. In the text they are mentioned as follows "(Tervoort, MV and Glimcher, J., unpublished data)". When unpublished results are cited, the data should be provided for the Editors' information when essential for proper evaluation, or if requested. A personal communication should be mentioned in the text as follows: "(Tervoort, MV, personal communication)". Authors should not make unauthorized use of personal communications. Personal communications are not to be included in the References section.

### Tables and Figures

(a) Tables should be numbered separately in Arabic numerals (Table 1, 2, 3, . . .) and must have a title.

(b) Figures should be numbered in Arabic numerals (Fig. 1, 2, 3, . . .). Illustrations will not be redrawn by the Publisher and therefore they should be submitted as either original ink drawings, computer generated prints (laser printer), or sharp, high contrast, unmounted photographs on glossy paper with the lettering proportional to the size of the illustrations taking reduction in size into account. Each illustration should be clearly marked on the reverse side with the name of the author(s), the number of the illustration and its orientation (top); use a soft pencil or preferably a felt-tipped pen. Illustrations should be designed for use in either a single column (7.5 cm) or a double column (16 cm). Actual magnification of all photomicrographs should be indicated. Reproduction in colour will have to be approved by the Editors. The extra costs of colour reproduction will be charged to the author(s).

(c) The appropriate position of each table and figure should be indicated in the margin of the manuscript.

(d) Legends to figures should be typed, double spaced, beginning on a separate page.

### Nomenclature and Abbreviations

Standard nomenclature should be used throughout; unfamiliar or new terms, arbitrary abbreviations, and trade names should be defined when first used. Unnecessary symbols and abbreviations should be avoided.

### Proofreading

Since acceptance is based upon the submitted version of the paper, it is essential that no new material be inserted in the text at the time of proofreading; furthermore, no alteration to style or meaning will be permitted at this stage. Any new material that the authors wish to introduce for reasons of scientific accuracy will be checked by the Editors, and a charge may be made for corrections. Authors are encouraged to return their proofs by fax.

### Reprints

Fifty reprints of each article will be supplied free of charge to the author(s). Additional reprints can be ordered at the prices shown on the reprint order accompanying proofs. Later orders cannot be filled since reprints are made at the time the journal is printed. There is no page charge.



J.M. Boggs, G. Rangaraj (Canada) <i>Greater partitioning of small spin labels into interdigitated than into non-interdigitated gel phase bilayers</i> . . . . .	1
O. Tirosh, R. Kohen, J. Katzhendler, A. Alon, Y. Barenholz (Israel) <i>Oxidative stress effect on the integrity of lipid bilayers is modulated by cholesterol level of bilayers</i> . . . . .	17
T. Paukku, S. Lauraeus, I. Huhtaniemi, P.K.J. Kinnunen (Finland) <i>Novel cationic liposomes for DNA-transfection with high efficiency and low toxicity</i> . . . . .	23
H. Brachwitz, Y. Thomas, J. Bergmann, P. Langen, W.E. Berdel (Germany) <i>New nucleoside-5'-alkylphosphonophosphates and related compounds containing 2'-deoxycytidine, thymidine and adenosine as nucleoside component. Syntheses and their effects on tumor cell growth in vitro</i> . . . . .	31
Q. Cheng, R.C. Stevens (USA) <i>Monolayer properties of monosialoganglioside in the mixed diacetylene lipid films on the air/water interface</i> . . . . .	41
M.S.F. Lie Ken Jie, S.H. Chau (Hong Kong) <i>Synthesis and nuclear magnetic resonance spectroscopic properties of some acetylenic tellura fatty acid esters</i> . . . . .	55
M. Brandl, M. Drechsler, D. Bachmann, K.-H. Bauer (Germany) <i>Morphology of semisolid aqueous phosphatidylcholine dispersions, a freeze fracture electron microscopy study</i> . . . . .	65
J. Kruk, M. Jemiola-Rzemińska, K. Strzałka (Poland) <i>Plastoquinol and <math>\alpha</math>-tocopherol quinol are more active than ubiquinol and <math>\alpha</math>-tocopherol in inhibition of lipid peroxidation</i> . . . . .	73
W. Jira, G. Spittler, A. Richter (Germany) <i>Increased levels of lipid oxidation products in low density lipoproteins of patients suffering from rheumatoid arthritis</i> . . . . .	81

*Cited/abstracted in: Current Awareness in Biological Sciences; Current Contents/Life Sciences; Chemical Abstracts; Excerpta Medica; Index Medicus*

© 1997 Elsevier Science Ireland Ltd. Copyright Reserved. No part of this publication may be reproduced, stored in a retrieval system, or transmitted, in any form or by any means, electronic, mechanical, photocopying, recording or otherwise, without the prior permission of the Copyright owner.

Published and Printed in Ireland

© The paper used in this publication meets the requirements of ANSI/NISO Z39.48-1992 (Permanence of Paper)

Library of Congress Catalog Number: 68-26533

The table of contents of *Chemistry and Physics of Lipids* is included in ESTOC – Elsevier Science Tables of Contents service – which can be accessed on the World Wide Web at the following URL addresses: <http://www.elsevier.nl/locate/estoc> or <http://www.elsevier.com/locate/estoc>



0009-3084(19970530)87:1;1-Q

08008



